LBL-165

c.1

ELLIPSOMETRY OF SURFACE LAYERS

Hiram Gu
(M.S. Thesis)

December 1971

AEC Contract No. W-7405-eng-48

For Reference

Not to be taken from this room

LBL-165

c.1

DISCLAIMER

This document was prepared as an account of work sponsored by the United States Government. While this document is believed to contain correct information, neither the United States Government nor any agency thereof, nor the Regents of the University of California, nor any of their employees, makes any warranty, express or implied, or assumes any legal responsibility for the accuracy, completeness, or usefulness of any information, apparatus, product, or process disclosed, or represents that its use would not infringe privately owned rights. Reference herein to any specific commercial product, process, or service by its trade name, trademark, manufacturer, or otherwise, does not necessarily constitute or imply its endorsement, recommendation, or favoring by the United States Government or any agency thereof, or the Regents of the University of California. The views and opinions of authors expressed herein do not necessarily state or reflect those of the United States Government or any agency thereof or the Regents of the University of California.

0 0 0 0 3 6 0 7 0 9 9

ELLIPSOMETRY OF SURFACE LAYERS

Contents

Abstract vii

I. Introduction 1

II. Theory 4

A. Definitions and Conventions 4

B. General Principle of Ellipsometric Measurements 7

C. Ellipsometry of a Film-Free Surface 7

D. Ellipsometry of a Film-Covered Surface 15

III. The Ellipsometer 24

IV. Adsorption Study of Carbon Monoxide on a Platinum Single Crystal 25

A. Equipment 25

B. Alignment 25

C. The Effect of Cell Windows 28

D. Specimen 28

E. Bare Substrate 28

F. Chemisorption of Carbon Monoxide 34

V. Study of Liquid Films on a Platinum Electrode 43

A. Equipment 43

1. Cell 43

2. Liquid Filling and Draining System 43

3. Cell Atmosphere Control System 43

4. Optical System 47

B. The Platinum Electrode 47

C. Preparation of Electrolytes 54

D. Preparation of Electrode Surface and Cleaning of the Cell 54

E. Alignment 55

F. The Effect of Cell Windows 56

G. Determination of the Optical Constants of the Platinum Electrode 58

H. KOH Films 61

1. Measurement of the Thinning of Film 61

2. Steady State Film Profile 65

3. Comparison with White Light Interference 65

4. Discussion 71

I. H_2SO_4 Film 75

1. Experimental 75

2. Discussion 78

VI. Design Considerations for an Automatic Ellipsometer . . . 79

Acknowledgments 83

Appendix I. Computer Programs 84

A. FORTRAN IV Computer Program "MOC" 84

B. FORTRAN IV Computer Program "AXCON" 88

C. FORTRAN IV Computer Program "MER" 94

D. FORTRAN IV Computer Program "LAYER" 100

E. FORTRAN IV Computer Program "SFILM" 110

F. FORTRAN IV Computer Program "FPLOT" 121

G. FORTRAN IV Computer Program "DLVPS" 130

Appendix II. Alignment and Calibration of the Ellipsometer on LEED Setup 133

A. Alignment of the Ellipsometer 133

B. Calibration of the Polarizer and the Analyzer Circles 134

C. Calibration of the Compensator Circle Setting 136

Appendix III. Alignment and Calibration of the Ellipsometer (Variable Angle of Incidence Setup) 142

A. Adjustment of the Collimator and Telescope Axes to be Coplanar and to Intersect the Rotational Axis of the Sample Table at Right Angles 142

B. Adjustment of the Horizontal Circle Readings (Angle of Incidence Readings) 144

C. Alignment of Rotational Axes of Table and Telescope . . 144

D. Calibration of Polarizer and Analyzer Circles 146

E. Calibration of the Quarter-Wave Plate 147

Appendix IV. Poincaré Sphere 149

Appendix V. Ellipsometric Parameters Δ and ψ From Polarizer and Analyzer Circle Readings in Different Zones 155

References 156

0 0 0 0 3 6 0 7 1 0 0

ELLIPSOMETRY OF SURFACE LAYERS*

Hiram Gu

Inorganic Materials Research Division, Lawrence Berkeley Laboratory
and Department of Chemical Engineering; University of California
Berkeley, California

ABSTRACT

Ellipsometry was used in two studies of films on platinum substrates: Chemisorbed carbon monoxide films and electrolyte films. Good qualitative correlation was found between ellipsometric and Auger Electron Spectroscopic measurements of surface contaminant layers. Steady-state film profiles of 2.62N and 6.05N KOH films obtained on a platinum electrode by ellipsometry compared well with those derived from the observation of interference colors. Ellipsometric measurements of 0.94N H_2SO_4 film could be interpreted in terms of a dielectric film while data of KOH films suggested absorption characteristics of the film which may be due to the inclusion of foreign particles. Detailed procedures for the alignment of ellipsometers of fixed and variable angle of incidence are given.

---

*M.S. Thesis, research conducted under the direction of R. H. Muller.

I. INTRODUCTION

The history of Ellipsometry can be dated back to 1808.[41] Due to its high resolution and the fact that it allows the performance of non-destructive optical measurements in situ, ellipsometry has become a versatile tool in surface research. Through the years, ellipsometry served in many areas of research such as determination of optical constants,[42-44,51] surface study of glass,[45] corrosion studies,[46,47] studies of oxide films,[48-50] organic films on metals,[59,60] polymer adsorption,[61] gas adsorption[20,24,62], ion adsorption,[36] and electrochemical studies.[63-65] Because of its ability to determine film thickness with a resolution of often less than 1Å, ellipsometry has mainly been used to measure thin films (optical path less than one wavelength). However, thick film measurements have also been made with ellipsometry.[66]

This work covers two aspects of ellipsometry--thin film measurement and thick film measurement. In addition, a brief account of a preliminary design for an automatic ellipsometer is given. The study of chemisorption of carbon monoxide on a platinum single crystal is the subject covered in thin film measurement, while the thick film measurement deals with the study of electrolyte films on a platinum electrode.

The hydrogenation of unsaturated hydrocarbons on transition metal catalysts is of great practical interest. To understand the catalytic reaction mechanisms, it is important to know how the adsorbed hydrocarbon molecules arrange themselves on the metal surface. Platinum has been most widely used for catalytic hydrogenation reactions. Conventionally, the adsorption of gases has been studied by low energy electron diffraction (LEED), mass-spectrometric techniques, work function technique, Auger electron spectroscopy (AES) and flash-desorption technique. These were carried out in an ultra-high vacuum

system. Carbon monoxide, a major ambient constitutent in the vacuum system was known to chemisorb readily on platinum substrates forming ordered strustures.[56] During the studies, the platinum surface may easily be contaminated by carbon monoxide, occupying available adsorption sites. It is therefore important to understant the interaction of carbon monoxide with platinum surfaces.

Morgan and Somorjai[57] have done LEED studies of carbon monoxide adsorption on platinum surfaces. Several authors[20-22,58] have reported on the merits of combining ellipsometry with LEED, or with Auger electron spectroscopy measurements. In this work, it was hoped that the adsorption studies of CO on a platinum crystal by ellipsometry could complement LEED and AES measurements by providing information on the amount of surface coverage.

Electrolyte films formed on electrodes have long been of interest. Will,[67,68] from his experiments involving oxidation of hydrogen in sulfuric acid on partially immersed platinum electrode, concluded that the presence of the film contributed appreciably to the charge transfer reaction. He was able to explain his experimental results in terms of a theoretical model. Bennion and Tobias,[69,70] and Maget and Roethlein[71] have done current distribution measurements on partially immersed electrodes. Weber, et al.[72] suggested the presence of electrolyte films in the pores of gas electrodes. They formulated an electrolyte film mechanism model for gas electrodes as opposed to the surface diffusion mechanism model suggested by Justi and Winsel.[73] Iczkowski[78] has made a comparison between the two models. The analysis of porous electrodes by Grens, et al.,[74] Katan, et al.,[76] and Rockett, et al.[75] also suggested that the pores of a gas electrode are covered by an electrolyte film.

Since it is believed that electrolyte films contribute markedly to

gas electrode reactions, the study of the thickness of electrolyte films is of importance for an explanation of the working mechanism of a porous gas diffusion electrode. Muller[29] has made optical studies of electrolyte films on partially immersed nickel and silver surfaces. Burshtein, et al.[77] have used a monochromatic interference method to study 1N KOH and 1N H_2SO_4 films on platinum electrodes. Turney[27] has used white light interference to study aqueous KOH films on platinum and stainless steel surfaces.

A second purpose of this work was to apply ellipsometry to the study of electrolyte films and to compare the results with white light interference measurements. It was also hoped that the results of ellipsometric measurements could help clarify a discrepancy between Turney's results and those previously obtained by Muller.

II. THEORY

Ellipsometry deals with the reflection of a monochromatic, collimated, polarized light. A polarized light wave can be represented by an electric vector, E, propagating through space, changing in amplitude and direction. The electric vector can be resolved into two components. One lies in the plane of incidence, and the other normal to the plane of incidence. The state of polarization is characterized by the phase and amplitude relationships between these two components. Upon reflection, the state of polarization will change. Ellipsometry employs the measurement of this change for the characterization of the reflecting surface.

A. Definitions and Conventions

It is important to recognize that many parameters in the theory of ellipsometry depend on definitions and conventions arbitrarily chosen.[1] In order to avoid confusion, a set of definitions, conventions, and the coordinate system used in the present work will be given here. All equations that follow are derived from these bases.

The complex index of refraction of an absorbing medium is defined as $n_c = n - ik$, where n is the refractive index and k, the index of extinction. For a dielectric medium, k is equal to zero and the medium is characterized by a real index of refraction n.

The coordinate system is shown in Fig. 1. The direction of a positive vector is represented by an arrow head. Subscripts p and s designate "in the plane of incidence" and "normal to the plane of incidence", respectively. Superscript (") denotes the reflected wave, and superscript (') denotes the transmitted wave. The medium containing the incident beam is assumed to be a dielectric medium with refractive

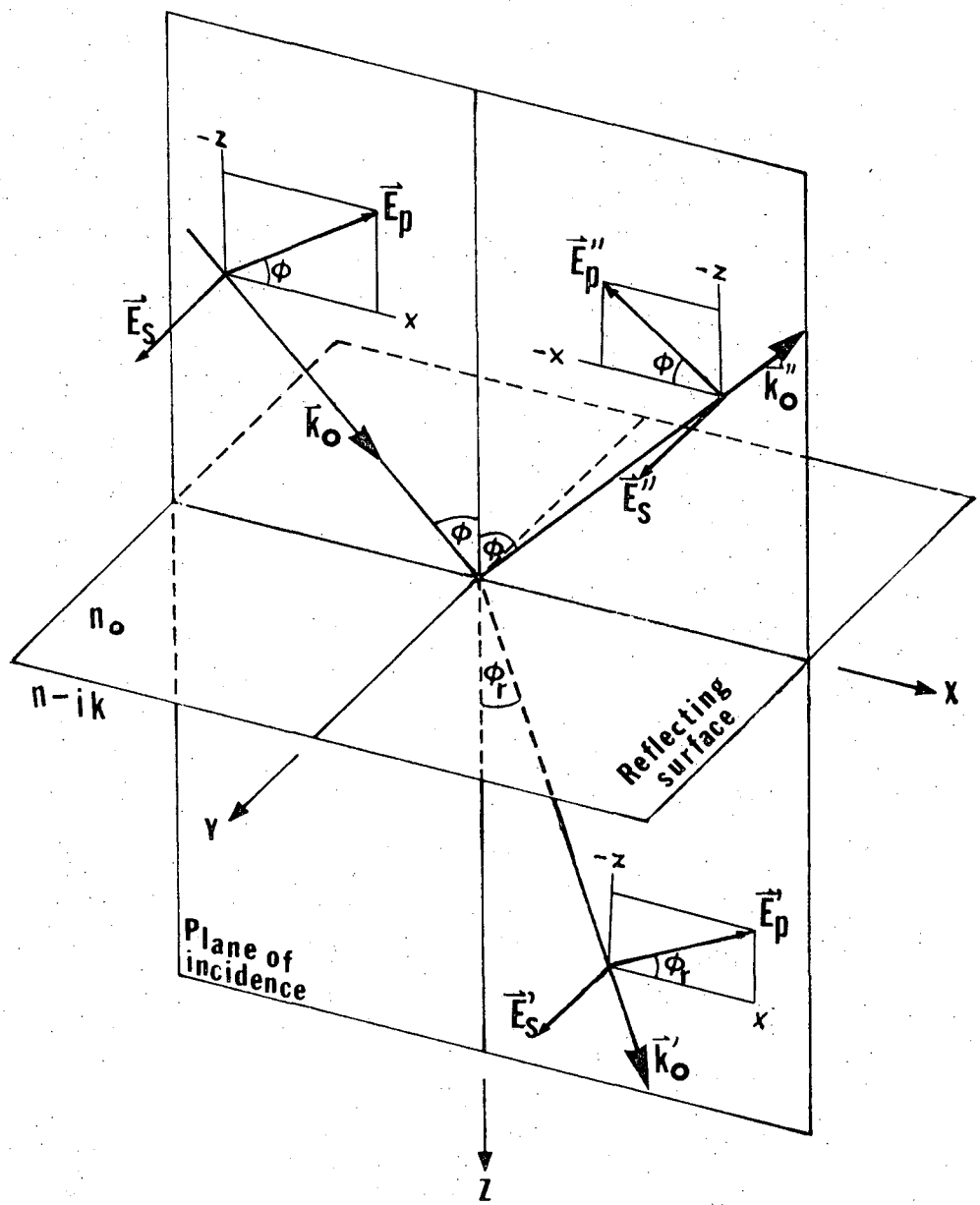

XBL 7110-7420

Fig. 1 Coordinate system and sign conventions for the electric field (positive direction of E_p and E_s in incident, reflected and refracted waves is indicated by arrows). The propagation vectors are represented by k_o, k_o' and k_o''. Subscript p stands for polarization parallel to the plane of incidence and subscript s stands for polarization normal to the plane of incidence. The complex index of refraction of the adsorbing medium is designated n-ik.

index, n_o. The effect of reflection is characterized by the relative phase change, Δ and the arctangent of the relative amplitude attenuation, ψ. They are defined as:

$$\Delta = (\varepsilon''_p - \varepsilon_p) - (\varepsilon''_s - \varepsilon_s) \tag{1}$$

$$\tan \psi = \frac{|E''_p/E''_s|}{|E_p/E_s|} \tag{2}$$

where epsilon represents the phase of a component with respect to an arbitrary time origin. $\varepsilon'' - \varepsilon$ can be termed the absolute phase change, δ.

The complex relative amplitude attenuation ρ is defined as the ratio of the Fresnel coefficients for the p and s components.

$$\rho = \frac{r_p}{r_s} \tag{3}$$

The Fresnel Coefficients are defined as the ratio E''_p/E_p and E''_s/E_s. They are in general, complex (when the reflecting surface is absorbing) and can be written as an amplitude ratio and a phase change:

$$r_p = \frac{E''_p}{E_p} = \frac{|E''_p|}{|E_p|} \frac{e^{i\varepsilon''_p}}{e^{i\varepsilon_p}} \tag{4}$$

$$r_s = \frac{E''_s}{E_s} = \frac{|E''_s|}{|E_s|} \frac{e^{i\varepsilon''_s}}{e^{i\varepsilon_s}} \tag{5}$$

Combining Eqs. (1), (2), (3), (4) and (5), we obtain the basic equation of ellipsometry:

$$\rho = \tan \psi \, e^{i\Delta} \tag{6}$$

B. General Principle of Ellipsometric Measurements

The principle of ellipsometric measurements of Δ and ψ is shown schematically in Fig. 2. Monochromatic collimated light after passing the polarizer becomes plane polarized in the direction which forms an azimuth angle p with the plane of incidence. The compensator, which is usually a quarter wave plate and in general with its fast-axis oriented at 45° or 135° to the plane of incidence, will shift the component parallel to its fast axis ahead of the component parallel to its slow axis by 1/4 λ_o* or 90°. The beam is thus made elliptically polarized. The reflection will restore the beam to plane polarized light with proper orientation of the transmission axis azimuth of the polarizer. The reflected beam can then be extinguished** by adjusting the analyzer. From the readings of the azimuth angle of the polarizer and analyzer, Δ and ψ can be determined easily with the help of the Poincaré sphere† treatment and spherical trigonometry.

C. Ellipsometry of a Film-Free Surface

When polarized monochromatic light is reflected from a dielectric-dielectric interface (see Fig. 3a), the Fresnel reflection coefficients are given by:[2]

$$r_s = \frac{E''_s}{E_s} = \frac{n_o \cos\phi - n_1 \cos\phi_r}{n_o \cos\phi + n_1 \cos\phi_r} = -\frac{\sin(\phi - \phi_r)}{\sin(\phi + \phi_r)} \tag{7}$$

$$r_p = \frac{E''_p}{E_p} = \frac{n_1 \cos\phi - n_o \cos\phi_r}{n_1 \cos\phi + n_o \cos\phi_r} = \frac{\tan(\phi - \phi_r)}{\tan(\phi + \phi_r)} \tag{8}$$

---

*λ_o is the vacuum wavelength of the incident light.

**In practice, complete extinction is not obtained due to the imperfectness of the optical components. The analyzer is only adjusted to obtain the minimum intensity. The minimum is determined by two off minimum readings.

†See Appendix IV.

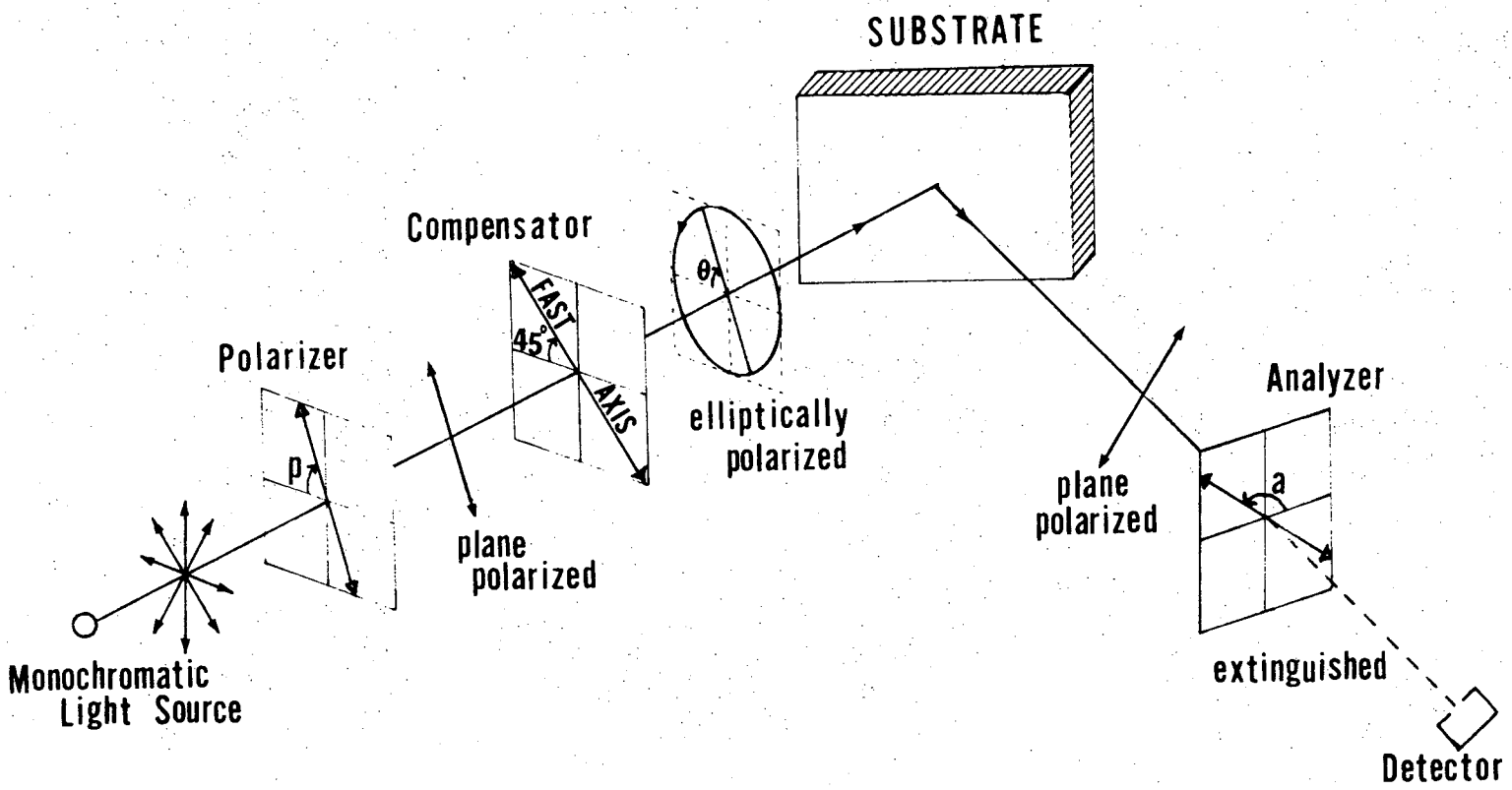

XBL 7110-7416

Fig. 2 Schematic representation of Ellipsometric Measurements. Azimuth angles are measured counterclockwise from plane of incidence when looking against the propagation vector.

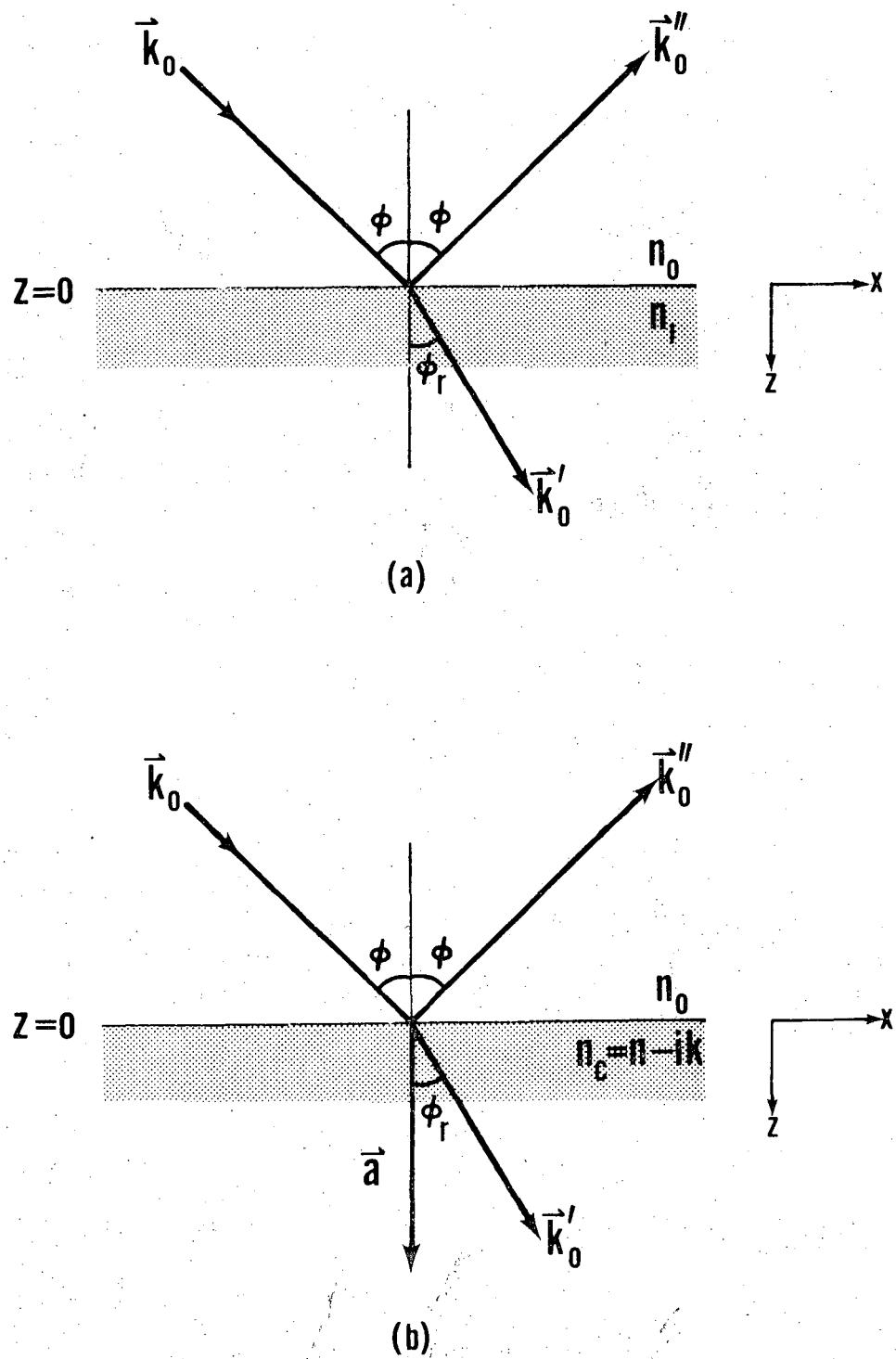

XBL 7110-7417

Fig. 3 a) Reflection from a transparent substrate, $n_0 \sin \phi = n_1 \sin \phi_r$. b) Reflection from an absorbing substrate. The propagation vector $\vec{k}_0'$ forms the real angle ϕ_r with the normal to the surface of the medium while the attenuation vector $\vec{a}$ lies along the normal. Planes of equal phase are normal to $\vec{k}_0'$ while planes of equal amplitude are normal to $\vec{a}$ in the absorbing medium.

where n_o is the refractive index of the incident medium and n_1, that of the substrate. The angle of incidence ϕ, is related to the angle of refraction ϕ_r by Snell's law:

$$n_o \sin \phi = n_1 \sin \phi_r \tag{9}$$

Eqs. (7) and (8) can thus be written in terms of n_o, n_1 and ϕ alone. Plots of r_p, r_s and their moduli R_p, R_s ($|r_p|$, $|r_s|$) as a function of the angle of incidence are shown in Figs. 4a and 4b.

For light incident from a transparent medium onto a plane surface of an absorbing medium (see Fig. 3b), the situation is more complicated. The Fresnel reflection coefficients are complex quantities and can be written as:

$$r_s = \frac{n_o \cos \phi - n_c \cos \phi'}{n_o \cos \phi + n_c \cos \phi'} = - \frac{\sin (\phi - \phi')}{\sin (\phi + \phi')} \tag{10}$$

$$r_p = \frac{n_c \cos \phi - n_o \cos \phi'}{n_c \cos \phi + n_o \cos \phi'} = \frac{\tan (\phi - \phi')}{\tan (\phi + \phi')} \tag{11}$$

In this case, ϕ' is the complex angle of refraction (not a real quantity, as ϕ_r is), and may be defined by the complex form of Snell's law:

$$n_o \sin \phi = n' \sin \phi_r \equiv n_c \sin \phi' \tag{12}$$

Again n_o is the refractive index of the incident medium and n_c is the complex index of refraction

$$n_c = n - ik \tag{13}$$

n' in Eq. (12) is defined in Eq. (14):

$$n_c' = n' - ik' \tag{14}$$

The quantities n' and k' are related to the metal constants n and k by[38]

$$n^2 - k^2 = n'^2 - k'^2 \tag{15}$$

and

$$nk = n'k' \cos \phi_r \tag{16}$$

n' and k' will be termed the alternate optical constants.

(It is noted that if n and k are taken to be constants, the alternate constants n' and k' will have a slight dependence on angle of incidence.[2])

The moduli of Eqs. (10) and (11) are given by[2,39]

$$R_s = \sqrt{\frac{A^2 + B^2 - 2A \cos \phi + \cos^2 \phi}{A^2 + B^2 + 2A \cos \phi + \cos^2 \phi}} \tag{17}$$

$$R_p = R_s \sqrt{\frac{A^2 + B^2 - 2A \sin \phi \tan \phi + \sin^2 \phi \tan^2 \phi}{A^2 + B^2 + 2A \sin \phi \tan \phi + \sin^2 \phi \tan^2 \phi}} \tag{18}$$

where

$$A = \sqrt{\frac{1}{2 n_o^2} \left[\sqrt{(n^2 - k^2 - n_o^2 \sin^2 \phi)^2 + 4n^2k^2} + (n^2 - k^2 - n_o^2 \sin^2 \phi) \right]} \tag{19}$$

$$B = \sqrt{\frac{1}{2 n_o^2} \left[\sqrt{(n^2 - k^2 - n_o^2 \sin^2 \phi)^2 + 4n^2k^2} - (n^2 - k^2 - n_o^2 \sin^2 \phi) \right]} \tag{20}$$

A plot of Eqs. (17) and (18) as a function of angle of incidence is shown in Fig. 5d.

The ellipsometric parameters Δ (relative phase change), ψ (arctangent of relative amplitude attenuation), δ_p (absolute phase change of p component), and δ_s (absolute phase change of s component) are also functions of angle of incidence. They are given by the following expressions:[2,39]

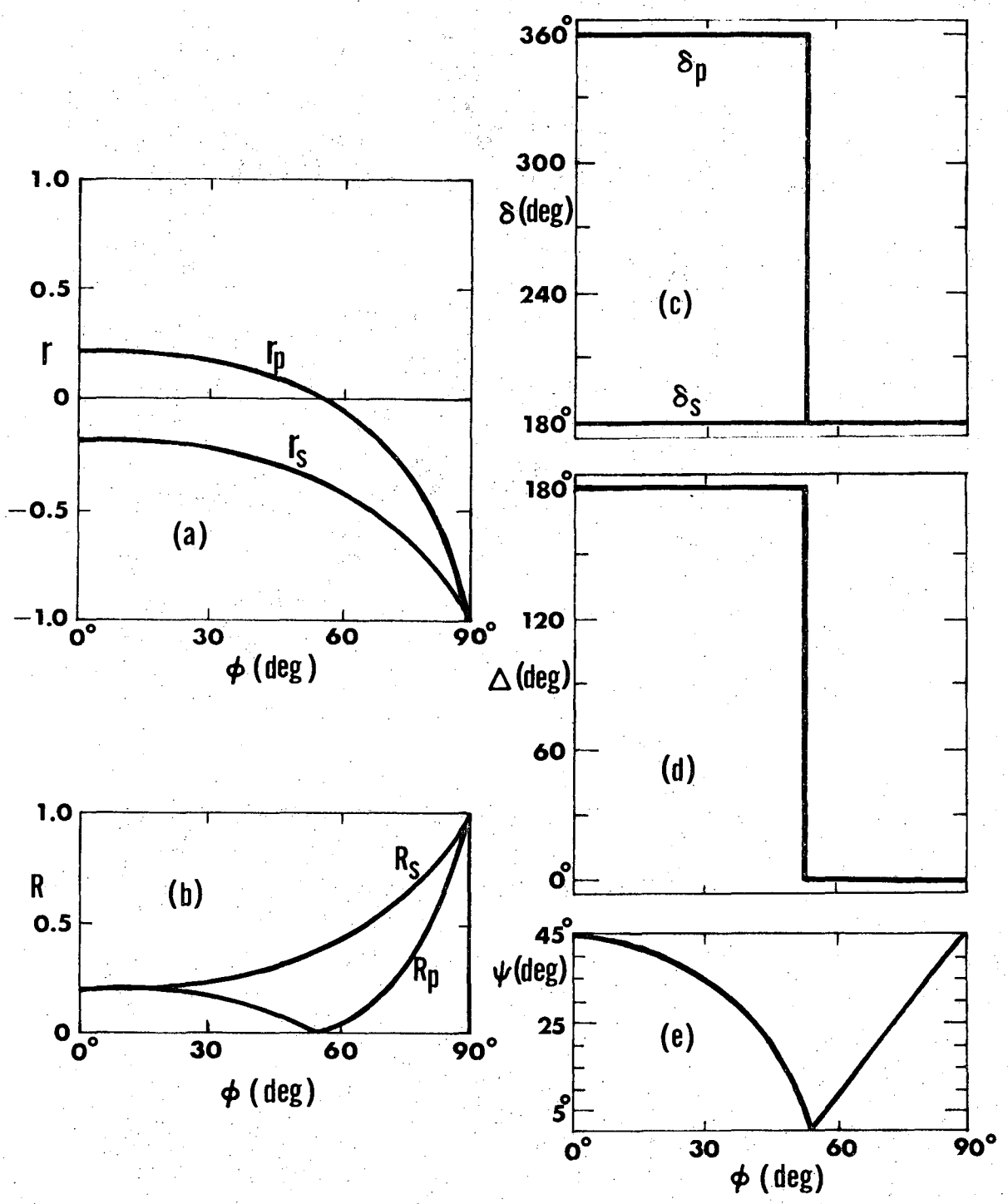

XBL 7110-7418

Fig. 4 Fresnel reflection coefficient r, modulus of reflection coefficient R, absolute phase change δ, relative phase change Δ, and arctangent of relative amplitude attenuation ψ as functions of angle of incidence ϕ for a transparent dielectric (glass), n = 1.5, k = 0.

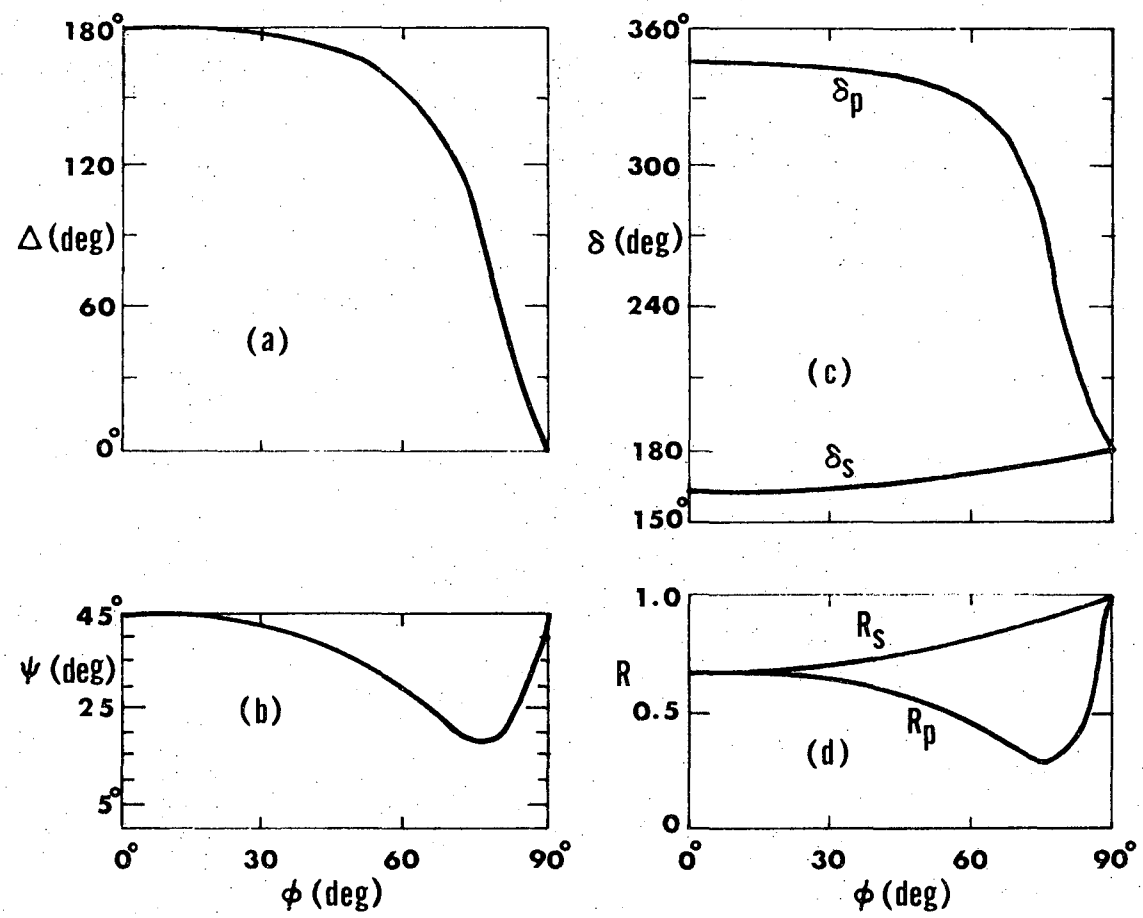

XBL 7110-7419

Fig. 5 Relative phase change Δ, arctangent of relative amplitude attenuation ψ, absolute phase change δ, and modulus of reflection coefficient R as functions of angle of incidence φ for a poor reflector (tantalum), n = 3.3, k = 2.21.

$$\Delta = \tan^{-1}\left(-\frac{2B \sin\phi \tan\phi}{A^2 + B^2 - \sin^2\phi \tan^2\phi}\right) \tag{21}$$

where $0 \leqslant \Delta \leqslant \pi$ for bare surfaces,

$$\psi = \tan^{-1}\left\{\sqrt{\frac{A^2 + B^2 - 2A \sin\phi \tan\phi + \sin^2\phi \tan^2\phi}{A^2 + B^2 + 2A \sin\phi \tan\phi + \sin^2\phi \tan^2\phi}}\right\} \tag{22}$$

where $0 \leqslant \psi \leqslant \pi/4$ for bare surfaces,

$$\delta_s = \tan^{-1}\left\{-\frac{2B \cos\phi}{A^2 + B^2 - \cos^2\phi}\right\} \tag{23}$$

where $0 \leqslant \delta_s \leqslant \pi$, and from Eqs. (1), (21) and (23),

$$\delta_p = \tan^{-1}\left\{\frac{2B \cos\phi\,(A^2 + B^2 - \sin^2\phi)}{A^2 + B^2 - \frac{1}{n_o^4}(n^2 + k^2)^2 \cos^2\phi}\right\} \tag{24}$$

These equations can also be applied to a non-absorbing substrate when we take k to be zero. An example of the dependence of Δ, ψ, δ_p and δ_s on angle of incidence is shown in Fig. 4 (for dielectric substrate) and Fig. 5 (for absorbing substrate).

The optical constants of a substrate in a transparent medium can be determined from ellipsometric measurements with the following equations:[2]

$$n = n_o \sqrt{1/2\left\{(D^2 - E^2 + \sin^2\phi) + \sqrt{(D^2 - E^2 + \sin^2\phi)^2 + 4D^2E^2}\right\}} \tag{25}$$

$$k = n_o \sqrt{1/2\left\{-(D^2 - E^2 + \sin^2\phi) + \sqrt{(D^2 - E^2 + \sin^2\phi)^2 + 4D^2E^2}\right\}} \tag{26}$$

where

$$D = \frac{\sin\phi \tan\phi \cos 2\psi}{1 + \sin 2\psi \cos\Delta}^{*} \tag{27}$$

$$E = \frac{\sin\phi \tan\phi \sin 2\psi \sin\Delta}{1 + \sin 2\psi \cos\Delta}^{*} \tag{28}$$

When the substrate is non-absorbing, Δ will be either zero or 180° (see Fig. 4) and D will be zero. According to Eq. (26), k is therefore also zero as expected.

D. Ellipsometry of a Film-Covered Surface

When polarized light is reflected from a film-covered surface, the change of state of polarization will depend both on the optical constants of the substrate, and on the thickness and optical constants of the film. Similar to a film-free surface, the change can be characterized by the ellipsometric parameters Δ and ψ.

As a ray of light falls upon a film-covered surface, multiple reflection occurs at the film surface and at the film-substrate interface as shown in Fig. 6a. It can be shown that the system of reflected and refracted waves shown in Fig. 6a is equivalent to the system shown in Fig. 6b, where E" is a wave equivalent to all waves reflected at the film, E' and E"' are the equivalents of all waves in the film and E_m is the equivalent of all waves in the metal.[3] The substrate is taken to be of infinite extent in the +z direction.[4,5]

With the help of Maxwell's equations,[6] the overall reflection coefficients are given[7] by:

---

*D and E are equal to A and B of Eqs. (19) and (20), respectively.

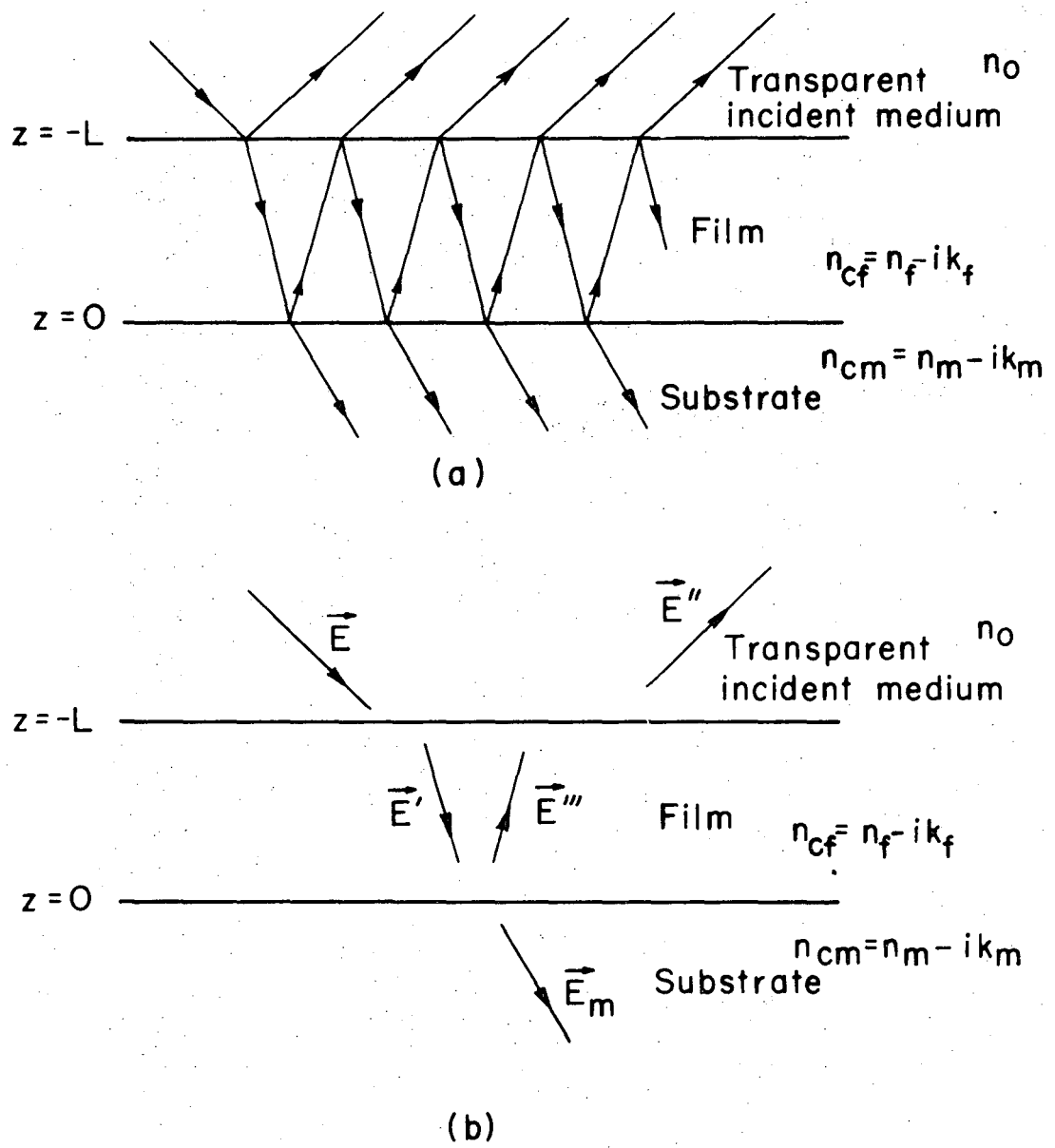

MUB-14178A

Fig. 6 Reflection from idealized film covered surface.
a) Representation by multiple beam reflection.
b) Representation in terms of equivalent waves.

$$r_s = \frac{E''_s}{E_s} = \frac{r_{1s} + r_{2s}\, e^{-id}}{1 + r_{1s}\, r_{2s}\, e^{-id}}\, e^{+id_o} \tag{29}$$

$$r_p = \frac{E''_p}{E_p} = \frac{r_{1p} + r_{2p}\, e^{-id}}{1 + r_{1p}\, r_{2p}\, e^{-id}}\, e^{+id_o} \tag{30}$$

where,

$$d = \frac{4\pi L}{\lambda_o}\, n_{cf} \cos \phi' \tag{31}$$

$$d_o = \frac{4\pi L}{\lambda_o}\, n_o \cos \phi \tag{32}$$

and

$$r_{1s} = \frac{E_{1s}}{E_s} = \frac{n_o \cos \phi - n_{cf} \cos \phi'}{n_o \cos \phi + n_{cf} \cos \phi'} \tag{33}$$

$$r_{1p} = \frac{E_{1p}}{E_p} = \frac{n_{cf} \cos \phi - n_o \cos \phi'}{n_{cf} \cos \phi + n_o \cos \phi'} \tag{34}$$

$$r_{2s} = \frac{E'''_s}{E'_s} = \frac{n_{cf} \cos \phi' - n_{cm} \cos \phi'_m}{n_{cf} \cos \phi' + n_{cm} \cos \phi'_m} \tag{35}$$

$$r_{2p} = \frac{E'''_p}{E'_p} = \frac{n_{cm} \cos \phi' - n_{cf} \cos \phi'_m}{n_{cm} \cos \phi' + n_{cf} \cos \phi'_m} \tag{36}$$

λ_o is the vacuum wave length of the incident light, ϕ' and ϕ'_m are the complex angle of refraction in the film and in the substrate respectively. From Eq. (12), the following relations hold:

$$\cos \phi' = \sqrt{1 - \frac{n_o^2 \sin^2 \phi}{n_{cf}^2}} \tag{37}$$

$$\cos \phi'_m = \sqrt{1 - \frac{n_o^2 \sin^2 \phi}{n_{cm}^2}} \tag{38}$$

n_{cf} is the complex refractive index of the film and n_{cm}, that of the substrate. r_1 is the Fresnel reflection coefficient at the film surface when the film is assumed to be infinitely thick and E_1 is the reflected electric field component under this condition. r_2 is the Fresnel reflection coefficient at the film-substrate interface.

Since,

$$\rho = \frac{r_p}{r_s} = \tan \psi \, e^{i\Delta} \qquad (3),(6)$$

applying complex algebra, we have

$$\Delta = \tan^{-1} \left\{ \frac{\mathrm{Im}\ (\rho)}{\mathrm{Re}\ (\rho)} \right\} \qquad (39)$$

and,

$$\psi = \tan^{-1} \left\{ |\rho| \right\} \qquad (40)$$

We can see from Eqs. (29) to (40) that both Δ and ψ are functions of the angle of incidence, the vacuum wave length, the refractive index of the incident medium, the optical constants of the substrate and the film, and the thickness of the film.

Several methods are available for determining the thickness of films on reflecting substrates from ellipsometric measurements.[3,5,8-12] When the angle of incidence, the optical constants of the film and of the substrate are known, values of Δ and ψ can be calculated for a given thickness, L, of the film using the exact Eqs. (29) to (40). Examples of a transparent film on transparent substrate, a transparent film on absorbing substrate and an absorbing film on absorbing substrate are shown in Figs. 7, 8, 9 and 10 respectively. Experimental values of Δ and ψ can be interpolated in such related graphs or tables to determine unknown thicknesses, without uncertainty if the thickness range

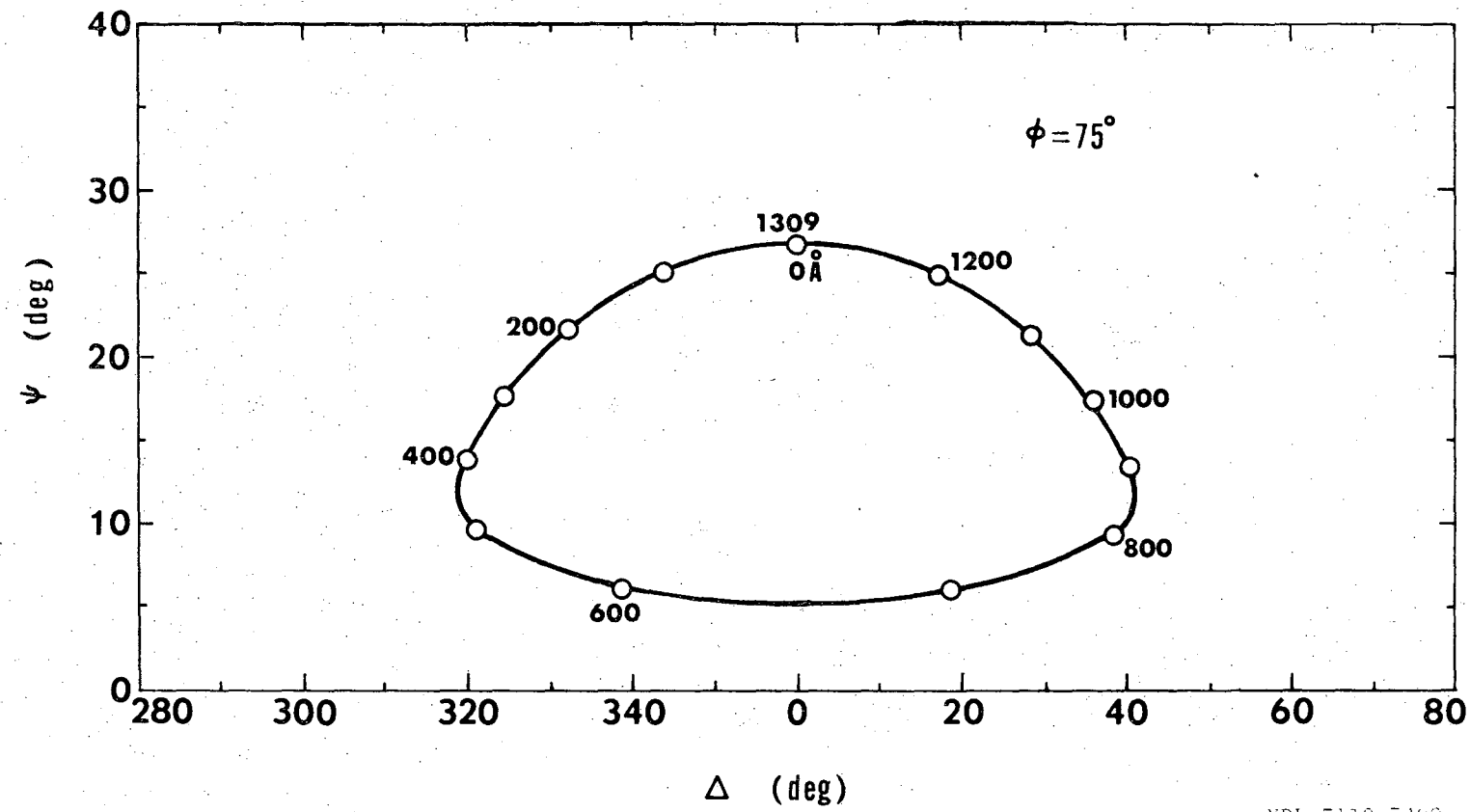

XBL 7110-7409

Fig. 7 Transparent Film on Transparent Substrate (ZnS on glass). Values of ψ and Δ calculated for increasing film thickness for wavelength 5461Å, angle of incidence 75°, base constants $n_m = 1.52$, $k_m = 0$ and film constants $n_f = 2.30$, $k_f = 0$. Film thickness in Å indicated as parameter. The curve closes on itself at 1309Å (optical thickness one wavelength).

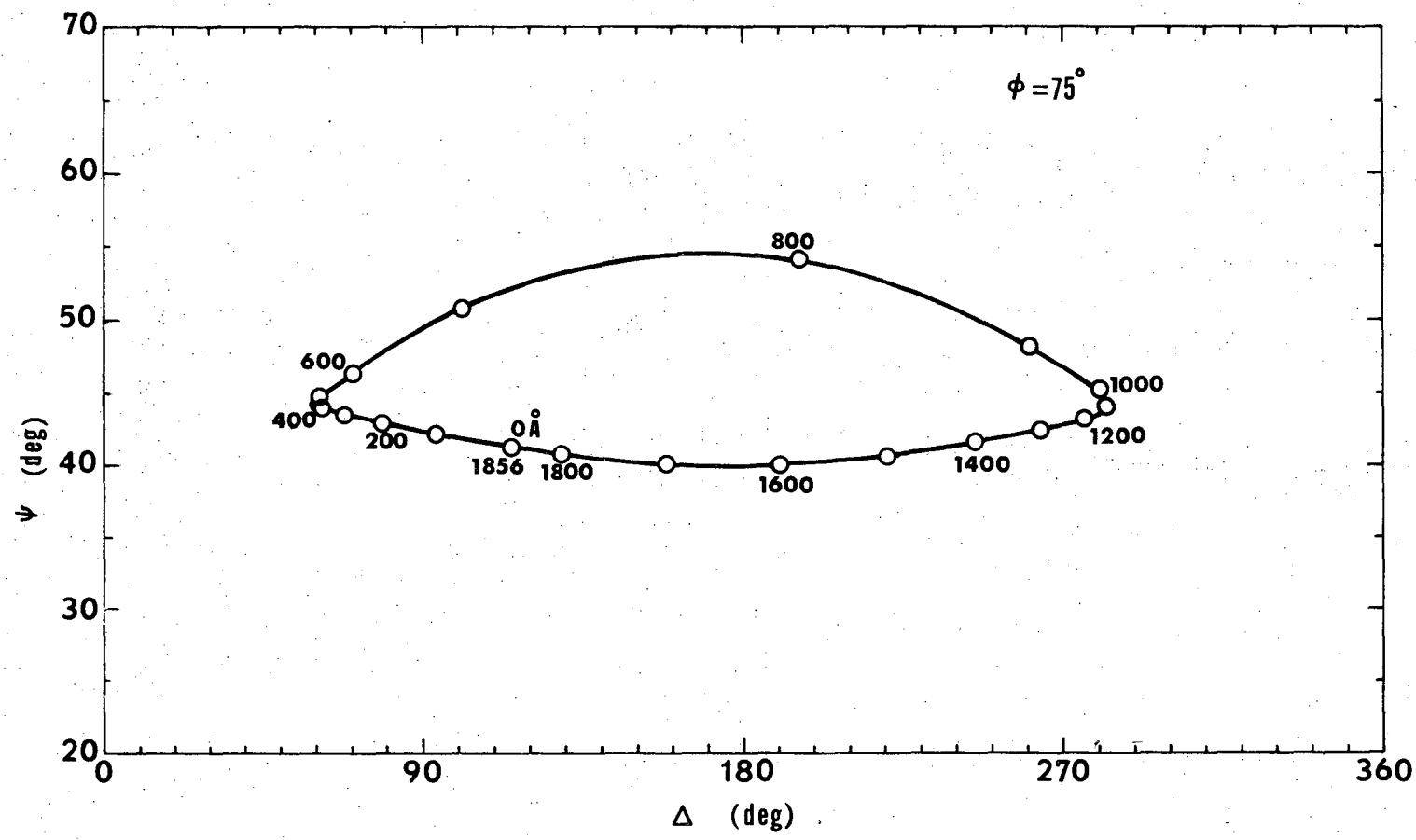

XBL 7110-7410

Fig. 8 Transparent film on absorbing substrate (aluminum oxide on aluminum). Values of ψ and Δ calculated for increasing film thickness for wavelength 5461Å, angle of incidence 75°, base constants $n_m = 0.81$, $k_m = 5.47$ and film constants $n_f = 1.76$, $k_f = 0$. The curve closes on itself at the thickness 1856Å.

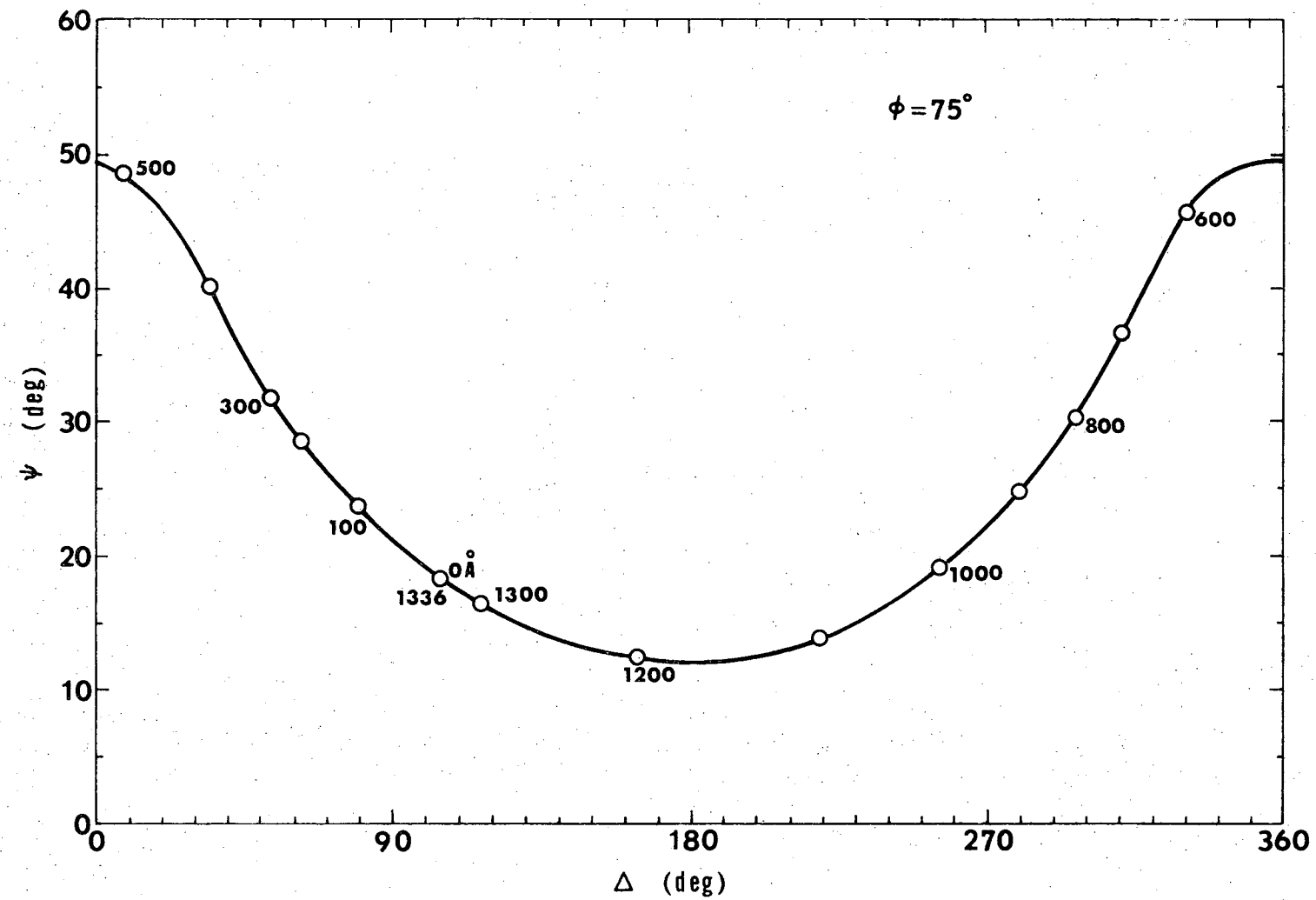

XBL 7110-7411

Fig. 9 Transparent film on absorbing substrate (tantalum oxide on tantalum). Values of ψ and Δ calculated for increasing film thickness for wavelength 5461Å, angle of incidence 75°, base constants $n_m = 3.5$, $k_m = 2.4$ and film constants $n_f = 2.26$, $k_f = 0$. The curve returns to bare tantalum values at 1336Å.

0 0 0 0 6 0 7 1 0 9

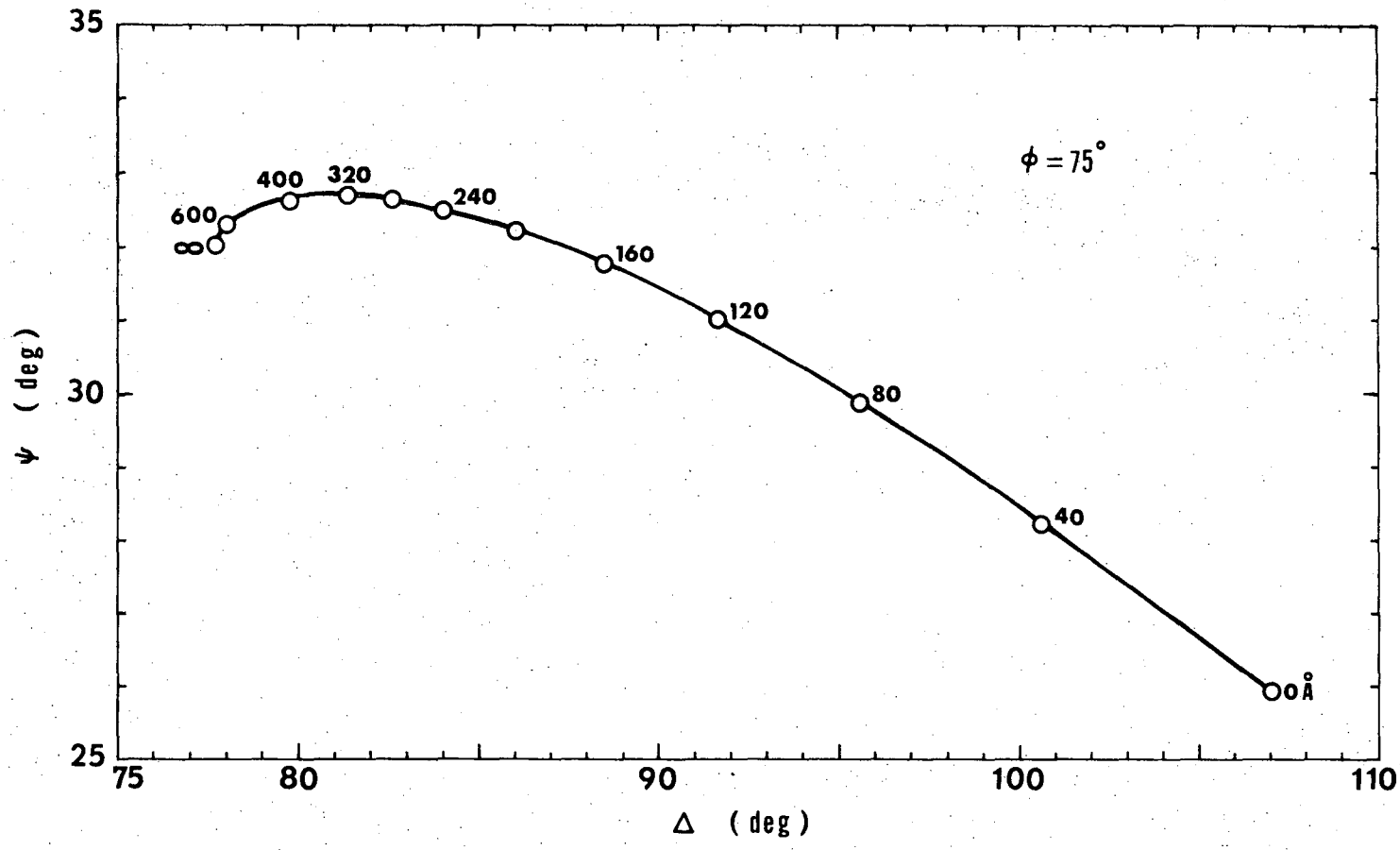

NBL 7110-7412

Fig. 10 Absorbing film on absorbing substrate (nickel on chromium). Values of ψ and Δ calculated for increasing film thickness for wavelength 5461Å, angle of incidence 75°, base constants $n_m = 2.96$, $k_m = 3.45$ and film constants $n_f = 1.4$, $k_f = 2.25$. The curve starts at the bare surface values for chromium and ends at the bare surface values for nickel (i.e. infinitely thick film).

is known*. Sometimes, it is possible to determine both the film thickness and its optical constants by trial and error with the help of high speed conputers.[10,12]

It must be noted that the above exact equations were derived on the basis that both the film and substrate are flat and uniform in properties. In real life, however, this is usually not the case. The film is usually inhomogeneous, rough or only partially covering the substrate. The ellipsometric equations shown above will in this case, predict a fictitious film of homogeneous properties with an average thickness.[13,16] Sometimes, the substrate surface itself may be rough. It this case the above predictions will be in error.[17] Berreman[18] has described a method to treat rough surfaces. Unfortunately, up to the present time, we still lack a satisfactory model to account for the roughness of the surface.

---

*For transparent films, these curves close on themselves, therefore, uncertainty exists if the thickness range is not known. As for an absorbing film, the curve ends at a value corresponding to that of a bare surface of the film material. The thickness of a thick absorbing film cannot be determined by ellipsometry.

III. THE ELLIPSOMETER

The Ellipsometer used is a Gaertner Model L119 Ellipsometer with 14 mm Glan-Thompson prisms. A mercury lamp (General Electric A-H4) with green filter (Gaertner L-541-E combination) was used as light source. The retardation plate is a quarter wave plate for the 5461Å line. The detector is a photomultiplier (RCA 931A, operated at -800v) coupled to a Lock-in-Amplifier (PAR model HR-8) and a chopper (PAR model BZ-1). This reduces the noise considerably and increases the accuracy of the measurements.

IV. ADSORPTION STYDY OF CO ON A PLATINUM SINGLE CRYSTAL

A. Equipment

The components of the Gaertner L119 ellipsometer are mounted on a specially built table which can be connected to the LEED vaccum system. The legs of the table are adjustable in the vertical direction and the table is positioned by the use of spacers and tapered pins. A detailed description of the instrumental arrangement has been given by Muller.[19,20] Figure 11 shows a picture of the system with a schematic sketch given in Fig. 12.

B. Alignment

Due to the configuration of the LEED chamber, a fixed angle of incidence of 45° had to be used. Therefore, the optical axes of the collimator and the telescope should be perpendicular to each other. This optical alignment and the calibration* of the ellipsometer were done independently, with the table separated from the LEED apparatus. The table was then rolled over part of the LEED apparatus. With a flat reflecting mirror attached to a chamber window with double face scotch tape, the collimator and the telescope were then autocollimated against the windows. Any misalignment was corrected by moving the table and adjusting the height of the table legs. The purpose of this is to align the light beam normal to the cell windows. This alignment has been shown by Muller et al.[20] not to be very critical. Misalignment of one degree from normal incidence ($\phi = 0°$) will affect the measured relative phase and amplitude parameters Δ and ψ by only 0.01°. After the components were aligned with the cell windows, spacers were fitted between the

---

*See Appendix II for the alignment and calibration procedures.

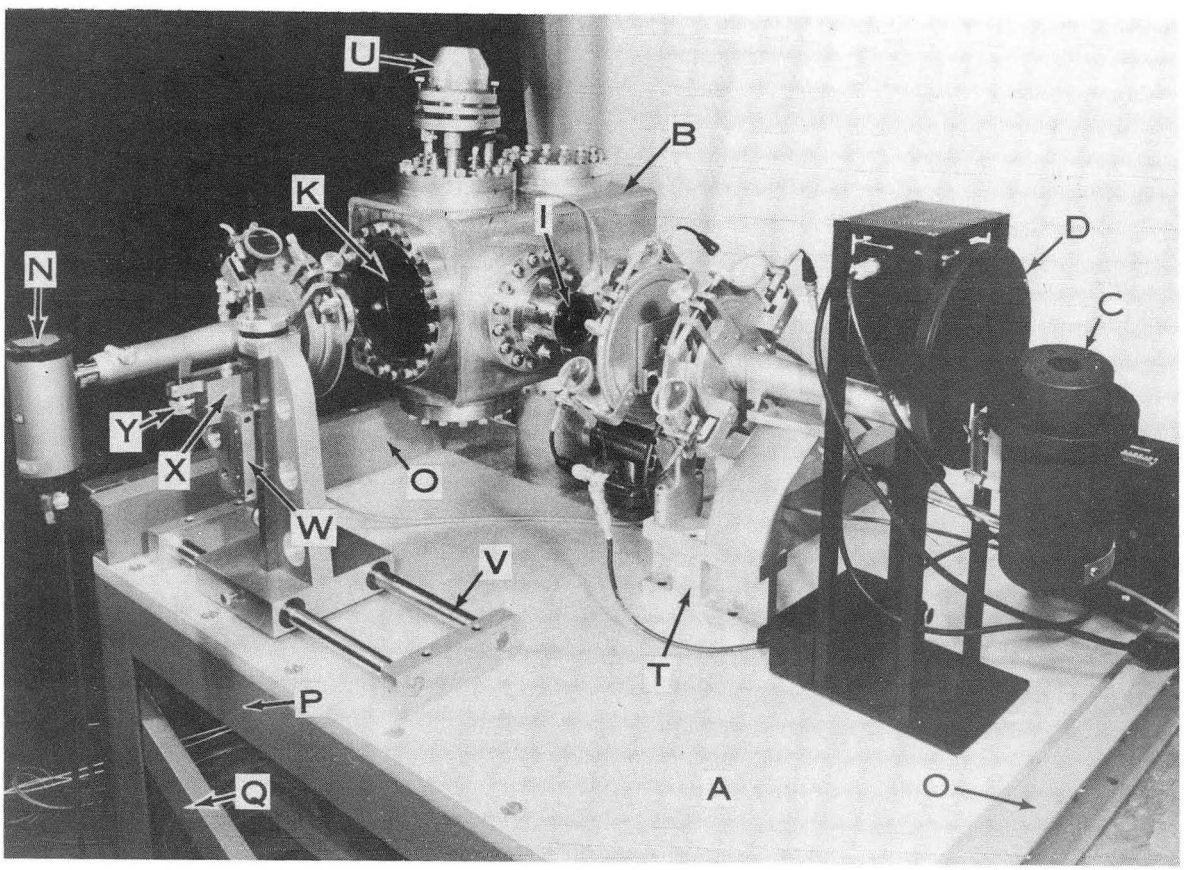

XBB 6712-7040A

Fig. 11

Ellipsometer attached to LEED apparatus[19]

A. Roll-on table which fits on LEED apparatus
B. LEED vacuum chamber
C. Mercury lamp with green filter, 5461Å
D. Light chopper
I. Side window
K. Optical view port on LEED chamber
N. Photomultiplier
O. Stiffening member for table top
P. Welded frame
Q. Braces
T. Spacer for fixed mounting of collimator and compensator assembly
U. Crystal manipulator
V. Rods for lateral translation of analyzer telescope with sleeves for reproducible positioning.
W. Dovetail carrier for vertical translation of telescope
X. Base for rotation of telescope in horizontal plane
Y. Screw for rotation of telescope in vertical plane

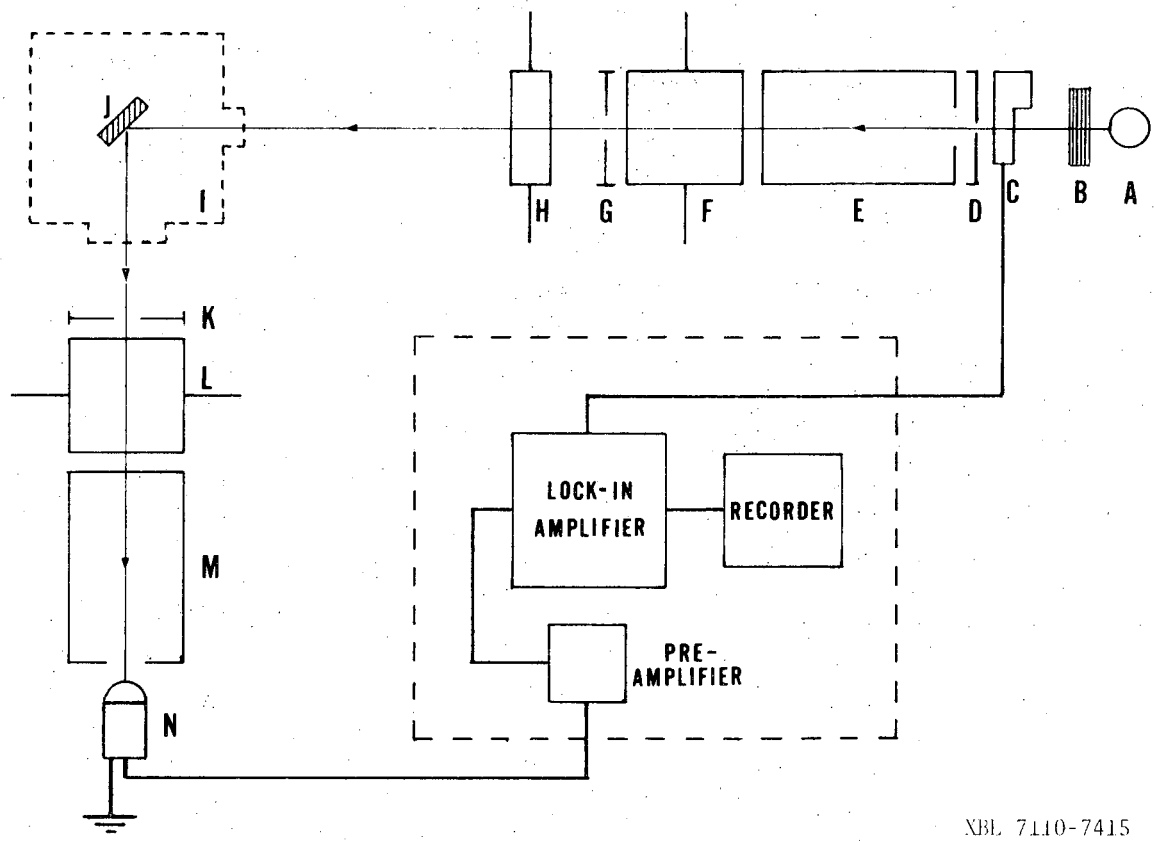

Fig. 12 Schematic of Ellipsometer Setup With LEED Chamber.

A. Light source, mercury lamp (General Electric A-H4)
B. Green filter, 5461Å (Gaertner L-541-E combination)
C. Light Chopper (PAR BZ-1)
D. Pinhole
E. Collimator
F. Polarizer
G,K. Iris diaphragms
H. Compensator, quarter wave plate, 5461Å
I. LEED vacuum chamber
J. Specimen, platinum crystal
L. Analyzer
M. Telescope
N. Photomultiplier (RCA 931A, operated at -800V)

frames of the LEED apparatus and the table. With the help of tapered pins, the table could be rolled back to the same position after it had been removed for baking out the vacuum system. This avoids the repetition of the tedious alignment procedure.

C. Effect of Cell Windows

Although the orientation of the cell windows with respect to the light beam is not very critical, the birefringence and optical inhomogeneities of the glass can be a problem in ellipsometric measurements. Corning 7056 boro-silicate glass (9.5 mm in thickness) was chosen as the glass for the windows for lack of inhomogeneities and birefringence. Table I shows the effect of the cell windows on the measured values of Δ and ψ. A marked increase in birefringence due to mechanical tightening of the windows was noted. This effect on Δ and ψ caused by the cell windows was used as a correction factor for later measurements. The thermal birefringence caused by the heating of the crystal is expected to be fairly small compared to that caused by mechanical stress, and was neglected.

D. Specimen

The substrate used for the measurements was a platinum single crystal cut at 9.5° off the (111) face.

E. Bare Substrate

Before the adsorption of CO can be studied by ellipsometry, the optical constants of the substrate must be known at the temperature to be employed.

For the measurement of the optical constants of the platinum crystal, the vacuum system was first baked out. The ellipsometer was then rolled

Table I. Effect of window birefringence and optical inhomogeneities on ellipsometric measurement of platinum crystal surface ($\phi = 45°$, wavelength = 5461Å).

	Measured Values		Difference from no Window Measurement	
	Δ	ψ	$D\Delta$	$D\psi$
Without Windows	165.22	41.24		
With Windows (bolts not tightened)	170.82	41.36	5.60	0.12
With Windows (bolts tightened)	175.40	41.77	10.18	0.53
With Windows (bolts tightened and chamber vacuum on)	174.86	41.97	9.64	0.73

onto the LEED apparatus and the platinum crystal aligned with the light beam. Measurements were made as the crystal cooled off from around 1000°C by adjusting the heating current. To calculate the optical constants n and k from measured values of Δ and ψ the computer program "MOC"* was used. A grid of ψ versus Δ with n and k as parameters (see Fig. 13) covering the expected values of platinum was also constructed so that the values of n and k could be determined graphically. The construction of the grid is accomplished by the use of computer program "MER".*

Figure 14 shows the change in Δ of the platinum crystal with temperature. The measurements were made at a vacuum of around 10^{-8} torr. As can be seen from the graph, the curve starts to bend down at around 400°C. If one assumes that the temperature dependence curve should extrapolate as shown in the graph, then the drop off must be due to surface contamination, (which is very possible with the low vacuum achieved). Auger electron spectroscopy (AES) measurements was applied and a carbon peak did show up at about 300°C. The carbon peak height increased as the temperature dropped. A comparison of the change of Δ with respect to the extrapolated clean surface values and the Auger carbon peak height is shown in Fig. 15. Good correlation is exhibited between the two curves. In addition, it shows that ellipsometry is more sensitive than AES to surface impurities.

Auger electron spectroscopy is a useful method to identify surface impurities. It is however, unable to determine the absolute degree of coverage. Low energy electron diffraction (LEED) has often been used in conjuction with AES to account for the surface coverage. The interpretation of LEED data, however, is usually not straightforward. Since

*See Appendix I.

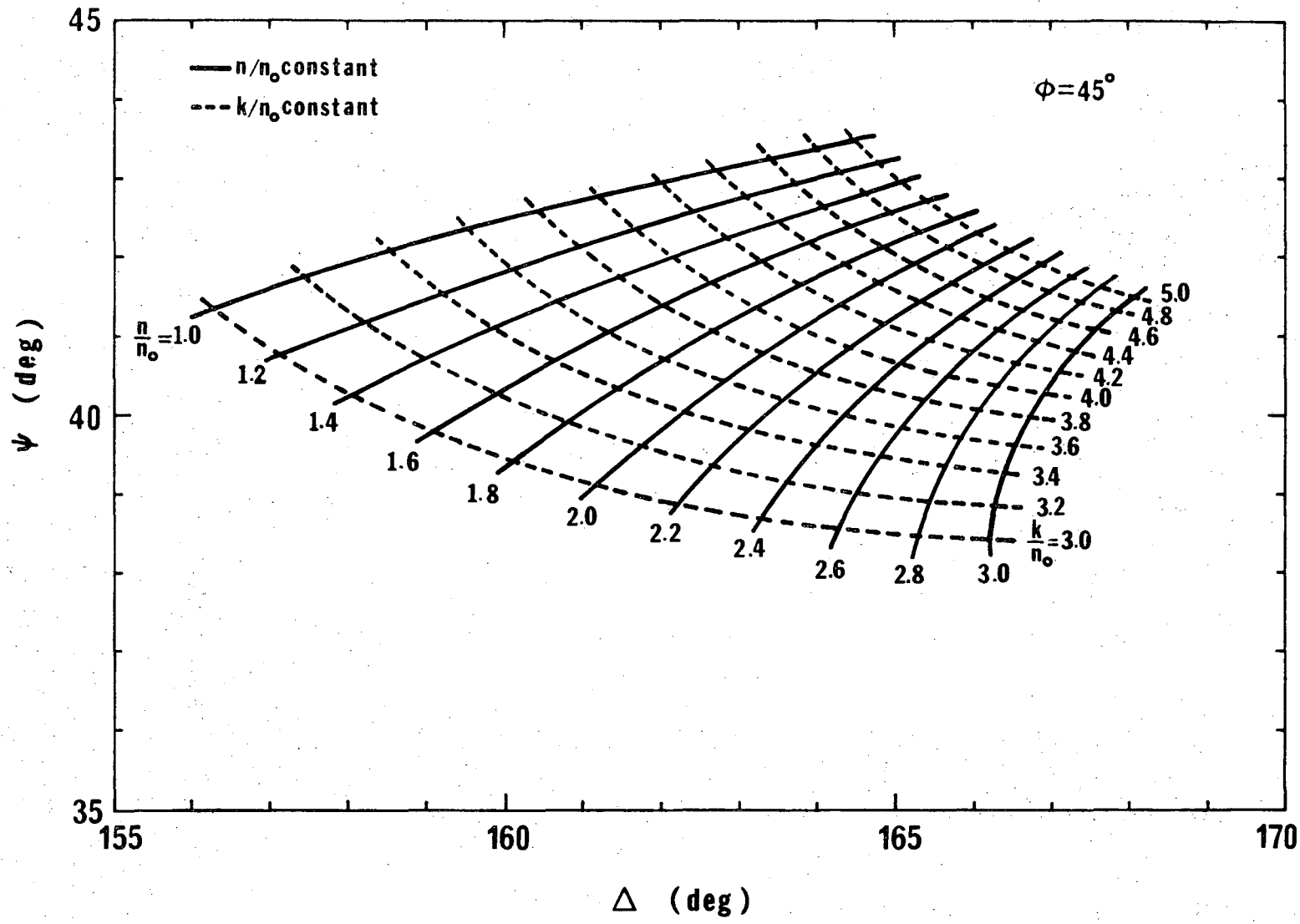

XBL 7110-7424

Fig. 13 Ellipsometric parameters ψ (arctangent of relative amplitude attenuation) and Δ (relative phase change) for reflection from a bare metal surface of optical constants n-ik. Angle of incidence, 45°.

0 0 0 0 3 6 0 7 1 1 4

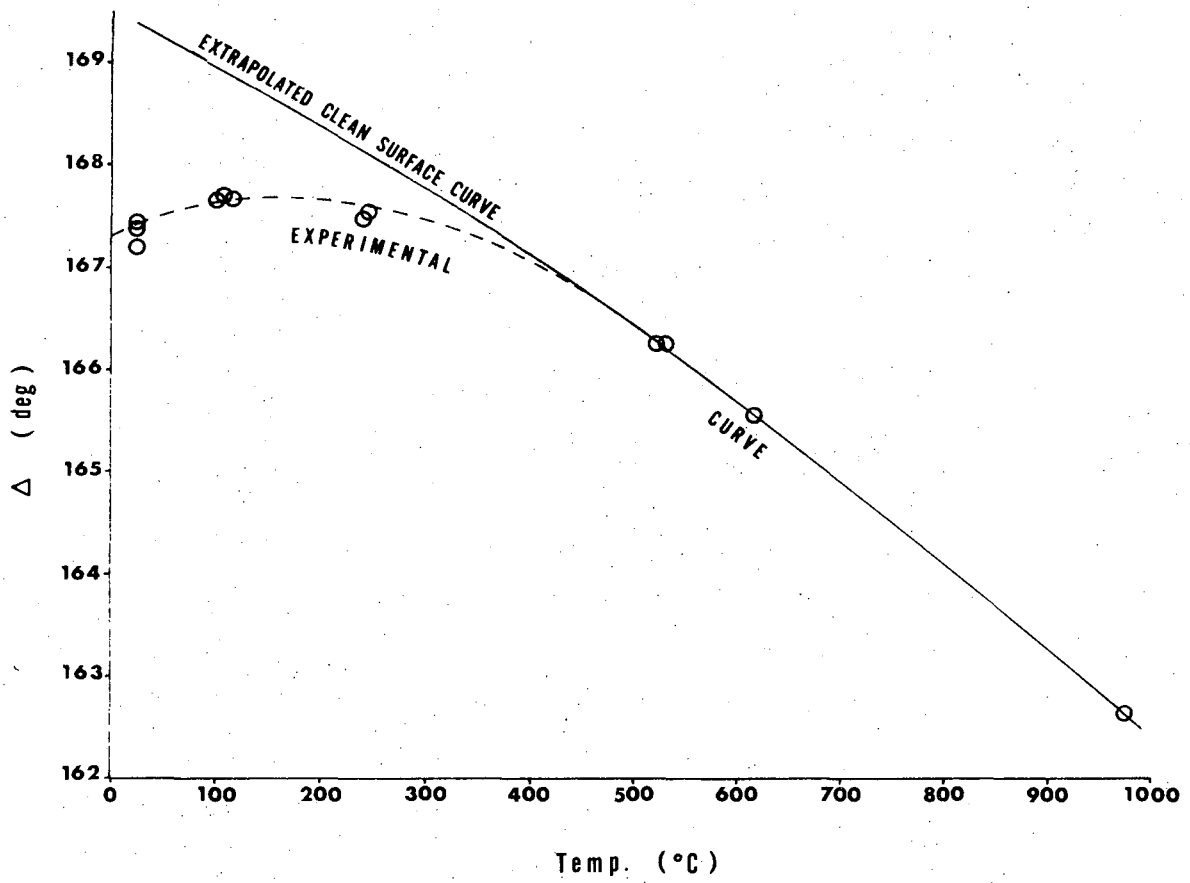

XBL 7110-7403

Fig. 14 Change in measured values of Δ with temperature. Specimen is platinum single crystal cut at 9.5 degrees off the (111) face. Pressure at 10^{-8} torr. Angle of incidence 45°.

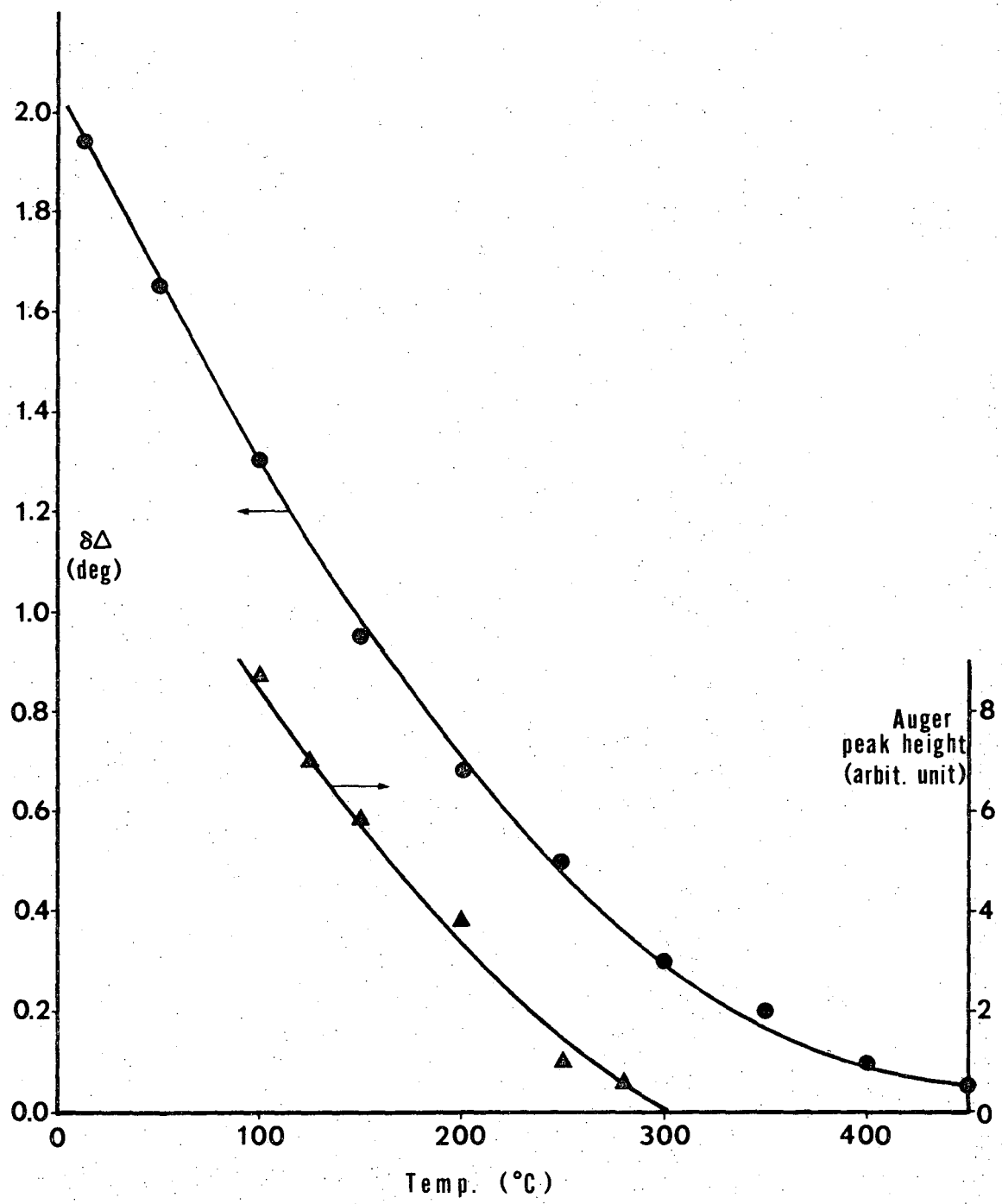

XBL 7110-7404

Fig. 15 Comparison of Ellipsometric measurement and Auger measurement.
δΔ is the difference of the measured Δ to clean surface Δ values.

the results of ellipsometric measurements are also coverage dependent, the combination of AES, LEED and ellipsometry can be very fruitful in surface research.[21,22]

The parameter ψ, varies only about 0.6° with temperature from 1000°C to room temperature. The build up of the contaminant layer contributes a change of about 0.2°.

It must be mentioned that no quantitative correlation could be made between AES and ellipsometric measurements in the present investigation. To make a quantitative correlation, we must be able to obtain clean surface data at below 400°C. This can only be accomplished with a vacuum higher than the 10^{-8} torr employed here. In addition, the optical constants of the adsorbant should be known to eliminate one variable. However, in the present case, the optical constants of the contaminant layer were unknown.

F. Chemisorption of Carbon Monoxide

Since the platinum crystal seemed to be contaminated at below 400°C, the adsorption of CO was studied at 410°C. After the vacuum chamber had been baked out, the platinum crystal was cooled down to and maintained at 410°C. Carbon monoxide was then admitted into the chamber and ellipsometric measurements (only two zones were used*) were taken continuously. The pressure in the chamber was 10^{-7} torr after the admission of CO (10^{-8} torr before admission). However, no apparent change was observed either in Δ or ψ even after 10 minutes. The LEED pattern taken immediately afterwards did, however, show coverage of CO

*Because of the lengthiness of a four-zone measurement, it is not practical to apply it to the following of film growth. McCrackin[11] has shown that two-zone average will suffice in reducing the errors.

of at least one monolayer. This discrepancy between ellipsometric measurement and LEED observation could be explained if: a) a CO layer was already present before the measurement by ellipsometry, or b) the changes in Δ and ψ produced by the CO film were too small to be observed.

Calculations were made to see what charges of Δ and ψ produced by the CO film can be expected at 45° angle of incidence. The result of the calculations is shown in Fig. 16. The refractive index used for the CO film is 1.2. Since no refractive index data was available for CO, this value is calculated from the molar refractivity, R,[23] using the Lorentz-Lorenz equation

$$R = \frac{n^2 - 1}{n^2 + 2} \frac{M}{\rho} \tag{41}$$

where, n = refractive index

M = molecular weight

ρ = density in gm/cc

The value of R was calculated from the contribution of atomic refractivity for sodium line (D-line). Table II gives the values used to calculate the refractive index of CO. It must be noted that n thus calculated is just an approximation. However, the use of n = 1.2 should give a fairly good estimation of the effect of a CO film on the ellipsometric parameters Δ and ψ. The accuracy of the film refractive index is not too critical for the determination of film thickness from changes in Δ and ψ as shown by Archer and Gobeli.[24]

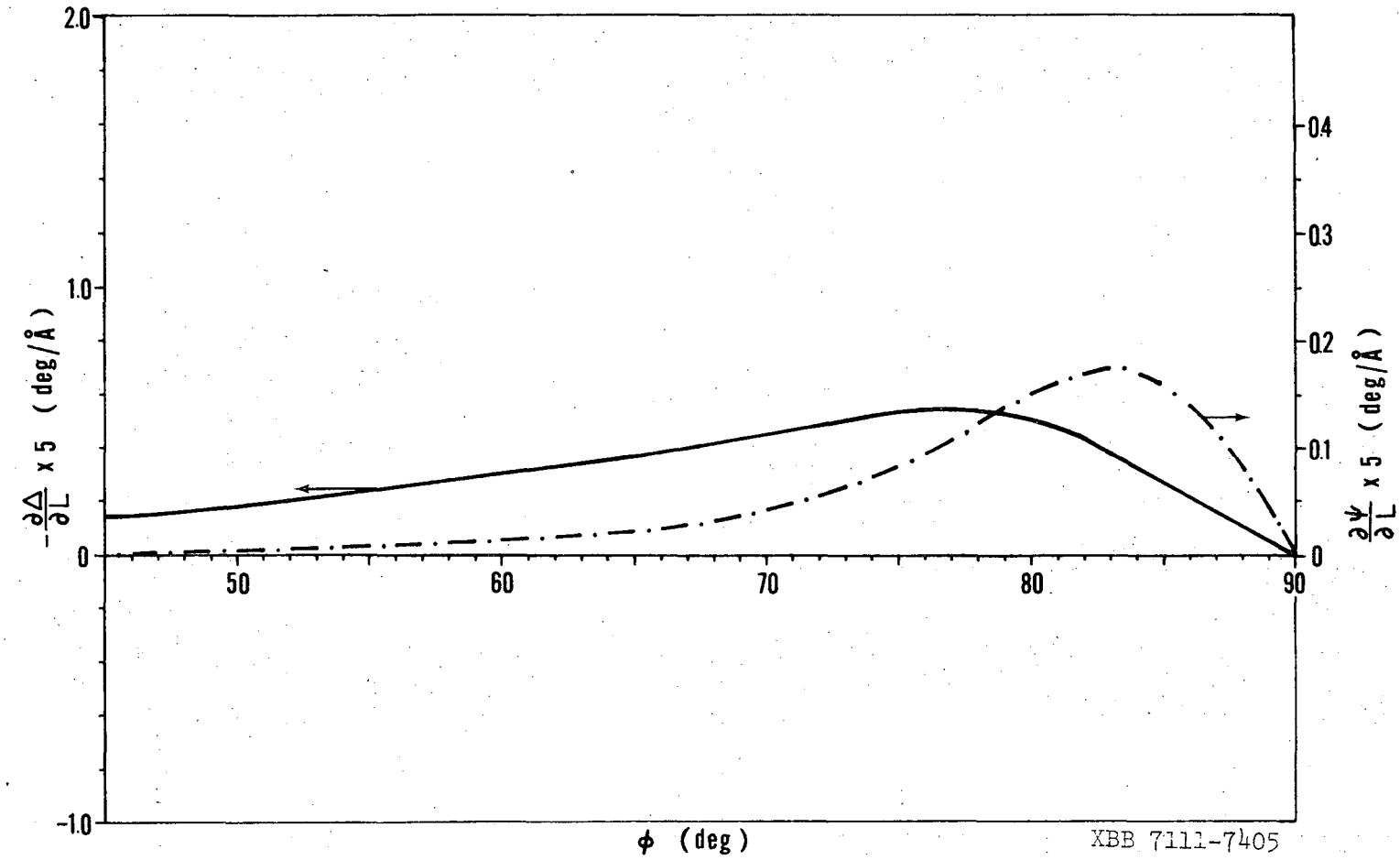

Fig. 16 Sensitivity of Δ and ψ to change in Film thickness at Different Angle of Incidence (carbon Monoxide on Platinum). Values calculated for wavelength 5461Å, film constants $n_f = 1.2$, $k_f = 0$ and substrate constants $n_m = 2.86$, $k_m = 4.42$. Scale calculated for the change of Δ and ψ to a 5Å film.

$$\left(\text{i.e. } \frac{\delta\Delta}{\delta L} = \frac{\Delta_{5\text{Å film}} - \Delta_{\text{no film}}}{5 - 0}\right)$$

Table II. Constants used in the calculation of carbon monoxide refractive index.

Compound	C	=O	CO
Atomic Refractivity values[23] for D-line	2.418	2.211	
Molar refractivity, R(cm^{-3})			4.629
Molecular weight, M(gm/mole)			28
Density,[31] ρ(gm/cm^3)			0.803

The calculation of the curve shown in Fig. 16 is accomplished by using the computer program "LAYER".* The calculation assumed that a film of 5Å is on the surface, which is at least a monolayer coverage of CO (assuming that the molecules are closely packed cubes on the surface.). The difference of the values of Δ and ψ for 5Å film to film free values divided by 5 gives the sensitivity of Δ and ψ to changes in film thickness. This is justified because the linear approximation of Δ and ψ to film thickness L usually holds well in this range of thickness.[25]

As one can see from Fig. 16, the change of Δ due to a 5Å film of CO at 45° angle of incidence is only 0.15°. The effect on ψ is only 0.001°.** Theoretically, the ellipsometer will not be able to detect the change in ψ, but a change of about 0.15° in Δ (if the CO film reaches 5Å thick) would be detectable (the resolution of the ellipsometer is 0.01°). However, due to an unusually high noise level encountered

---

*See Appendix I-D.

**ψ is less sensitive to changes in film thickness than Δ and often only changes in Δ are measurable.

during the measurements and the probability that the CO film was less than 5Å thick, the ellipsometer was unable to resolve the changes in Δ produced by the film. At 77° angle of incidence (optimum angle of incidence), however, the sensitivity of Δ to changes in film thickness is almost four-fold that at $\phi = 45°$. The effect on ψ also goes up to about 0.1°. The angle of incidence at which ψ reaches a maximum coincides with the principal angle of incidence.

The sensitivity of Δ to changes in CO film thickness on platinum is at its maximum at about 77° angle of incidence. When n_m, the real part of the refractive index of the metal, is not very large and k_m, the imaginary part, is large as compared to n_m, a low sensitivity of Δ to changes in dielectric film thickness can be expected. This is so even at optimum angle of incidence (sensitivity about 0.1 deg/Å or less). An example of CO film, this time on silver substrate (n_m small and k_m large), is shown in Fig. 17. When n_m is large and k_m is small as compared to n_m, the sensitivity of Δ to changes in dielectric film thickness will be much higher at optimum angle of incidence. A good example was given by Archer[26] for germanium and silicon substrates. Figures 18 and 19 show the two sensitivity curves scaled for 5Å CO film. The change in Δ at maximum sensitivity is larger, especially for silicon substrate when k_m is much smaller than n_m. Another interesting thing is the abrupt sign change of the Δ curve. The sensitivity curve of Δ has actually two maxima with the higher maximum occurring at a smaller angle of incidence. The principal angle of incidence lies between these two maxima (at the maximum of the ψ curve). Judging from the results of a series of calculations, in which different substrate optical constants were employed, it appears that the transition from the Δ curve

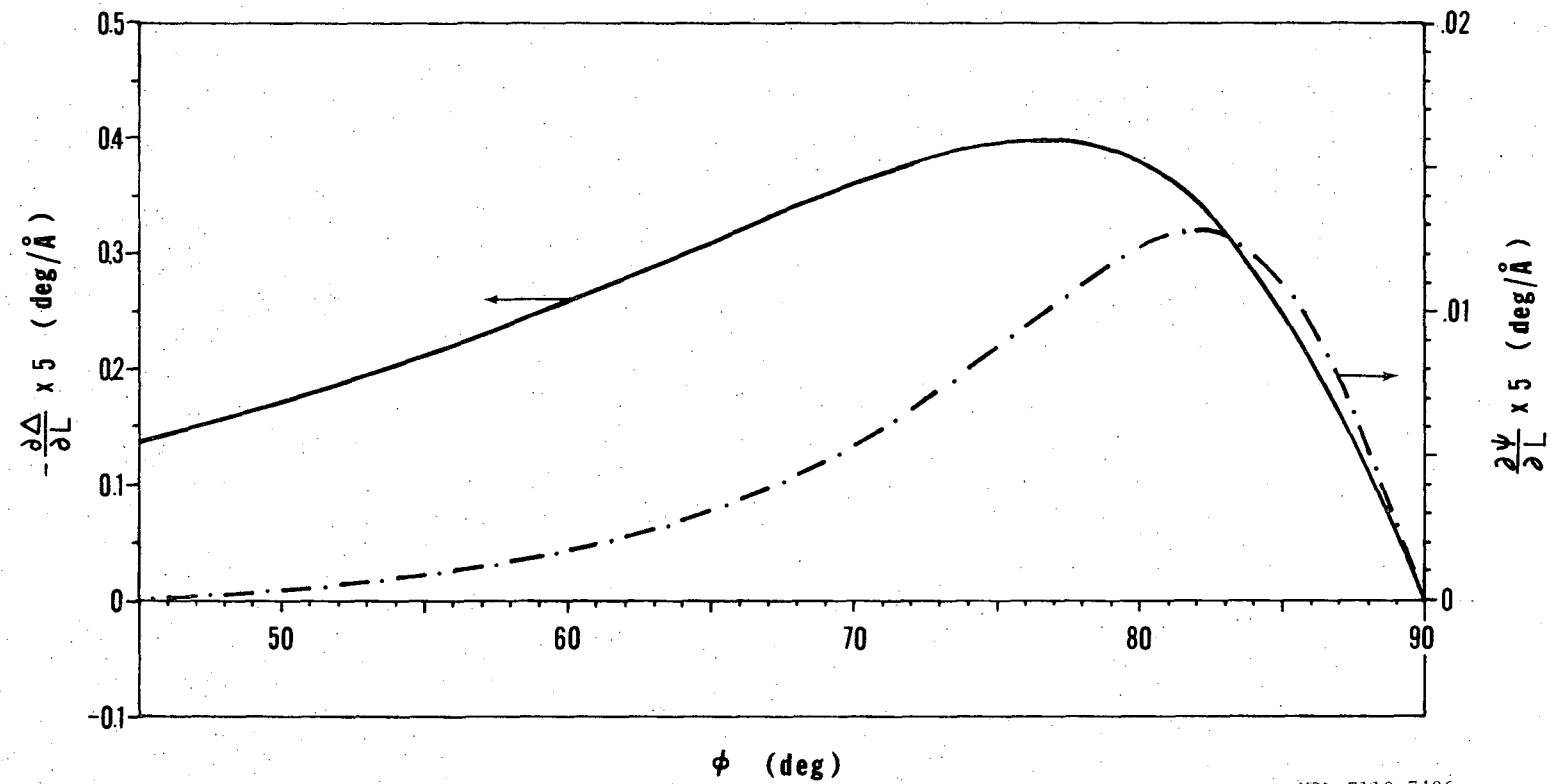

XBL 7110-7406

Fig. 17 Sensitivity of Δ and ψ to changes in film thickness at Different Angle of Incidence (Carbon Monoxide on Silver). Values calculated for wavelength of 5461Å, film constants $n_f = 1.2$, $k_f = 0.0$ and substrate constants $n_m = 0.2$, $k_m = 4.0$. Scale calculated for the changes of Δ and ψ to a 5Å film.

Note: The $\frac{\delta\Delta}{\delta L}$ curve may be in small error, since the approximation of linear change in Δ to film thickness does not hold well when n_m is small.

0 0 0 0 3 6 0 7 1 1 8

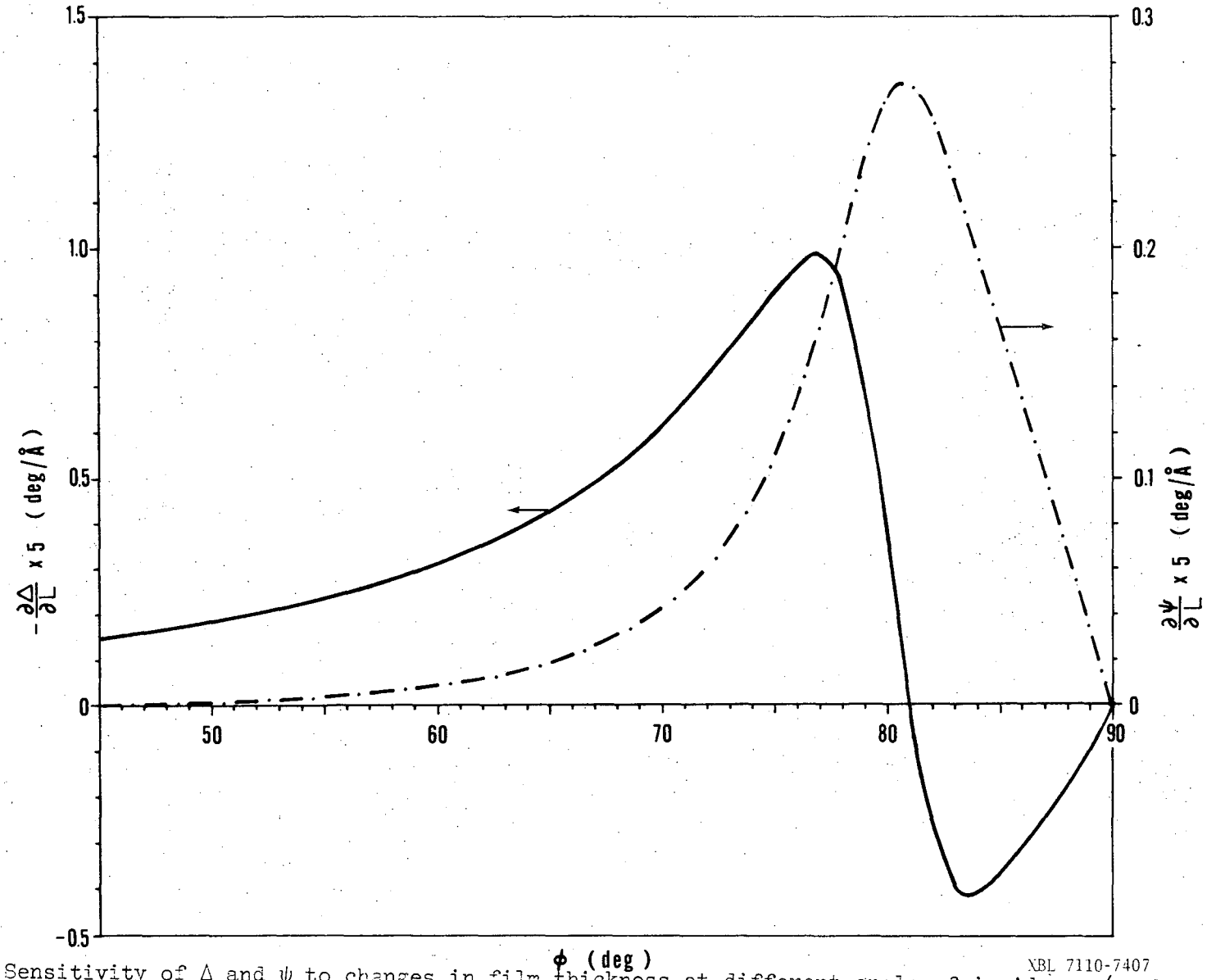

XBL 7110-7407

Fig. 18 Sensitivity of Δ and ψ to changes in film thickness at different angle of incidence (carbon monoxide film on germanium substrate). Values calculated for the wavelength of 5461Å, film constants $n_f = 1.2$, $k_f = 0$ and substrate constants $n_m = 5.1$, $k_m = 1.9$. Scale calculated for the change of Δ and ψ to a 5Å film.

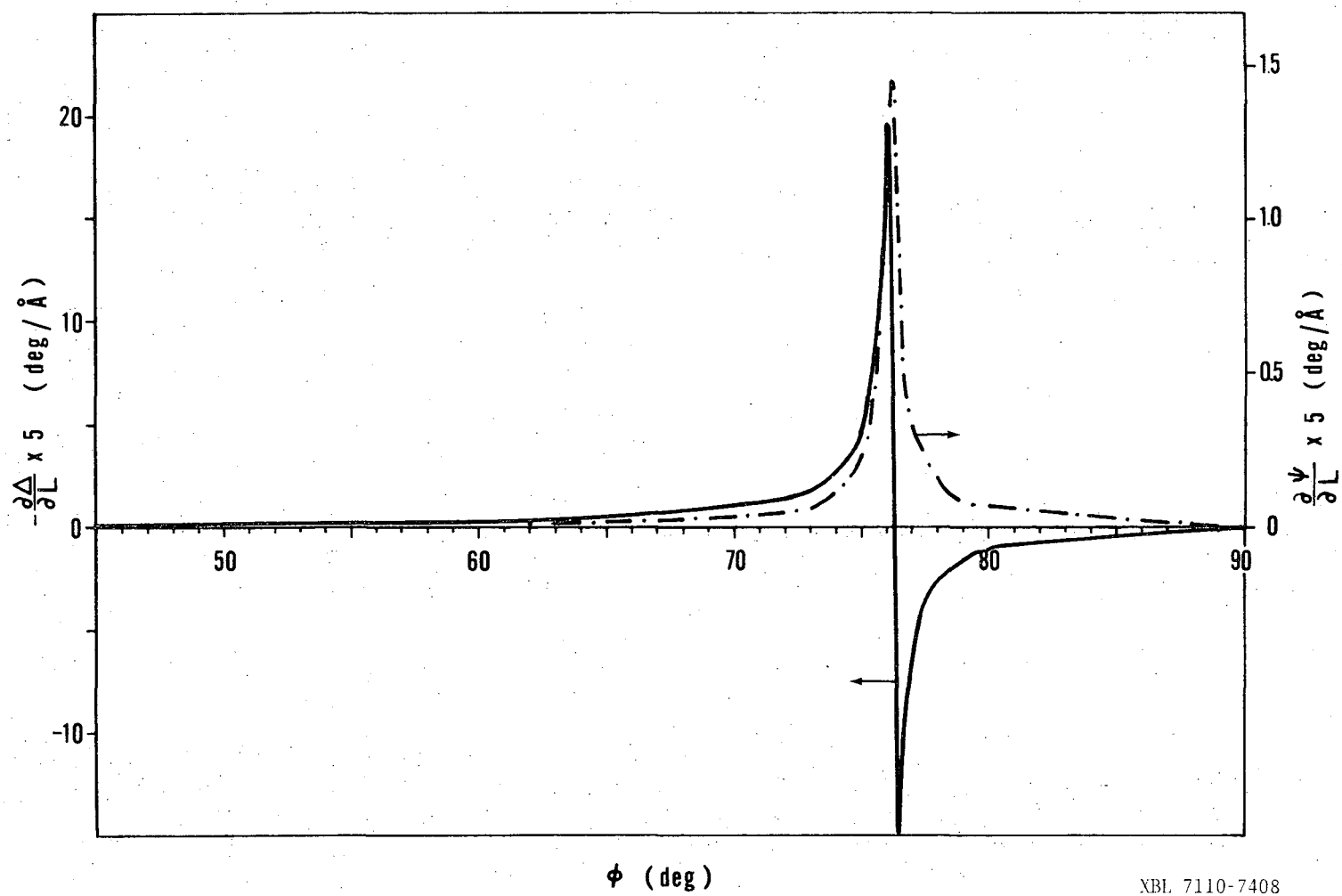

XBL 7110-7408

Fig. 19 Sensitivity of Δ and ψ to changes in Film Thickness at Different Angle of Incidence (Carbon Monoxide on Silicon). Values calculated for the wavelength of 5461Å. Film $n_f = 1.2$, $k_f = 0$ and substrate constants $n_m = 4.05$, $k_m = 0.028$. Scale calculated for the change of Δ and ψ to a 5Å film.

Note: The $\frac{\delta\psi}{\delta L}$ curve may be in small error since the approximation of linear change in ψ to film thickness does not hold well when k_m is small.

0 0 0 3 6 0 7 1 1 9

in Fig. 17 to that shown in Fig. 18 for a transparent film occurs at about $n_m/k_m = 1$. When this ratio is less than one, the curve has only one maximum. When the ratio is larger than one, two maxima in sensitivity occur. Winterbottom[5] has given some criteria for the dependence of the shape of the Δ and ψ sensitivity curves on the optical constants of the film and substrate.

The sensitivity of Δ to changes in film thickness is small for the study of gas adsorption on a platinum substrate at a 45° angle of incidence (unless a thick absorbed film is deposited). A vacuum chamber is now under design so that an angle of incidence of 75° can be used for the ellipsometric measurements. The ellipsometric study of the chemisorption of CO on platinum should be repeated with this chamber.

V. STUDY OF LIQUID FILMS ON A PLATINUM ELECTRODE

A. Equipment

1. Cell

In order to study liquid films on electrodes, a cell was constructed which allows the formation of a film on an electrode by draining the liquid in which the electrode had been totally immersed. The cell construction has been described in detail by Turney.[27] A top sectional view and a side sectional view of the cell are shown in Fig. 20a and 20b. The glass windows of the cell are oriented at 75° to each other. Therefore, an angle of incidence of 75° can be used for the measurement. This angle is close to the principal angle of incidence and is in the sensitive region for the measurement of films on a platinum surface. The outside of the glass windows is coated with an anti-reflection coating to minimize the reflection from the window surfaces which may cause an error in the measurements. Unlike Turney, during the present experiments, the nuts holding the windows to the cell were tightened to only 20 in.-lb which was found to be sufficient to prevent the cell from leaking. Mechanical stress imposed on the windows by the tightening of nuts will cause birefringence in the windows. The smaller the torque applied to the nuts, the lower the birefringence in the windows.

2. Liquid Filling and Draining System

The cell is filled and drained by gravitational flow. The cell's filling and draining system has also been described by Turney.[27] A diagram of the flow system is shown in Fig. 21.

3. Cell Atmosphere Control System

In order to keep a stable film on the platinum electrode, it is necessary to keep a saturated atmosphere in the cell. Nitrogen saturated

Fig. 20 a. Side sectional view of liquid film experimental cell.
b. Top sectional view of liquid film experimental cell.[27]

1. Studs for clamping windows to cell body
2. Gas inlet
3. Gas outlet
4. Clamp and electrical contact
5. Gas outlet for counter-electrode chamber
6. Main chamber
7. Glass capillary for reference electrode
8. Platinum electrode
9. Liquid drain
10. Counter-electrode
11. Counter-electrode chamber
12. Liquid inlet
14. Passage between chambers
15. Weir to establish liquid level
16. Frame to hold windows
17. Plate glass windows

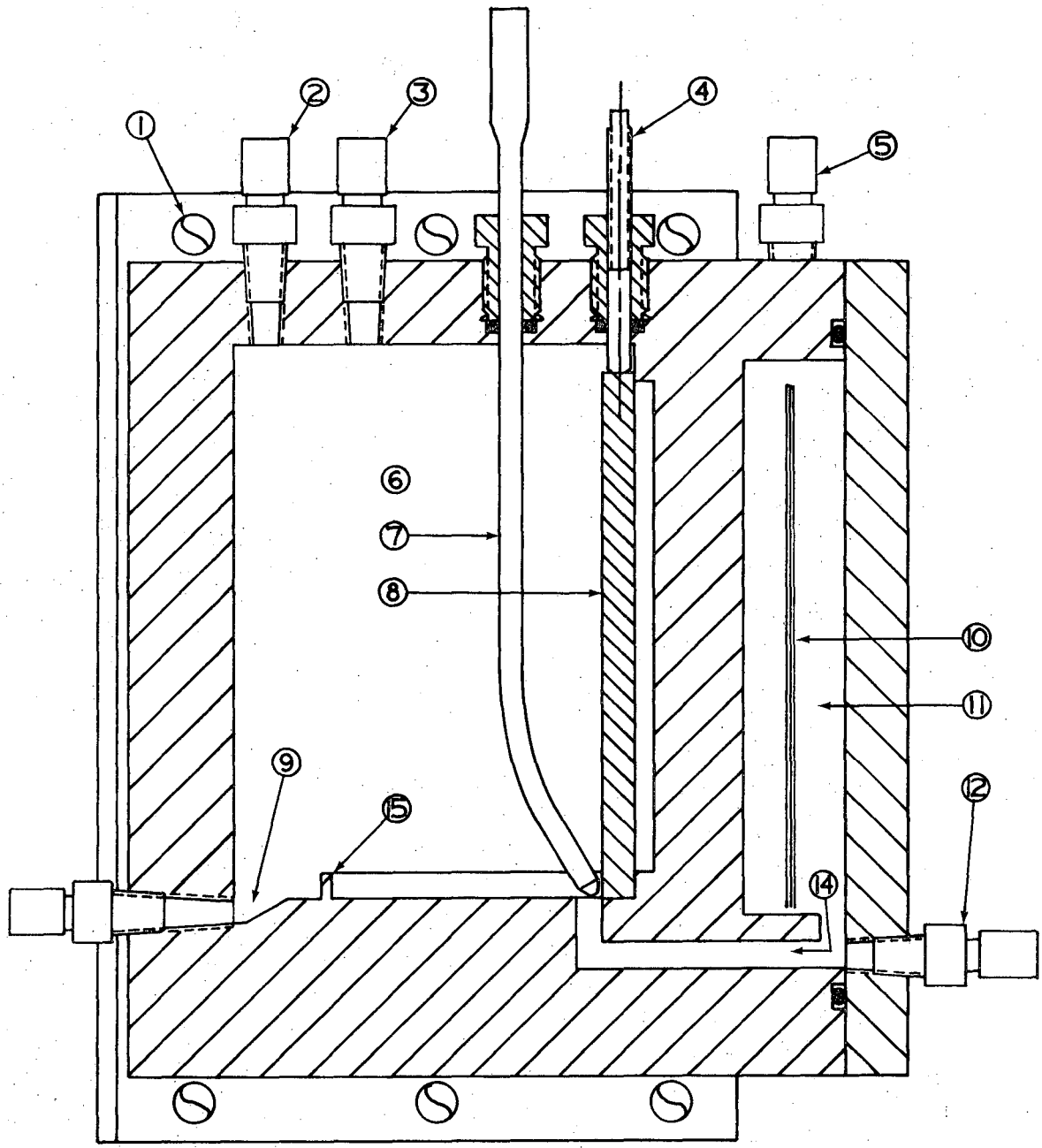

XBL 711-6409

Fig. 20a

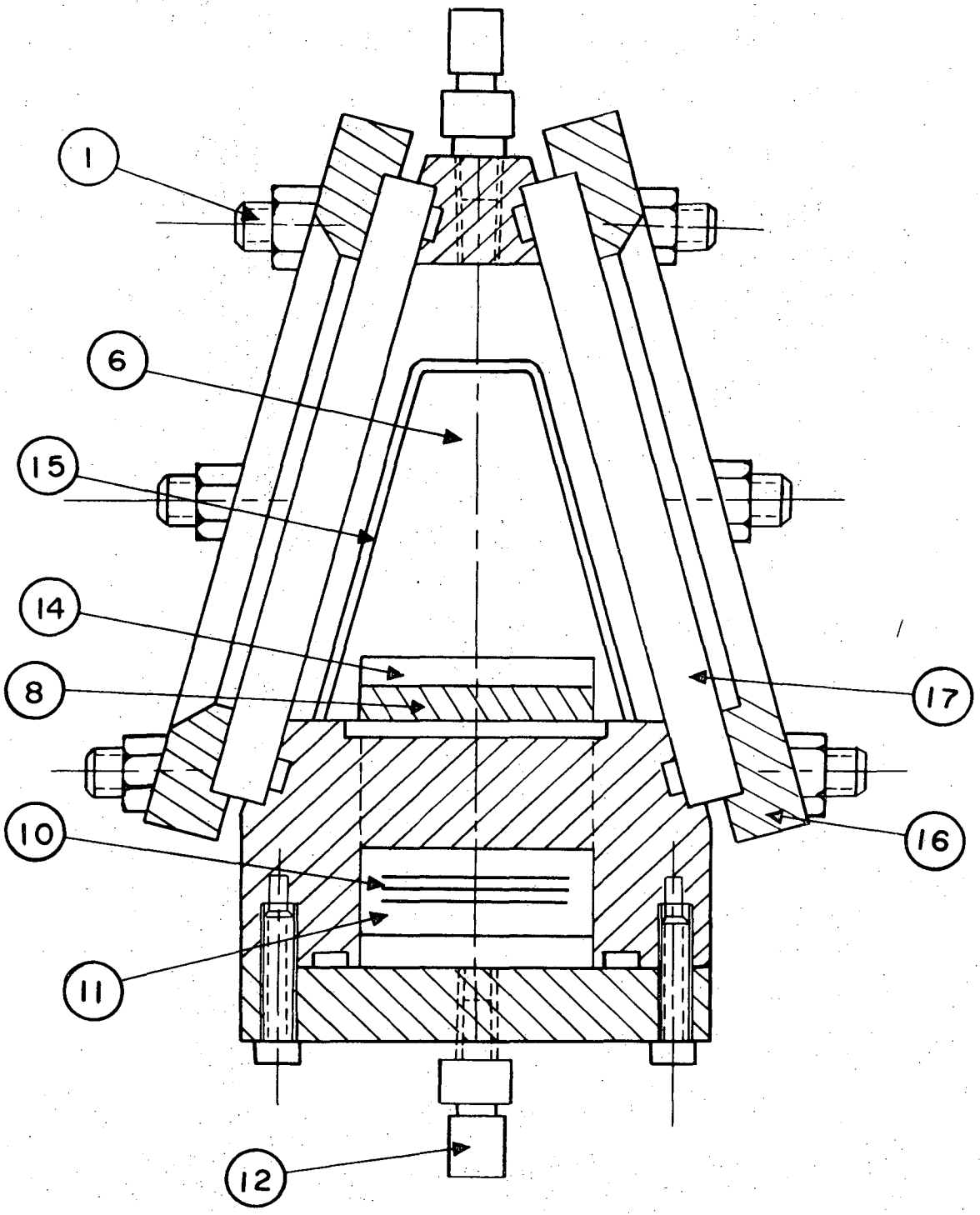

XBL711-2544

Fig. 20b

with the film solution was fed to the cell to control the atmosphere and to keep carbon dioxide and oxygen out of the cell. These gases may react with the film or oxidize the electrode surface. The gas saturation system has been described by Turney[27] and a sketch of it is shown in Fig. 22.

4. Optical System

An ellipsometric setup allowing variable angle of incidence measurements was used for the study. The polarizer parts and the compensator are stationed on a fixed arm, while the analyzer parts rest on a movable arm which can be rotated around an axis to change the angle of incidence. These arms have been extended away from the sample table in order to accommodate the cell. The sample table with three screws for tilting movement, was mounted on a motor driven dovetail carrier which has a vertical movement of about 11 cm. This movement allows measurements to be made along the electrode. A photograph of the setup with the cell in place is shown in Fig. 23. A simplified schematic sketch of the system is shown in Fig. 24.

B. The Platinum Electrode

The platinum electrode was constructed from a platinum sheet (10 cm × 4 cm × 0.05 cm) soldered to a 1/4 in. thick stainless steel backing. The surface of the platinum was optically polished. Except for a small area on the top, the sides and back of the electrode were coated with Kynar,* which is highly corrosion resistant under most acid or base environment. Electrical connection was made with a stainless steel (316) pin in contact with the bare area on the top edge. This pin also serves

*Trade mark of Pennsalt Chemical Corporation for a Vinylidene Fluoride polymer.

Fig. 21

Liquid filling and draining system.[27]

1. Dust and carbon dioxide filters
2. 500 ml flasks containing solution used for cathodic cleaning of electrode
3. 500 ml flasks containing experimental solution
4. System flushing drain
5. Experimental cell
6. Drain vent
7. Flexible connecting line
8. Liquid drain

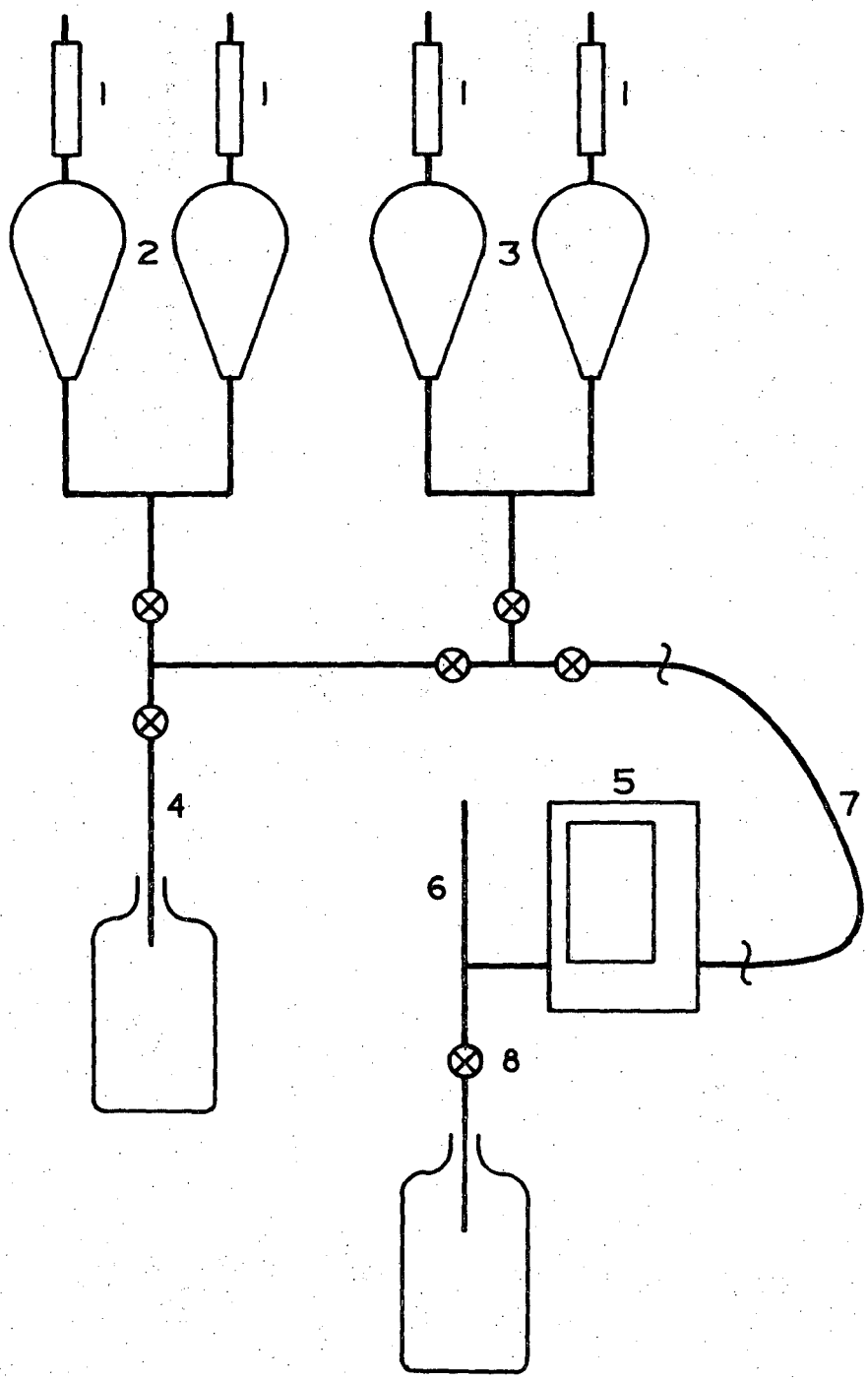

XBL 709-6668

Fig. 21

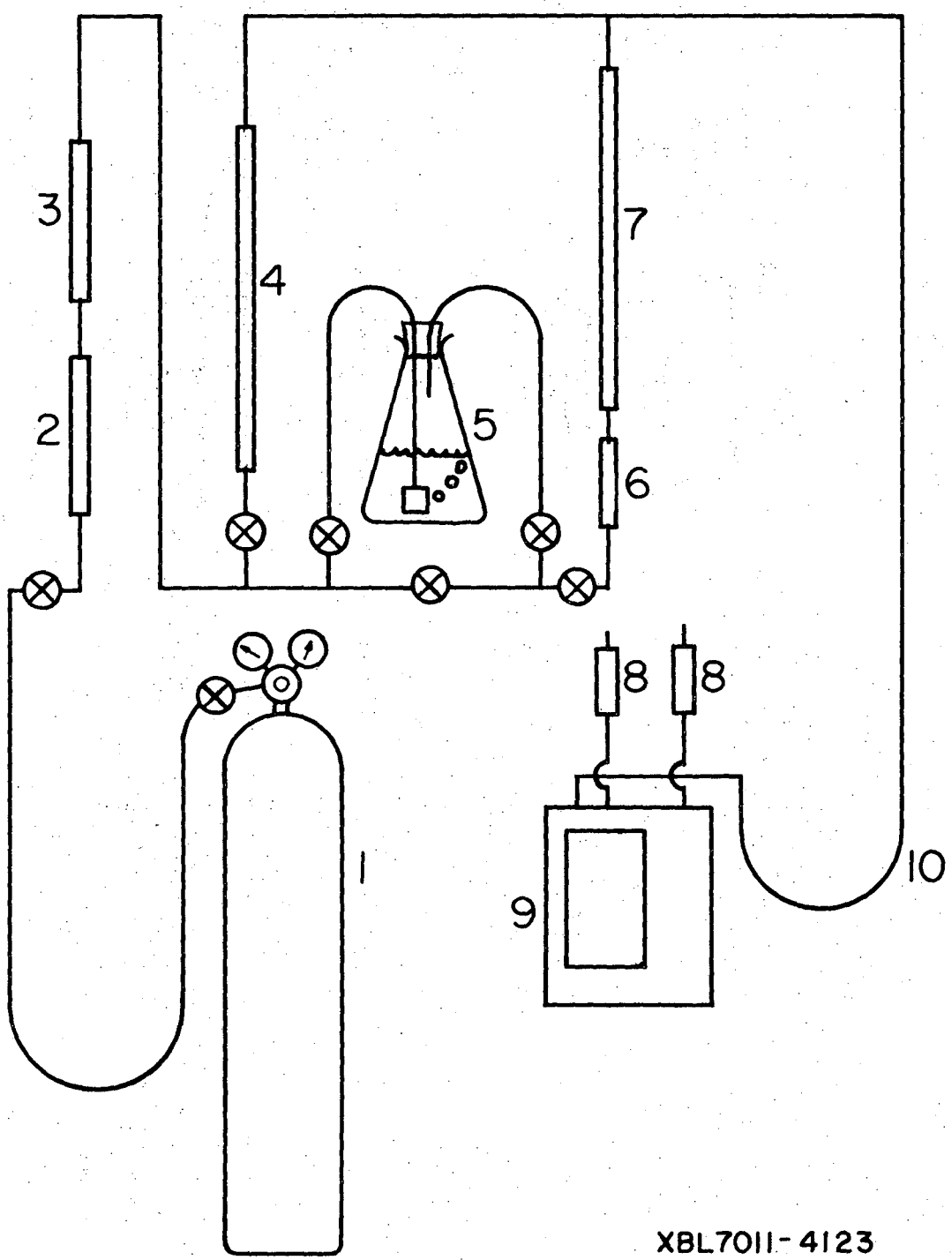

Fig. 22

Cell atmosphere control system.[27]

1. Gas supply cylinder (N_2)
2. Drying tube
3. Glass wool dust filter
4. Dry gas flow rate rotameter
5. Sparger with same solution as in experimental cell
6. Glass wool mist filter
7. Saturated gas flow rate rotameter
8. Dust and carbon dioxide filter
9. Liquid film experimental cell
10. Flexible connecting line

0 0 0 0 3 6 0 7 1 2 4

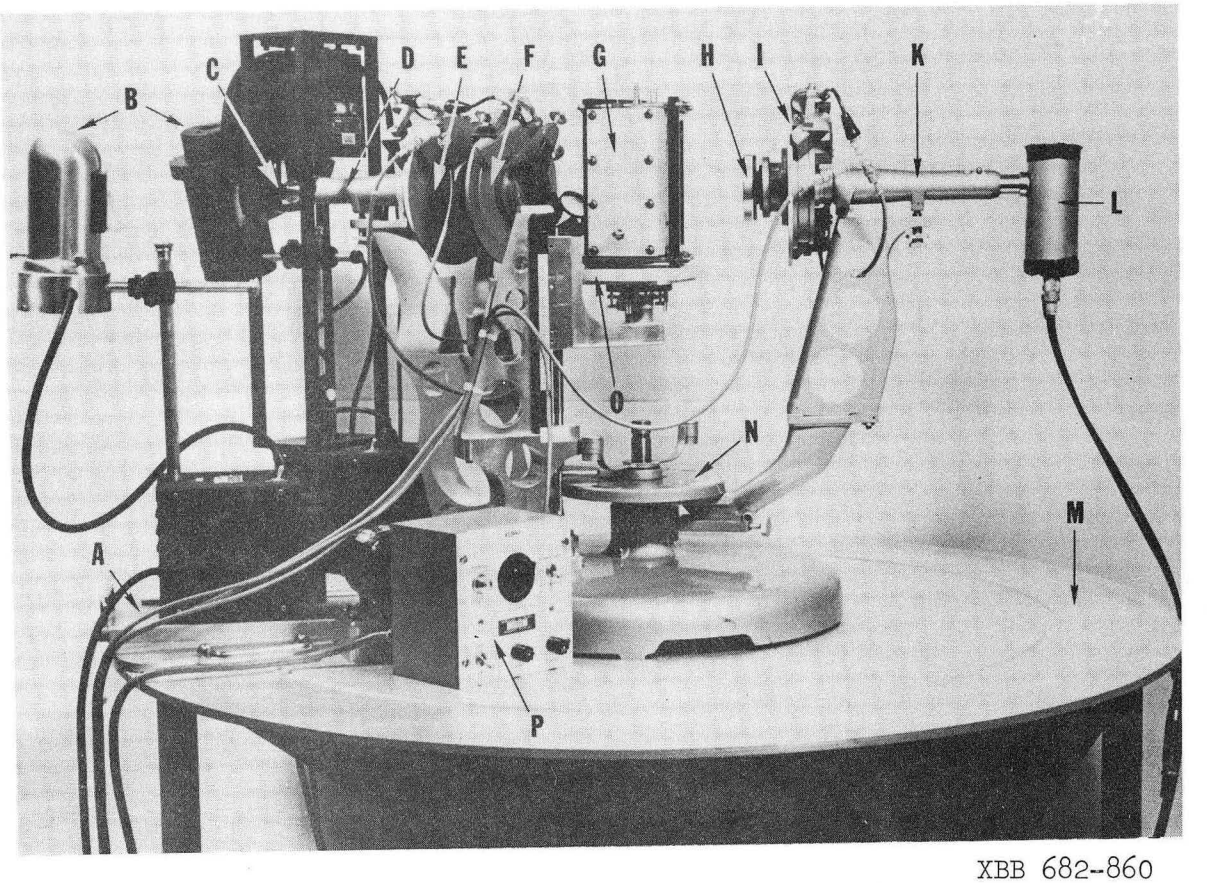

XBB 682-860

Fig. 23

Modified ellipsometer with experimental cell in place.[84]

A. Moveable carriage for light source
B. Exchangeable monochromatic light source
C. Light chopper and generator of reference signal for phase-sensitive detector
D. Collimator tube with pinhole entrance
E. Polarizer circle with illuminated scale
F. Compensator circle with illuminated scale
G. Experimental cell
H. Iris diaphragm for control of observed specimen area
I. Analyzer circle with illuminated scale
K. Telescope tube with pinhole exit
L. Photomultiplier
M. Table
N. Angle of incidence circle
O. Sample table with vertical movement
P. Motor drive control unit for vertical movement of sample table

Fig. 24

Simplified schematic of ellipsometer setup with the cell in place.[85]

A. Light source
B. Pinhole
C. Collimator lens
D. Polarizer prism
E,J. Iris diaphragms
F. Quarter wave plate
O,I. Cell windows with anti-reflection coatings to minimize parasitic beam (---)
H. Reflecting specimen (platinum electrode)
K. Analyzer prism
L. Telescope lens
M. Telescope pinhole serves to block most of the parasitic beam (---)
N. Photomultiplier
___ Main beam
--- Parasitic beam

0 0 0 0 5 6 0 7 1 2 5

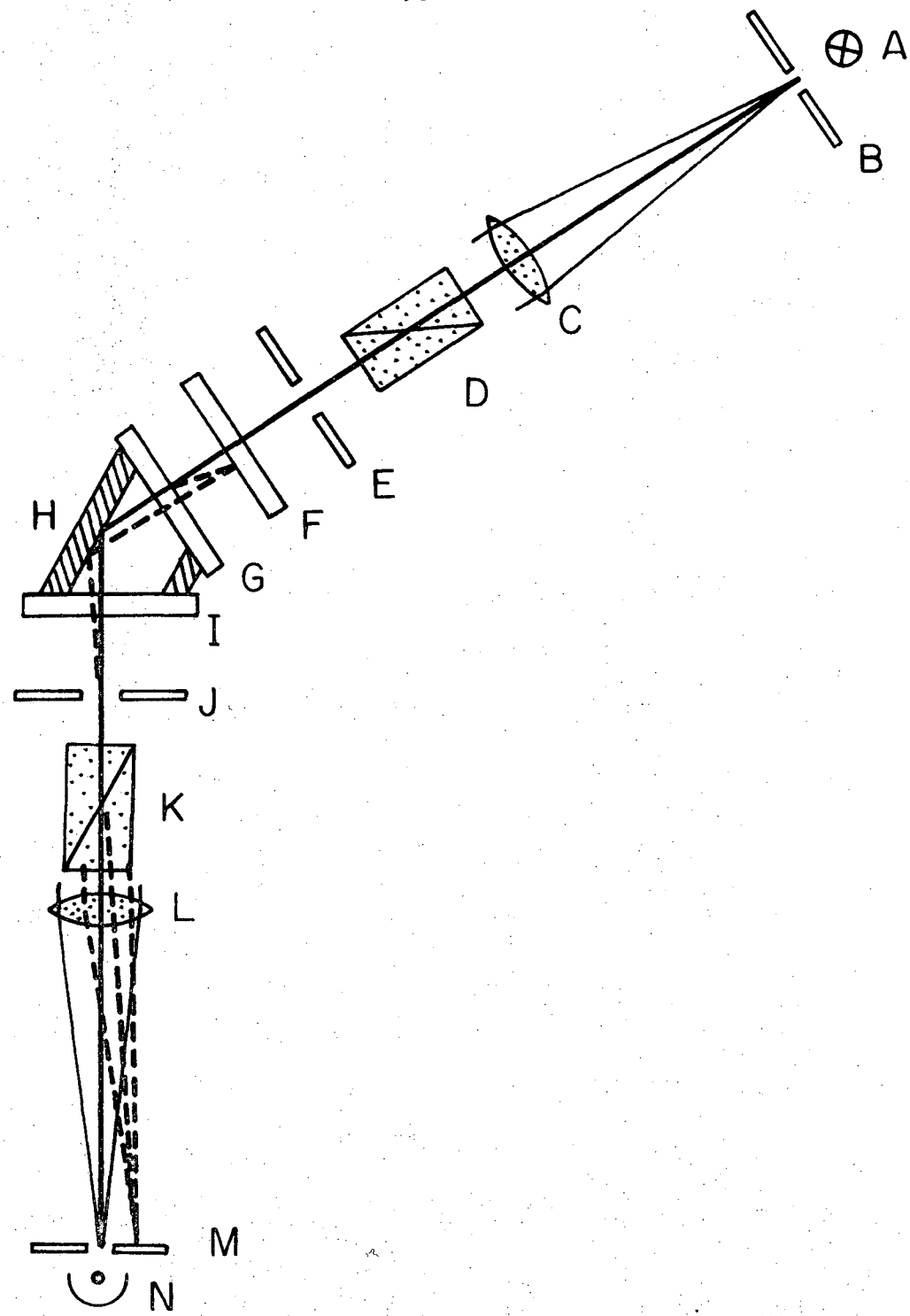

XBL719-4444

Fig. 24

to clamp the electrode in place.

C. Preparation of Electrolyte

The potassium hydroxide solutions were prepared from reagent grade pellets and distilled water. Since KOH attacks both glass and paper filters, teflon filters (Chemware Filter Membranes, Chemplast Inc.) were used with a polypropylene funnel to vacuum filter the solution. The finest teflon filter which was available had a porosity of 5μ (fine). After filtration, the solution was purged with nitrogen for the least 24 hours before it was used.

The sulfuric acid solution was prepared from reagent grade concentrated sulfuric acid. The solution was then vacuum filtered through a glass filter (porosity approx. 1μ) and pruged with nitrogen before being used.

D. Preparation of Electrode Surface Cleaning of the Cell

Before the cell was assembled, the platinum electrode was cleaned with isopropanol to remove grease and organic contaminants, followed by a cleaning with nitric acid. The cell body was cleaned with chromic acid and distilled water. The cleaning of the cell windows was rather laborious. One side of the windows is coated with anti-reflection coating. Cleaning could not be done easily with chromic acid without destroying part of the coating. For experiments with potassium hydroxide solution, the cleaning of windows was omitted because the potassium hydroxide solution etches the glass and therefore wets it very well. However, for experiments with dilute sulfuric acid, the glass windows had to be cleaned since dilute sulfuric acid does not etch glass, and liquid drops would form on the window surface when drained. This would introduce great error in the measurements. In order not to damage the coating of the windows during cleaning, the cell was first assembled,

then filled with chromic acid and followed by repeated rinsing with distilled water to wash the whole cell.

Before the performance of every experiment, the cell was filled with the electrolyte and the platinum electrode was cathodically cleaned (current density, 750 ma/cm^2) by intermitent evolution of large quantities of hydrogen to insure the presence of a clean platinum surface. Two counter-electrodes were used in succession for the cleaning process. Nickel screens were used as the counter-electrode for cleaning when experiments were performed with potassium hydroxide electrolyte. When working with dilute sulfuric acid, a platinum plate was used instead. Sometimes the cathodic cleaning had to be repeated many times to achieve a uniform wetting of the platinum surface.

To begin an experiment, the cell was filled with electrolyte and the gas saturation system turned on. The cell was then drained as fast as possible. When the liquid level reached the top of the weir,* timing began for the measurement of the thinning of the film.

E. Alignment

The alignment and calibration of the ellipsometer with variable angle of incidence setup is much easier than that described for use with the LEED setup because the polarizer and analyzer telescopes can be easily brought into "straight through position" (i.e. optical axes coincident with each other). Essentially, the McCrackin alighment procedures[11] were followed. The procedures are outlined by steps in Appendix III.

---

*The weir separates the solution contacting the electrode and that near the glass windows since the KOH solution attacks glass. The weir also serves to set the liquid level.

The angle between the two windows when the cell was assembled, did not differ from 75° by more than one degree. The electrode surface should form equal angles with the faces of the windows. This alignment of the electrode surface with respect to the windows was estimated to be accurate within half a degree. To align the cell with respect to the light beam at 75° angle of incidence, the cell was moved until the pin-hole image reflecting from the electrode fell on the cross-hairs of the analyzer telescope eyepiece. When this is accomplished, the light beam should be normal to the windows, with a deviation of less than one degree. As was mentioned before, one degree misalignment affect the state of polarization only very slightly.[20] It was not necessary to align the cell windows with respect to the light beam.

F. The Effect of Cell Windows

The effect of inhomogeneities and birefringence in the cell windows on Δ and ψ was determined by first measuring Δ and ψ for the platinum electrode with cell windows removed and then with windows in place. The difference in ψ and Δ between the two measurements were applied as correction factors. This measurement of the cell window effect was performed every time that the cell was taken apart and reassembled. Table III shows the results of the window effect measurement and the correction factors determined. For determination of the optical constants of the platinum electrode, the four-zone average[11] correction factors for windows were used. When measuring films on the platinum electrode, two-zone average correction factors were used since film measurements were only made in two zones (compensator circle reading at 45°, quarter-wave plate fast axis at 135° to plane of incidence).

It must be mentioned that measurement of the cell window effect was only made at one point on the window. The inhomogeneities of the

Table III. Effect of the cell windows on Δ and ψ (Reflecting surface: Platinum electrode; $\phi = 75°$; wavelength = 5461Å).

		Two-Zone Average (quarter-wave plate fast axis at 135°)			Four-Zone Average		
Measurement No.		1	2	3	1	2	3
1. No Windows	Δ (deg.)	99.94	100.94	97.00	99.65	100.60	96.74
	ψ (deg.)	34.13	33.71	33.33	34.12	33.76	33.32
2. Windows On, Finger Tight	Δ	98.16			97.82		
	ψ	34.14			34.12		
3. Windows On, Nuts Tightened to 20 in.-lb Torque	Δ	96.11	100.67	97.46	95.79	100.19	97.14
	ψ	34.17	33.78	33.36	34.15	33.76	33.32
Difference from No Window Measurement 2 - 1	$D\Delta$	-1.78			-1.83		
	$D\psi$	0.01			0.00		
Difference from No Window Measurement 3 - 1 (Correction factors are the negative of these values listed)	$D\Delta$	-3.83	-0.27	0.46	-3.86	-0.41	0.40
	$D\psi$	0.04	0.07	0.03	0.03	0.00	0.00

0 0 0 0 0 9 0 1 2 7

glass were probably the same along the window. However, to account for the variation of birefringence along the window caused by mechanical stress, measurements should actually be made at points where film study measurements would be made. The task of determining the effect of cell windows at different points was not carried out because it was considered too lengthy and laborious. A slight uncertainty, therefore, does exist in the effect of the cell windows on measured values of Δ and ψ at points where measurements were not made. When placing the windows onto the cell, care was taken to tighten the nuts uniformly to avoid unnecessary birefringence. Except for one pair of windows, which was later discarded, the effect of cell windows was only of the order of half a degree in Δ and neglegible in ψ. The uncertainty limit of the effect of the windows at different points was estimated to be of the same order of magnitude but not higher. From calculations, it was shown that an error in Δ of $\pm 0.5^{\circ}$ will introduce an error in the film thickness of about ± 2Å.

G. Determination of the Optical Constants of the Platinum Electrode

To obtain the optical constants of a clean platinum surface, the measurement was made with the cell filled with electrolyte and the electrode cathodically cleaned. This insured that the surface measured would be free of oxide layer and other contaminants. The optical constants of the platinum electrode measured in air and measured when surrounded by electrolyte are compared in Table IV. Four-zone average of Δ and ψ were used to determine the optical constants. The constants obtained are close to that reported in literature.[34,35,36]

When measurements of optical constants were made with the cell filled with electrolyte, the alignment of the windows with respect to

Table IV. Optical constants of the platinum electrode ($\phi = 75°$, wavelength = 5461Å).

	Δ (deg.) (Four-zone average)	ψ (deg.) (Four-zone average)	n	k
1. Measurement made with the electrode in air	100.65	33.80	1.70	3.85
2. Measurements made with the electrode surrounded by electrolyte (electrode cathodically cleaned)				
In 1N KOH solution (refractive index = 1.3444)	81.96*	35.46*	1.47	3.82
Electrode Re-Polished				
In 2.62N KOH solution (refractive index = 1.3595)	81.85**	32.48**	1.93	3.71
In 6.05N KOH solution (refractive index 1.3853)	81.77**	32.70**	1.93	3.79
In 0.94N H_2SO_4 solution (refractive index = 1.3393)	82.71†	32.60†	1.90	3.72

*Window effect correction factors set 1 of Table III applied.

**Window effect correction factors set 2 of Table III applied.

†Window effect correction factors set 3 of Table III applied.

the light beam was more critical[28] because it could cause false angle of incidence. A check was made to see how much the reflected light beam had deviated from its original position after the cell was filled with electrolyte. It was found that the reflected light beam was deflected only by two minutes by the electrolyte. This means that the alignment of the windows with respect to the light beam was very good. The autocollimation check of the windows with respect to the light beam was not made because the anti-reflection coating would give a reflection too weak to be observed, and because the attachment of a mirror onto the window might destroy the coating.

Table IV shows that the optical constants of the platinum electrode measured in 1N KOH was greatly different from the rest of the measurements. The reason for the discrepancy is not clear. One of the following reasons may explain the difference. a) At the time of measurement the surface could have been contaminated by corrosion products* which originated from the top of the electrode. Making the measurement near the bottom of the electrode may not have avoided the problem. b) Since the measurement was made near the bottom of the electrode, and measurement of the effect of windows was made at the middle of the electrode,** an uncertainty exist in the correction factors for window effect. The pair of windows used at the time showed high inhomogeneities

*The corrosion product was produced because of an anodic dissolution process during cathodic cleaning. The pin in contact with the electrode was at the time made from 304 stainless steel while the backing of the platinum electrode was 316 stainless steel. Due to the roughness of the contact area, a small gap was present. This problem of corrosion was solved after the contact area was smoothed. In addition, a 316 stainless steel pin was used later.

**Except with 1N KOH, measurement of the optical constant were made at the middle of the electrode where cell window effect measurements were made. This avoided any uncertainty in the effect of windows on measured values of Δ and ψ.

and birefringence (see Table III). Therefore, the uncertainty range might very well be large. c) The electrode was re-polished after the measurement with 1N KOH. The surface of the electrode may be very different before and after the hand-polishing.

It might be noted that the optical constants of platinum falls in the range where n and k are quite sensitive to changes in ψ and Δ (especially to changes in ψ) at 75° angle of incidence (see Fig. 25). For instance, a change of ψ of approximately 3° will change the calculated values of n/n_o from 2.0 to 1.5 and k/n_o from 3.5 to about 3.8.

H. KOH Films

In the study of KOH films on the platinum electrode, an unexpected problem arose. Measurements could be interpreted only by assuming a small index of extinction, k in the film (potassium hydroxide film should be transparent). Detailed dicussion will be given in section V-H-4.

1. Measurement of the Thinning of the Film

The measurement of the thinning of potassium hydroxide films was made at 3.83 cm from the top edge of the electrode. Measurements began as soon as the electrolyte level reached the top of the weir. As the electrolyte was drained, some of it was collected for refractive index and concentration determination. The refractive index was determined using the Bausch and Lomb precision refractometer. The concentration was determined by titration with standard 1N HCl (phenolphthalein end point).

Figures 26 and 27 show the thinning curves of 2.62N and 6.05N KOH films. The results show what was expected, the thinning rate of 6.05N KOH film was slower than that of the 2.62N film since 6.05N KOH had a higher viscosity (approximatly one and a half times higher) and only

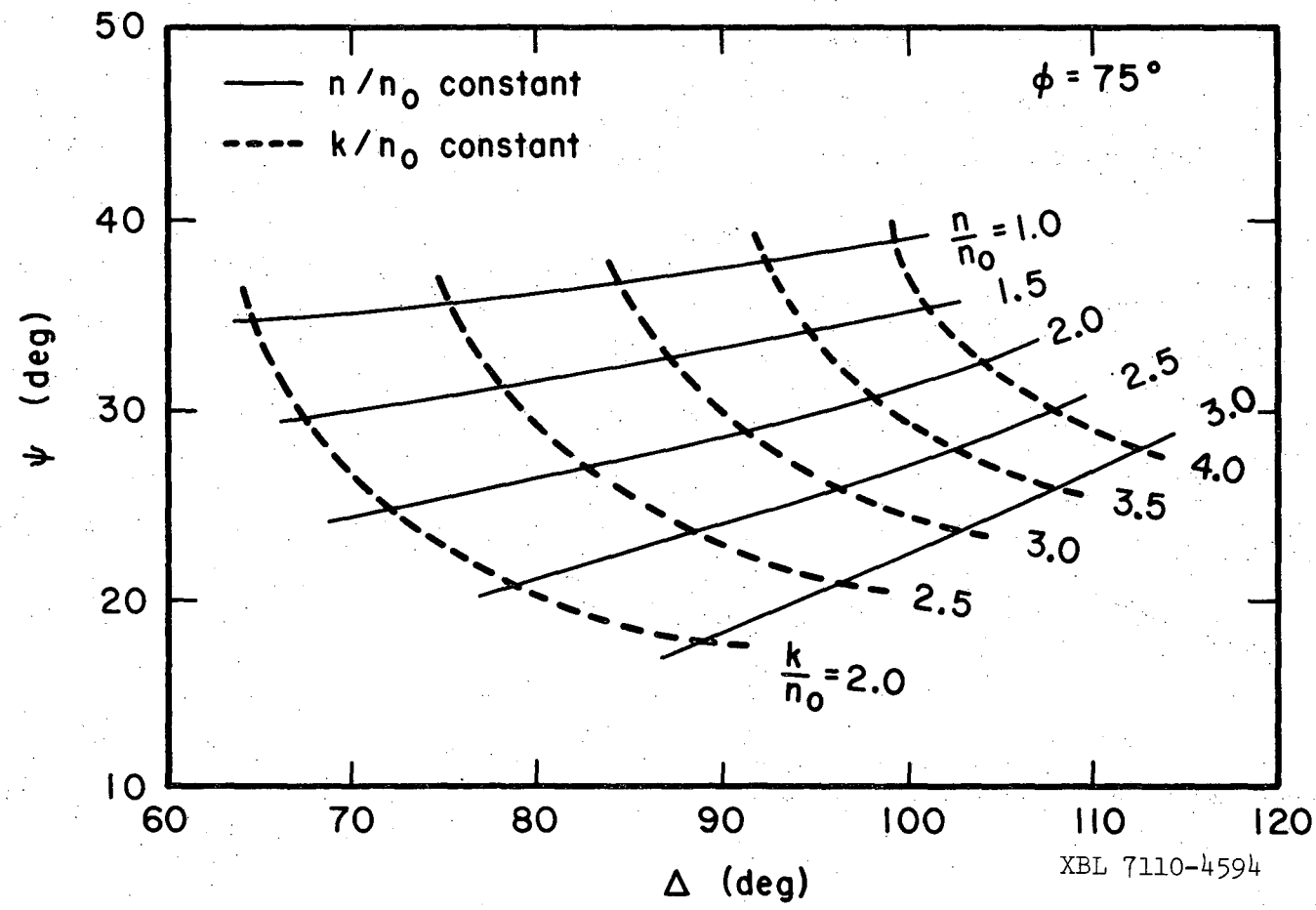

Fig. 25 Ellipsometric parameters ψ and Δ for reflection from a bare metal surface of optical constants n-ik. Angle of incidence 75°.

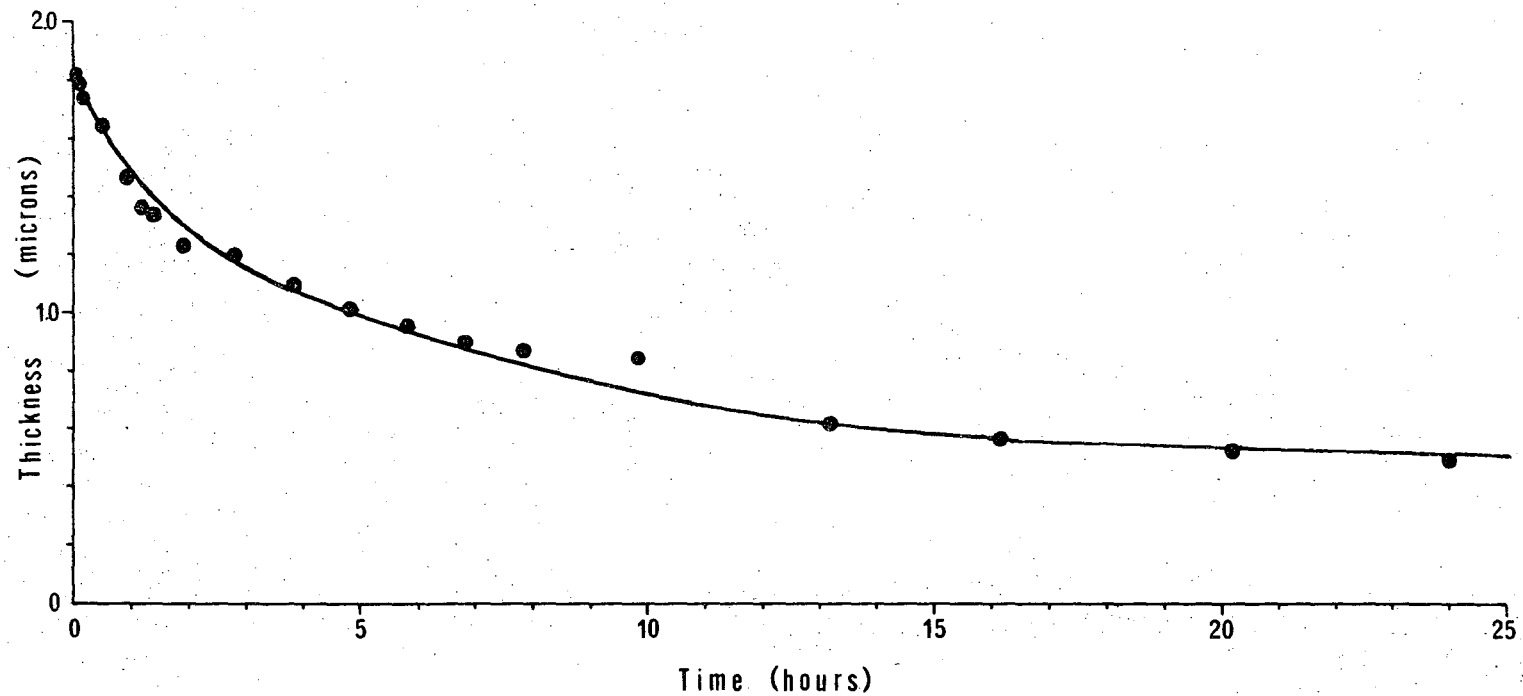

NBL 7110-7415

Fig. 26 Thinning of 2.62N KOH film on platinum electrode. Measurement made at 3.83 cm from top edge of electrode.

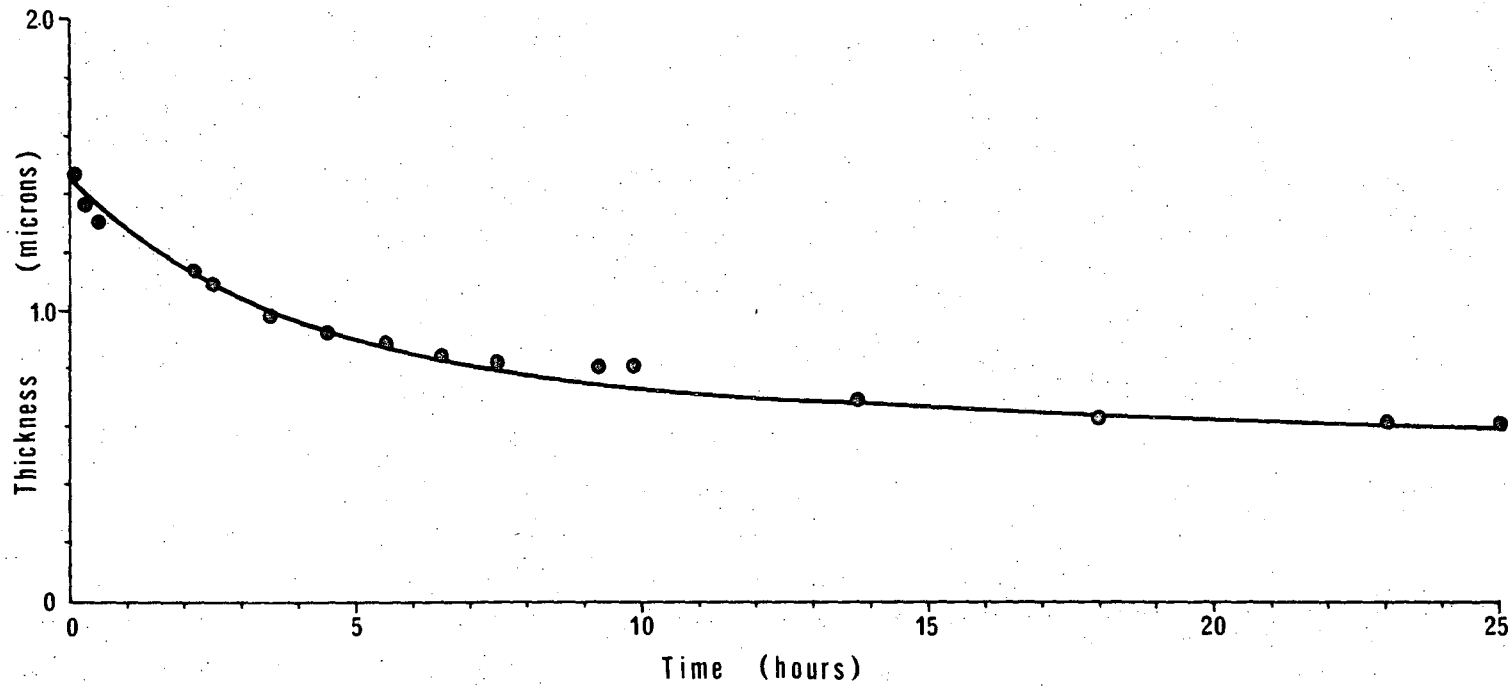

NBL 7110-7426

Fig. 27 Thinning of 6.05N KOH film on platinum electrode. Measurement made at 3.83 cm from top edge of electrode.

a slightly higher density. However, as opposed to results obtained by Muller,[29] thinning curves did not obey Eq. (42)[30]

$$L = (\mu/\rho g)^{1/2} z^{1/2} t^{-1/2} \tag{42}$$

where L = film thickness

z = vertical coordinate, measured from the upper electrode down

t = time

μ = viscosity

ρ = density

g = gravitational constant

2. Steady State Film Profile

The film profile was obtained by making ellipsometric measurements at selected points along the electrode after the drained film had reached steady state. Limitations in the movement of the sample table restricted measurements to parts of the surface higher than one centimeter above the liquid level. The film profiles for 1N, 2.62N and 6.05N KOH film are shown in Fig. 28. The film profiles seem to show waviness.

3. Comparison with White Light Interference

It was of interest in this work to see how ellipsometry can be applied to thick film measurement and how it compares with film interference measurements.

White light interference measurement was made immediately after the ellipsometric measurement. With the angle of incidence remaining at 75° and the cell unmoved, the mercury lamp was replaced by a white microscope light. The quarter-wave plate was removed, and the polarizer set either at the p or s position (transmission axis in the plane of incience or normal to the plane of incidence). The interference colors were

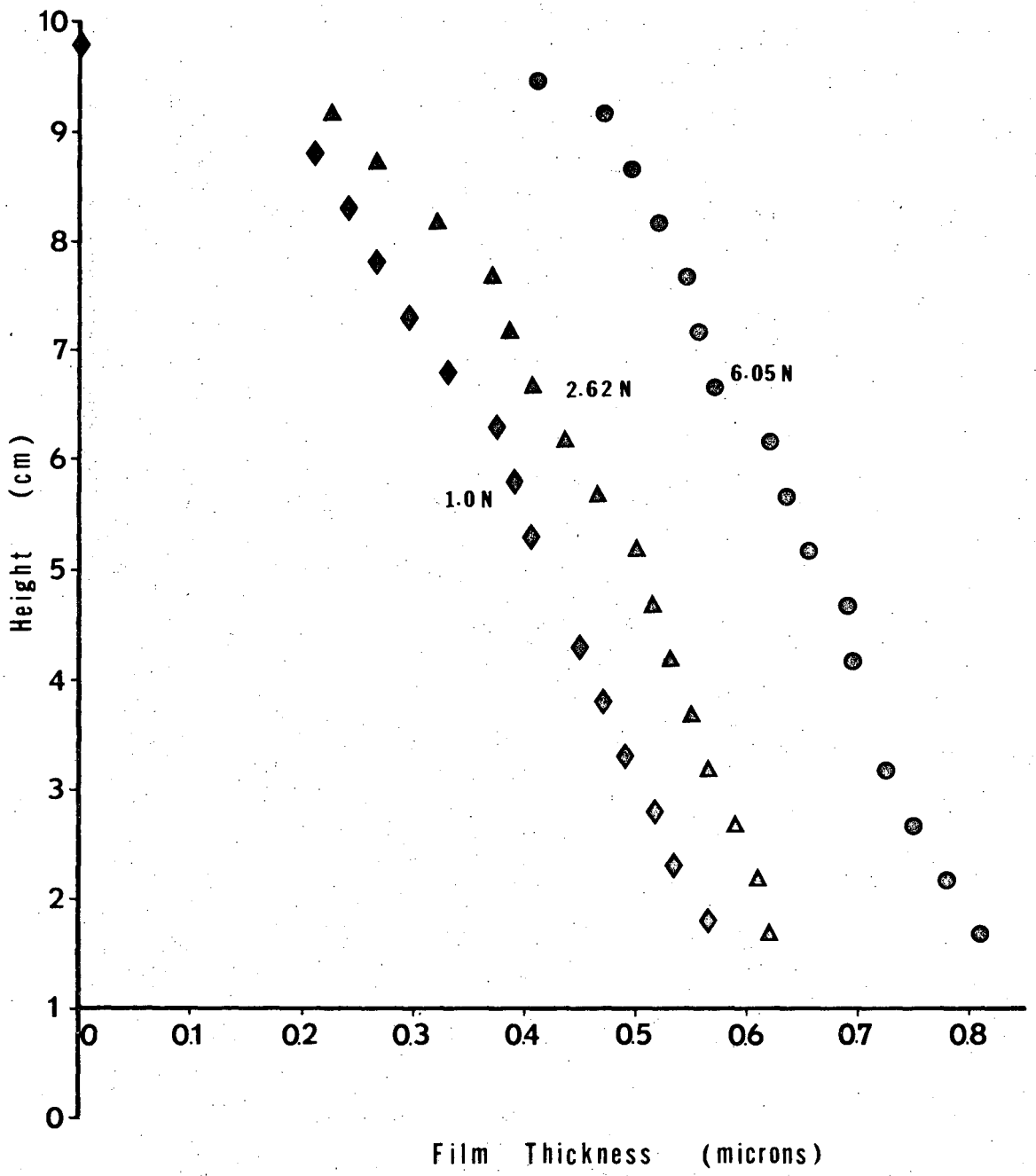

XBL 7110-7402

Fig. 28 Ellipsometrically determined steady state film profiles of KOH films on platinum. Measurements made 24 hrs after the forming of films.

observed with the analyzer transmission axis at 45° to the plane of incidence.

Comparison of ellipsometric measurements and film interference measurements for 2.62N and 6.05 KOH films are made in Figs. 29 and 30. An excellent agreement exist between the two types of measurements. The ellipsometric measurement, as a matter of fact, shows less scatter than interference measurements.

To obtain local film thickness from the interference colors, the color scales (Fig. 31) constructed by Turney[27] was used. The use of Fig. 31 requires the knowledge of δ_{tot} (total phase change due to reflection)

$$\delta_{tot} = \delta_3 - \delta_1 \tag{43}$$

where δ_3 is the absolute phase change due to reflection at the air-film interface and δ_1, the absolute phase change at the film-metal interface.

The abscissa in Fig. 31 is the optical path difference, ΔS, through the film,

$$\Delta S = 2\, n_f L \cos \phi' \tag{44}$$

where n_f is the refractive index of the dielectric film, ϕ' the angle of refraction* in the film and L the film thickness.

A color series for platinum electrode is taken from Fig. 31 for p- and s-polarization respectively. The values of δ_{tot} for both polarizations were calculated from Eq. (43). The absolute phase changes for p- and s-polarization, respectively, at the air-film interface and film-platinum interface were determined using the computer program "MER" (Appendix I-C). The color series obtained are compared with those

---

*ϕ' in Eq. 44 is not a complex quanity as in Eq. (31), since the film is assumed to be dielectric.

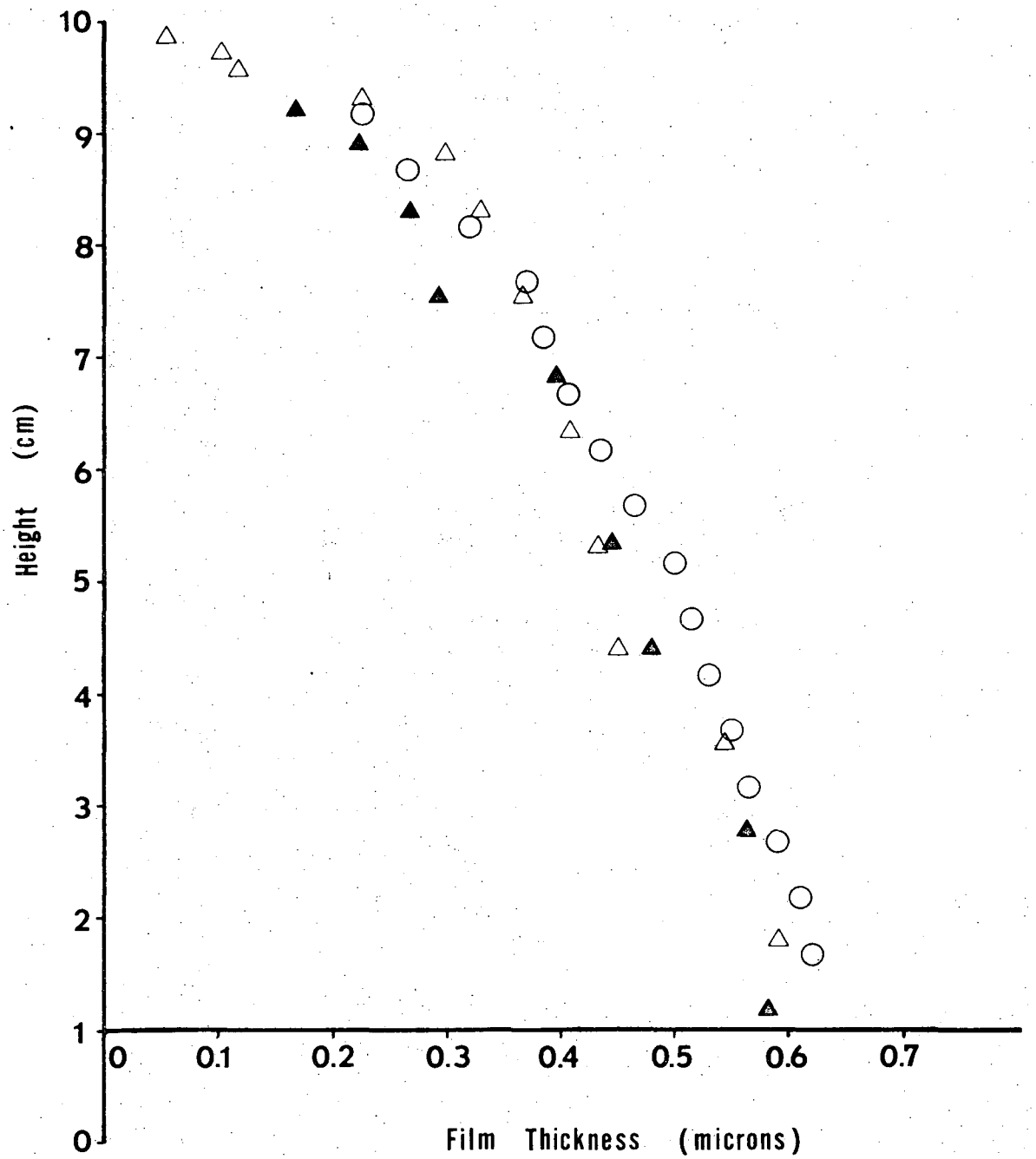

XBL 7110-7422

Fig. 29 Comparison of ellipsometrically determined steady state film profile with white light interference determination. 2.62N KOH film on platinum.
○ - Determined by ellipsometry
△,▲ - Determined by interference color observation
△ - s polarization
▲ - p polarization

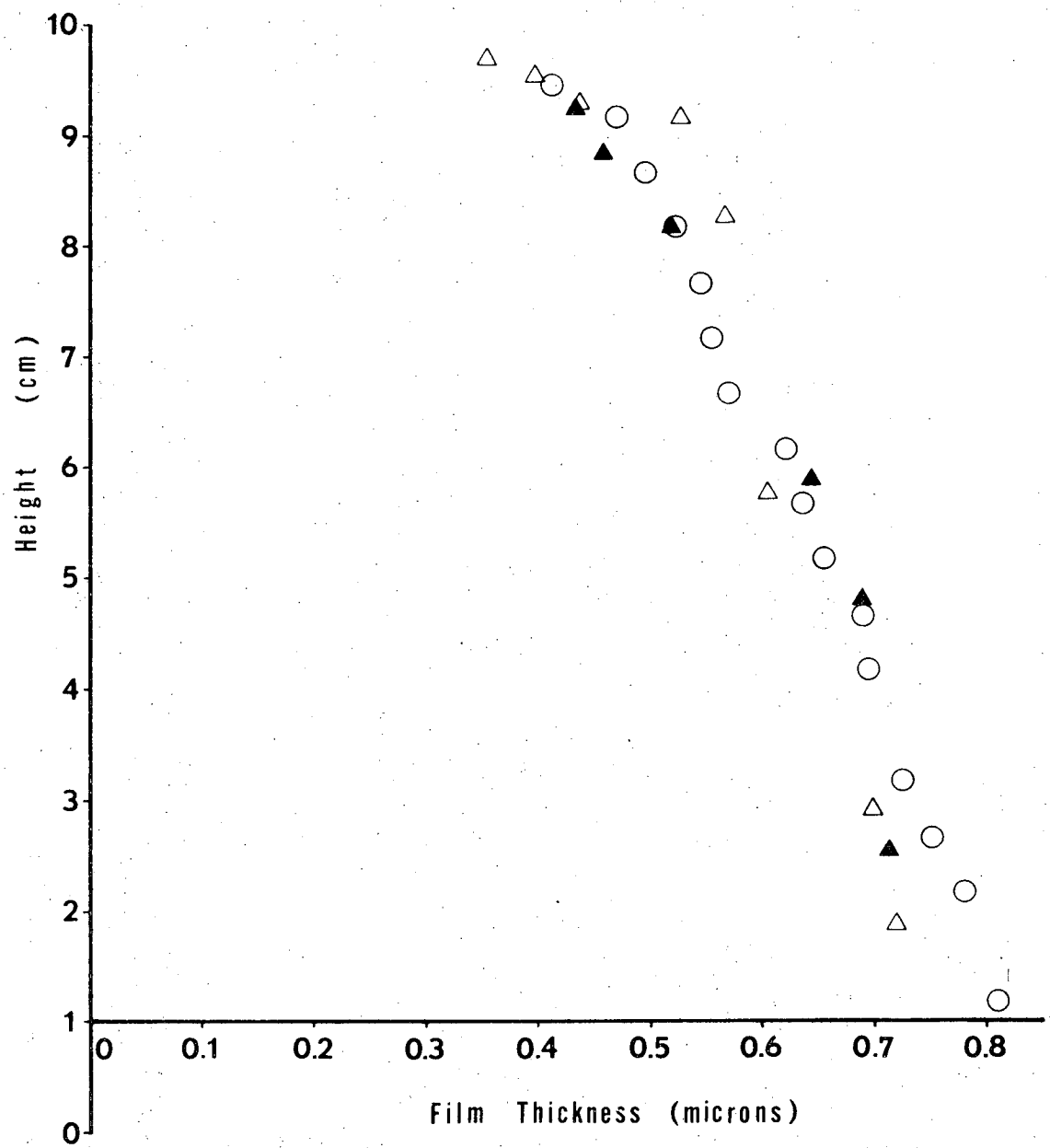

XBL 7110-7423

Fig. 30 Comparison of ellipsometrically determined steady state film profile with white light interference determination. 6.05N KOH film on platinum.
○ - Determined by ellipsometry
△ ▲ - Determined by interference color observation
△ - s polarization
▲ - p polarization

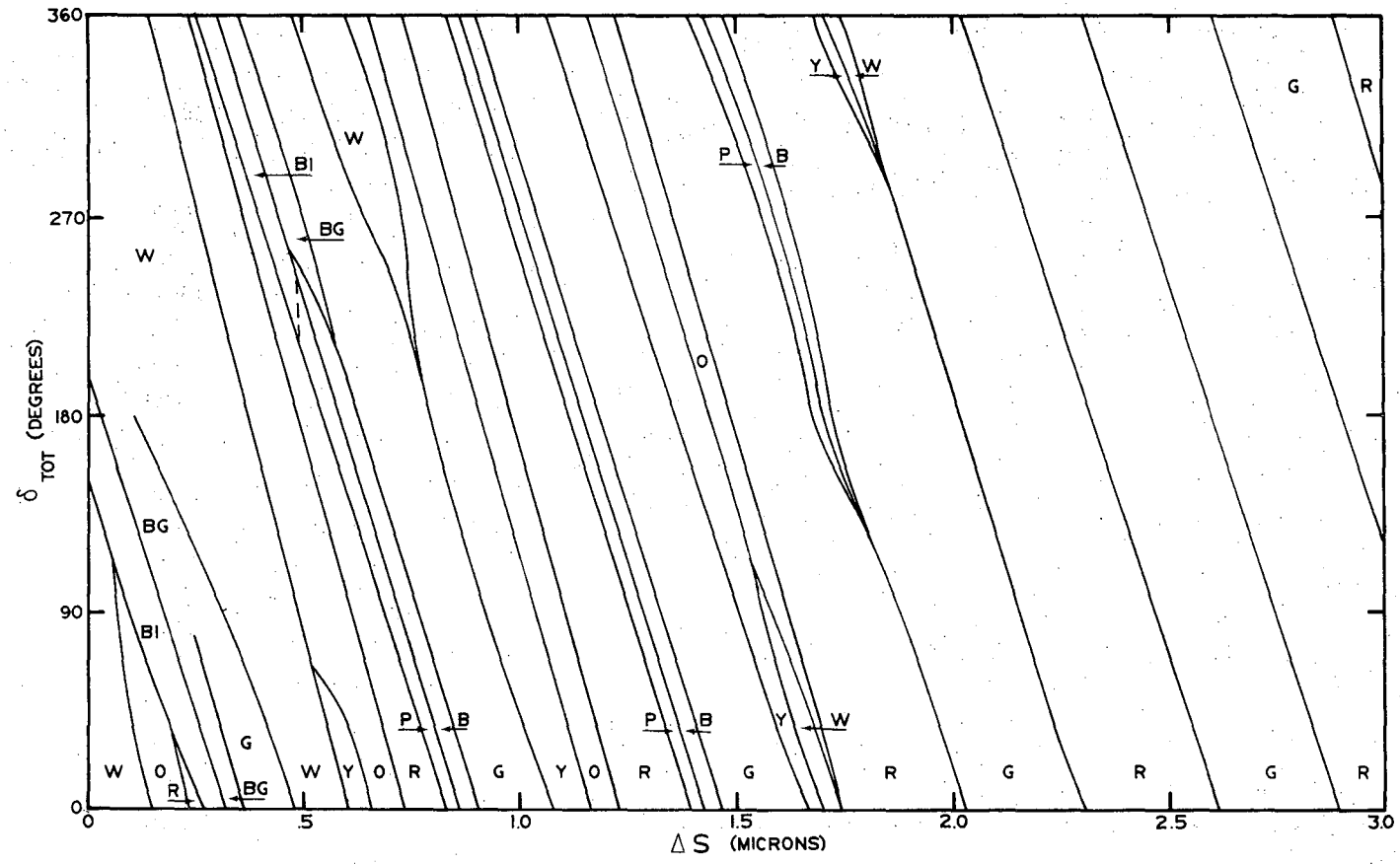

XBL 707-1577

Fig. 31 Multiple beam interference. Generalized inteference color chart.[27] (Typical for dielectric film on platinum or stainless steel substrate). W - white, O - orange, R - red, B - blue, BG - blue green Bl - black, G - green, P - purple, Y - yellow.

obtained by Turney[27] in Fig. 32. For the p-polarization, a difference in ΔS of about 0.1 microns exists between the present results and Turney's, while for s-polarization the difference is 0.05 μ. A good agreement, however, is obtained between the presently used color series and the ones used by Muller.

4. Discussion

To obtain the thickness of the film, the computer program "DLVPS" (Appendix I-G) was used to plot the experimental data on the ψ versus Δ plane. Theoretical curves of ψ versus Δ with different film optical constants were also calculated using computer program "FPLOT" (Appendix I-F). The thickness was retrieved by comparing the experimental ψ and Δ with theoretical ψ and Δ, when a best fit was found between the data and the theoretical curve.

Potassium hydroxide solution is transparent and colorless. Therefore, KOH films should be non-absorbing and could be characterized by a real refractive index n_f (determined by refractometer). However, it was found necessary to assume a small index of extinction for the film (especially for the thinner part). Table V gives, for different thicknesses of film, the values of index of extinction required for the film in order to fit the theoretical curve thus calculated to experimental data.

The absorption characteristics shown by the KOH films probably could be explained by the inclusion of foreign particles in the solution. Since the finest porosity of the teflon filter used was 5 μ, any particles smaller than 5 μ would remain in the solution. When the film was formed, these particles acted as scattering or absorbing centers. The results of ellipsometric measurements thus showed that the film had absorption characteristics. In the thinner part of the film, the volume

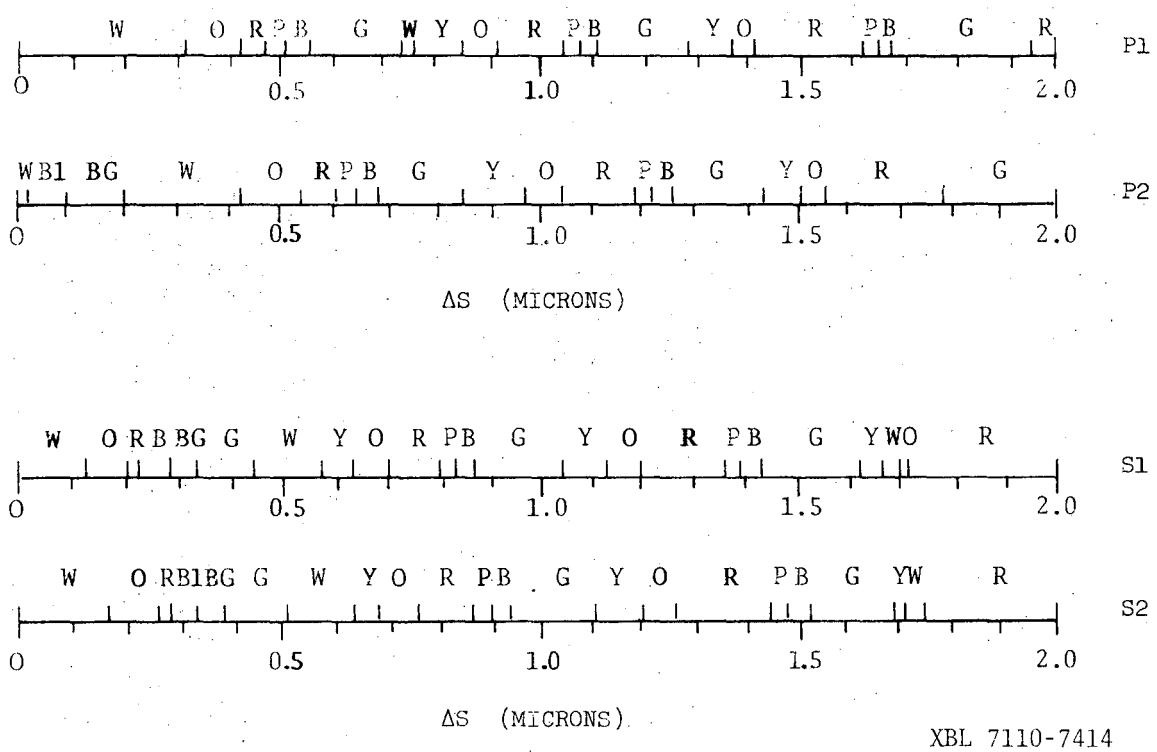

XBL 7110-7414

Fig. 32 Thin film interference color series for a platinum substrate. Comparison of the series constructed for the present work with those constructed by Turney.[27]

p polarization

P1 - Present work $\delta_{tot} = 226°$

P2 - Turney's $\delta_{tot} = 138°$

s polarization

S1 - present work $\delta_{tot} = 23°$

S2 - Turney's $\delta_{tot} = 338°$

Table V. Film optical constants used for the determination of KOH film thickness on the Pt electrode.

Experiment	Concentration	Optical Constants n_f (measured)	k_f (fitted)	Film Thickness Range (Microns)
KOH Film Profile Measurements	1N	1.3444	0.03	0.06 - 0.6
	2.62N	1.3595	0.04	0.2 - 0.4
			0.015	0.44 - 0.65
	6.05N	1.3853	0.02	0.4 - 0.65
			0.01	0.7 - 0.8
KOH Film Thinning Measurements	2.62N	1.3595	0.02	0.5 - 0.95
			0.01	1.0 - 1.9
	6.05N	1.3853	0.02	0.6 - 0.95
			0.01	0.98 - 1.2
			0.00	1.3 - 1.5

percentage of particles was higher. A higher index of extinction therefore existed in the thinner part of the film. This reasoning is supported by the experiments with sulfuric acid (Section V-I).

In calculating the theoretical values of ψ and Δ with changes in film thickness, the substrate optical constants were assumed to be those measured when the platinum electrode was surrounded by electrolyte (see Table IV). When analyzing the results for 1N KOH film, it was borne in mind that the substrate constants might be in error as mentioned in Section V-G. However, it was found that the theoretical ψ versus Δ curve based on substrate constants of $n_m = 1.47$, $k_m = 3.82$, and film constants of $n_f = 1.3444$, $k_f = 0.03$ fitted quite well with the data. If the platinum optical constants were in error, this fit would mean that the accuracy of substrate constants is not critical in determining the film thickness.

Two ψ versus Δ curves, with film thickness as the parameters were computed with substrate constants $n_m = 1.47$, $k_m = 3.82$ and film constants $n_f = 1.3444$, $k_f = 0$ and $n_f = 1.3444$, $k_f = 0.03$. These two curves were compared with the two curves calculated using substrate constants $n_m = 1.93$, $k_m = 3.71$* and the same film constants. For the transparent film ($n_f = 1.3444$), the maximum difference between the two is 4° in ψ and 5° in Δ which corresponds to an error in thickness of about 30Å. These maximum differences occur within the Δ range of 120° to 220°. For the slightly absorbing film ($n_f = 1.3444$, $k_f = 0.03$), the same maximum differences between the two curves also occured within the range of 120° to 220° in Δ. The differences in ψ and Δ, however, increase with film thickness. Since the present study deals with thick KOH films,

---

*These substrate constants were obtained with the electrode surrounded by 2.62N KOH electrolyte. They are expected to be accurate.

an inaccuracy of ±50Å in film thickness is tolerable. The accuracy in the results for 2.62N and 6.05 KOH film, however, is expected to be much better than ±50Å.

I. H_2SO_4 Film

Further support for the arguments presented in Section V-H-4 to explain the absorbing character of KOH films has been obtained by the observation of liquid films free of solid particles on the same platinum electrode. Dilute sulfuric acid as the liquid was chosen for the following reasons.

a) Reagent grade concentrated sulfuric acid is obtained by distillation and therefore it is free of inert particles. b) Dilute sulfuric acid does not attack glass as KOH does. A glass filter (with a porosity of approximately 1μ, Corning ultra fine) could be used to vacuum filter the solution. Therefore, any particles still present can be filtered out of the solution down to a size much smaller than was possible with KOH. c) Sulfuric acid is of practical interest in fuel cells and corrosion processes.

1. Experimental

The thinning of 0.94N sulfuric acid films was measured at 4.32 cm from the top of the electrode. The result is shown in Fig. 33. The thinning rate of 0.94N KOH films was much faster than that of 2.62N and 6.05N KOH films since the viscosity of 0.94N H_2SO_4 is much lower. The film reached steady state in about 11 hours, compared to 20 to 22 hours needed by the KOH films to reach steady state. However, like the KOH films, the time dependence of the thinning with H_2SO_4 did not obey Eq. (42).

The results of the film profile measurement is shown in Fig. 34. A tapered film of thickness of 50Å to 200Å wetted the electrode. The

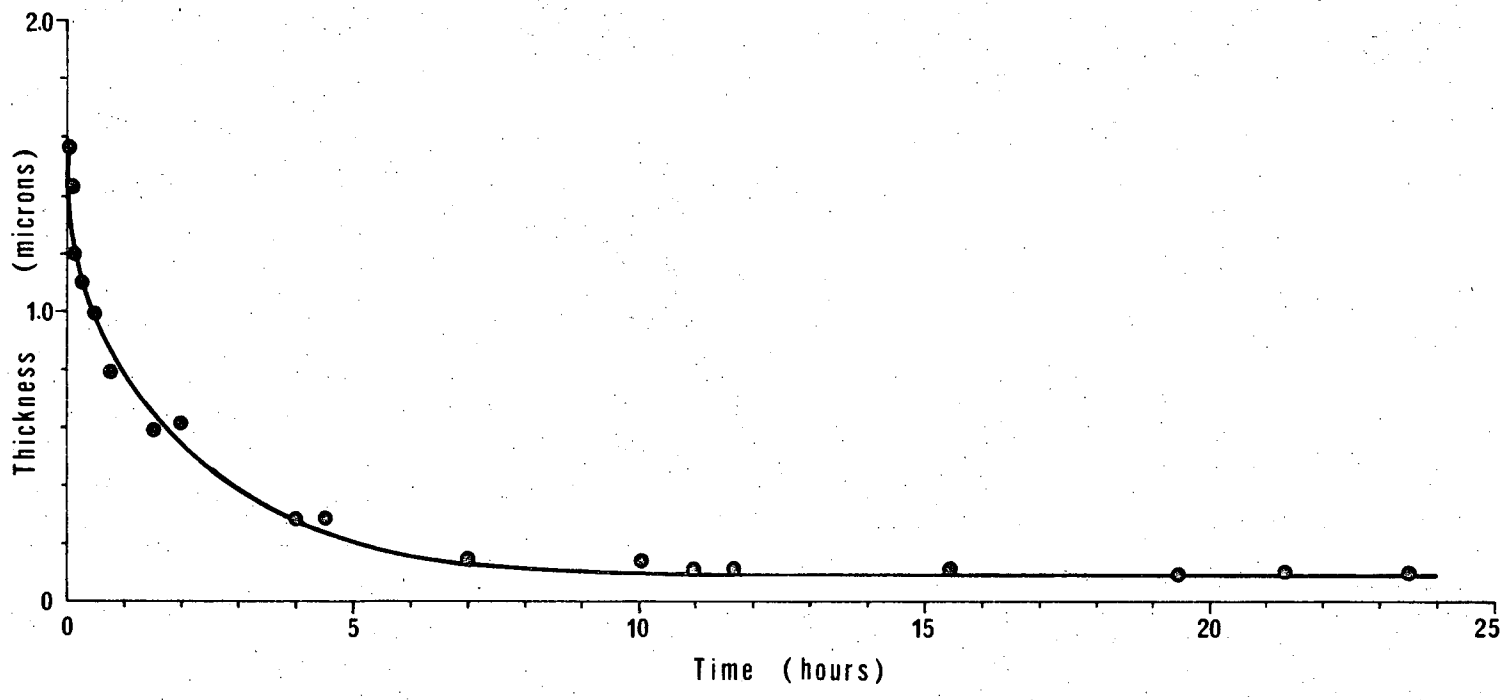

XBL 7110-7425

Fig. 33 Thinning of 0.94N H_2SO_4 film on platinum electrode. Measurement made at 4.32 cm from top edge of electrode.

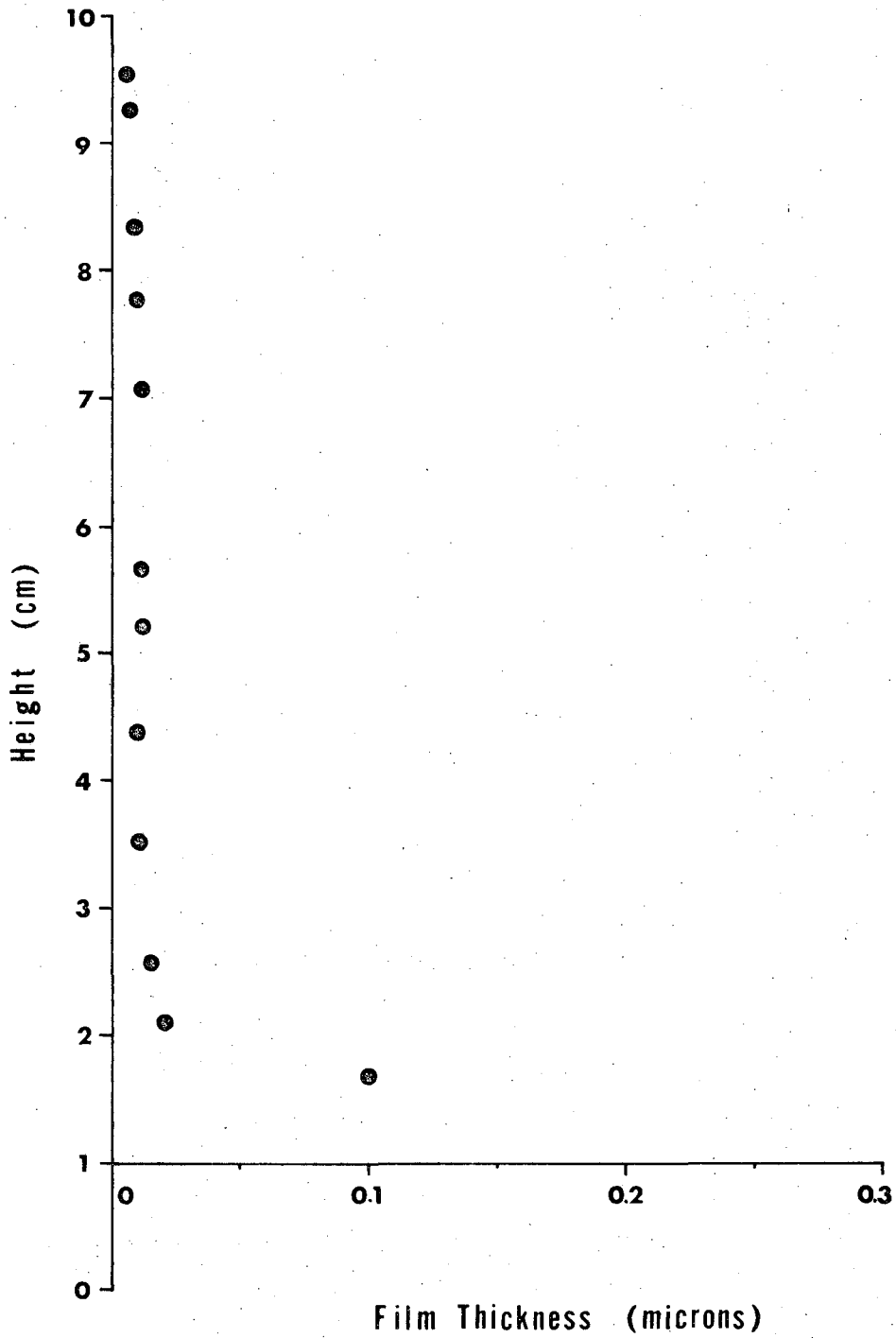

XBL 7110-7401

Fig. 34 Ellipsometrically determined steady state film profile of 0.94N H_2SO_4 film on platinum. Measurement made 24 hrs after the forming of the film.

thickness of the film seemed to increase greatly at about 2 cm above the liquid level. Due to the limited traveling distance of the sample table, data could not be obtained closer to the liquid level.

No film interference color was observable because the film was too thin. This again shows one of the superiorities of ellipsometry over interferometry when applied to film measurement.

2. Discussion

In order to derive thickness values from the experimental values of ψ and Δ the calculated theoretical ψ versus Δ curves were fitted to the experimental points. In contrast to KOH results, measured points could be connected by a theoretical curve based on a real refractive index for the film (n_f = 1.3393, measured by refractometer, and k_f = 0.) The substrate constants used were the ones measured when the electrode was surrounded by 0.94N H_2SO_4 electrolyte (see Table IV).

As was mentioned before, the 0.94N sulfuric acid was prepared from reagent grade concentrated sulfuric acid and filtered through a glass filter. Therefore, the solution used was free of particles larger than 1μ. The ellipsometric results showed what was expected--a transparent sulfuric acid film on a metallic substrate (platinum). The sulfuric acid film also had a smoother appearance than the KOH films when observed through the analyzer telescope. These results may not be a solid evidence that the absorption characteristic of KOH films was due to foreign particles, however, they certainly contribute a substantial support for the argument.

VI. DESIGN CONSIDERATIONS FOR AN AUTOMATIC ELLIPSOMETER

Ellipsometry is very useful in the study of films. However, with equipment operated manually, which requires several minutes for each measurement, it is limited to the investigation of steady-state films or transient films with a slow change in thickness. An automatic ellipsometer with fast response time would increase the scope of film measurements to include the study of transient adsorption and oxidation processes.

There are various reports on automatic ellipsometers. Several techniques such as computer control,[52] servo-motor control,[53] electro-optic and magneto-optic modulation[54,55] have been employed. In the present design of an automatic ellipsometer, the scheme used is similar to that described by H. P. Layer[55]--the use of two Faraday rotators for modulation.

The Faraday rotation can be described by the following equation[23]

$$\theta = VH\ell \tag{45}$$

where θ = the Faraday rotation, minutes of arc

V = the Verdet constant, min/Oe-cm

H = magnetic field applied, Oersteds

ℓ = length of light path through the material, cm

A good Faraday rotator is a material which has a high Verdet constant.

Since solids are convenient to handle, glass was chosen to be used as Faraday cells in the automatic ellipsometer. Selection of the most suitable glass as Faraday rotator should be based on the following considerations (besides high Verdet constant): small absorbance, small reflection loss and small residual birefringence. Also, the glass should have a low stress optical coefficient since a stable and uniform temperature is difficult to achieve in a Faraday cell.

The absorbance, α has been defined by Robinson[33] in the following equation

$$I(d) = I(0)\, e^{-\alpha d} \tag{46}$$

where $I(0)$ = incident light intensity

$I(d)$ = transmitted light intensity

d = distance between glass surfaces where $I(0)$ and $I(d)$ are measured

Equation (46) account only for the absorption loss in the glass. Fresnel reflection loss is not included.

Three glasses were considered for use as Faraday rotator: 1) Corning 8463 extra heavy lead glass, 2) Schott SFS-6 extra heavy lead glass, and 3) Chance-Pilkington, zero stress optical coefficient glass.

Comparison between the Corning 8463 and Schott SFS-6 glasses as Faraday cells has been reported in the literature.[33] Very few data,[40] however, were available for the Chance-Pilkington zero stress optical coefficient glass. Some of the properties of these glasses are listed in Table VI for comparison.

Table VI. A comparison of glasses used as Faraday rotator.

	Corning 8463	Schott SFS-6	Chance-Pilkington Zero Stress Opt. Coef.
Density (gm/cm^3)	6.22	5.18	5.75
Verdet Const.[33,40] at 5461Å (min/Oe-cm)	0.15	0.14	0.10
Refractive Index n_D	1.980	1.806	1.844
α, absorbance[33] at 5461Å (cm^{-1})	0.056	0.015	

The Corning 8463 has the highest Verdet constant. However, it also has a high absorbance. Calculations showed that after passage through 12 inches* of the glass, 82% of the light is absorbed. From informations[32] gathered, the Corning 8463 has large residual birefringence and a high stress optical coefficient. The residual birefringence can be removed by proper annealing. However, the glass is still very sensitive to strain-induced birefringence.

The Schott glass has a high Verdet constant and a small absorbance (only 36% of the light is absorbed after passage through 12 inches of the glass). It is an attractive glass to be used as a Faraday cell. No data were available on its residual phase retardation and its stress optical coefficient. These properties, if not favorable, may be a hinderance to the use of Schott glass as Faraday cells.

The Chance-Pilkington glass, which has the smallest Verdet constant of the three possesses a phase retardation of less than 0.01° per centimeter. As claimed by the manufacturer, the zero stress optical coefficient glass has a zero stress optical coefficient at wavelength of 5890Å and a stress optical coefficient of 0.04 Brewsters at 4300Å. No value on the absorbance of the Chance-Pilkington glass was available. If it has a small absorbance, the zero optical coefficient glass will be the most favorable glass to be used as Faraday rotator in the automatic ellipsometer. With a glass core of 6 inches in length, a Verdet constant of 0.1 min/Oe-cm will rotate a plane polarized light approximately 30 degrees** (maximum) under a magnetic field intensity of 1180

---

* Twelve inch path length was used because Faraday cells of 6 inches long each were planned for the automatic ellipsometer. One Faraday cell is located behind the polarizer and the other before the analyzer.

** A dynamic range of 30° was planned for the polarizer and the analyzer.

Oersteds (which is not difficult to achieve).

When a glass is chosen to be used as Faraday cell, its faces should be coated with anti-reflection coating to reduce the Fresnel reflection loss. Here, a glass with high refractive index is an advantage, since the reflectance can be reduced greatly by only a single $\lambda/4$ coating of MgF_2.

The solenoids used for Faraday cells will have three separate windings. The inner AC winding will be used for the modulation. The outermost DC winding will be used to rotate the plane of polarization. The middle AC winding will be used to shield the inner AC winding from the DC winding to prevent coupling. The solenoids will be water cooled. The purpose of the AC modulation of the magnetic field of each solenoid is to produce a control signal for a feedback circuit which regulates the current in each DC winding to achieve minimum transmitted light intensity. It is hoped that the automatic ellipsometer will have a response time of 10 msec.

ACKNOWLEDGMENTS

I would like to express my gratitude to Dr. Rolf H. Muller for his guidance and encouragement throughout the course of this work.

My thanks to Mr. Raul E. Acosta, Professor Lee F. Donaghey and Professor Yeun Ron Shen for reviewing the manuscript.

Miss Jean Wolslegel has done an excellent job in typing the manuscript.

This work was performed under the auspices of the United States Atomic Energy Commission.

APPENDIX I. COMPUTER PROGRAMS

A. FORTRAN IV Computer Program "MOC"

This computer program (Metal Optical Constants) calculates the optical constants from relative phase change, Δ, and arctangent of relative amplitude attenuation, ψ.

1. Equations Used in the Program

$$D = \frac{\sin\phi \tan\phi \cos 2\psi}{1 + \sin 2\psi \cos\Delta} \tag{27}$$

$$E = \frac{\sin 2\psi \sin\phi \tan\phi \sin\Delta}{1 + \sin 2\psi \cos\Delta} \tag{28}$$

$$n^2 = \frac{n_o^2}{2}\left[\sqrt{(D^2 - E^2 + \sin^2\phi)^2 + 4D^2E^2} + (D^2 - E^2 + \sin^2\phi)\right] \tag{25}$$

$$k^2 = \frac{n_o^2}{2}\left[\sqrt{(D^2 - E^2 + \sin^2\phi)^2 + 4D^2E^2} - (D^2 - E^2 + \sin^2\phi)\right] \tag{26}$$

2. Variables Employed in the Program

Name	Symbol	Description
PHID	ϕ (degrees)	angle of incidence
PHI	ϕ (radians)	angle of incidence
DELD	Δ (degrees)	relative phase change
DEL	Δ (radians)	relative phase change
PSID	ψ (degrees)	arctangent of relative amplitude attenuation
PSI	ψ (radians)	arctangent of relative amplitude attenuation
D	D	intermediate variable
E	E	intermediate variable
TN	n	real part of the complex refractive index
TK	k	imaginary part of the complex refractive index (index of extinction)
TNO	n_o	refractive index of transparent incident medium

3. Input Data for Program "MOC"

The input data for the program MOC are arranged on cards as illustrated below

Card	Col. 1	Col. 11	Col. 21	Col. 31	Col. 41	Col. 51	Col. 61
1	Title and comments (up to 80 columns may be used).						
2	n_o						
3	ϕ_1	ϕ_2	ϕ_3	ϕ_4	ϕ_5	ϕ_6	ϕ_7
4	Δ_1	Δ_2	Δ_3	Δ_4	Δ_5	Δ_6	Δ_7
5	ψ_1	ψ_2	ψ_3	ψ_4	ψ_5	ψ_6	ψ_7

Card 1 is printed verbatim on the first page of the printout. These 5 cards constitute a set of input data. Any number of sets may follow this first set. The last set of cards must be followed by two blank cards. The data should contain a decimal point and may be located anywhere in the field beginning with the column indicated and ending in the column preceding the next field.

The program together with a sample output is reproduced on the following pages.

```
      PROGRAM MOC (INPUT,OUTPUT)
C MOC METAL OPTICAL CONSTANTS
      DIMENSION PHID(7),PHI(7),DELD(7),DEL(7),PSID(7),PSI(7),D(7),DSQ(7)
     C,E(7),ESQ(7),TN(7),TNSQ(7),TK(7),TKSQ(7)
      DIMENSION TITLE (8)
    1 READ 2, TITLE
    2 FORMAT (8A10)
    3 PRINT 4, TITLE
    4 FORMAT (1H1, 8A10)
    9 FORMAT (F10.5)
   10 FORMAT (7F10.5)
   11 FORMAT (7F10.0)
    5 FORMAT (////1X,5HTNO =,F10.5)
   12 FORMAT(////3X,4HPHID,6X,4HDELD,6X,4HPSID,8X,1HD,9X,1HE,9X,2HTN,7X,
     C2HTK)
   14 FORMAT(1H0//30X,43H----------METAL OPTICAL CONSTANTS---------- )
      READ 9,TNO
      IF(TNO.EQ.0.0) GO TO 305
      PRINT 14
      PRINT 5, TNO
   25 READ 11, (PHID(M),M=1,7)
      READ 11, (DELD(M),M=1,7)
      READ 11, (PSID(M),M=1,7)
      DO 101 M=1,7
      PHI(M)=PHID(M)*0.01745329252
      DEL(M)=DELD(M)*0.01745329252
      PSI(M)=PSID(M)*0.01745329252
  101 CONTINUE
      DO 201 M=1,7
      SPH=SIN (PHI(M))
      CPH=COS (PHI(M))
      TPH=SPH/CPH
      SD=SIN (DEL(M))
      CD=COS (DEL(M))
      STPS=SIN (2.0*PSI(M))
      CTPS=COS (2.0*PSI(M))
      D(M)=+SPH*TPH*CTPS/(1.0+CD*STPS)
      DSQ(M)=D(M)*D(M)
      E(M)=+SPH*TPH*SD*STPS/(1.0+CD*STPS)
      ESQ(M)=E(M)*E(M)
      F=DSQ(M)-ESQ(M)+SPH*SPH
      TNSQ(M)=0.5*(SQRT (F*F+4.0*DSQ(M)*ESQ(M))+F)*TNO**2
      IF (TNSQ(M)) 150,152,152
  150 TN(M)=0
      GO TO 154
  152 TN(M)=SQRT (TNSQ(M))
  154 TKSQ(M)=TNO*TNO/2.*(SQRT(F*F+4.0*DSQ(M)*ESQ(M))-F)
      IF (TKSQ(M)) 156,158,158
  156 TK(M)=0
      GO TO 201
  158 TK(M)=SQRT (TKSQ(M))
  201 CONTINUE
      PRINT 12
      DO 301 M=1,7
  301 PRINT 10 , PHID(M),DELD(M),PSID(M),D(M),E(M),TN(M),TK(M)
      GO TO 1
  305 RETURN
      END
```

PROGRAM MOC -- SAMPLE OUTPUT (SILVER)

----------METAL OPTICAL CONSTANTS----------

TNO = 1.00000

PHID	DELD	PSID	D	E	TN	TK
2.00000	179.96520	44.99910	.20702	4.00236	.20703	4.00221
40.00000	164.86780	44.63550	.19747	4.05120	.19999	4.00001
45.00000	160.29340	44.53170	.19693	4.06186	.19997	3.99999
50.00000	154.78380	44.41140	.19643	4.07251	.19999	3.99999
70.00000	115.79420	43.77840	.19471	4.10864	.19999	3.99999
75.00000	97.62860	43.65930	.19443	4.11470	.20000	3.99999
80.00000	72.86210	43.71020	.19420	4.11915	.19999	3.99998

B. FORTRAN IV Computer Program "AXCON"

Similar to the computer program MOC, the FORTRAN IV program, AXCON, (Auxiliary Constants) calculates the metal optical constants n and k from given values of ψ, Δ and ϕ. In addition, the program finds the alternate constants n', k', electrical conductivity σ, dielectric constant ε and penetration depth.

1. Equations Used in the Program

$$D = \frac{\sin\phi \tan\phi \cos 2\psi}{1 + \sin 2\psi \cos\Delta} \qquad (27)$$

$$E = \frac{\sin\phi \tan\phi \sin 2\psi \sin\Delta}{1 + \sin 2\psi \cos\Delta} \qquad (28)$$

$$n^2 = \frac{n_o^2}{2}\left[\sqrt{(D^2 - E^2 + \sin^2\phi)^2 + 4D^2E^2} + (D^2 - E^2 + \sin^2\phi)\right] \qquad (25)$$

$$k^2 = \frac{n_o^2}{2}\left[\sqrt{(D^2 - E^2 + \sin^2\phi)^2 + 4D^2E^2} - (D^2 - E^2 + \sin^2\phi)\right] \qquad (26)$$

$$n' = n_o \sin\phi \sqrt{1 + \frac{\tan^2\phi \cos^2 2\psi}{(1 + \sin 2\psi \cos\Delta)^2}}$$

From (12) (15) (16) (25) and (26)

$$k' = \frac{n_o \sin\phi \tan\phi \sin 2\psi \sin\Delta}{1 + \sin 2\psi \cos\Delta}$$

From (12) (15) (16) (25) and (26)

$$\sigma = \frac{nk\omega}{2\pi} \qquad (47)^2$$

$$\varepsilon = n^2 - k^2 \qquad (48)^2$$

$$\text{penetration depth} = \frac{c}{2\omega k'} \qquad (49)^2$$

2. Variables Employed in the Program

Name	Symbol	Description
C	c	speed of light in vacuum
PI	π	ratio of circumference to diameter of circle
WAVEL	λ_o	vacuum wavelength
OMEGA	ω	angular frequency
PHI	ϕ (radians)	angle of incidence
PHID	ϕ (degrees)	angle of incidence
DEL	Δ (radians)	relative phase change
DELD	Δ (degrees)	relative phase change
PSI	ψ (radians)	arctangent of relative amplitude attenuation
PSID	ψ (degrees)	arctangent of relative amplitude attenuation
D	D	intermedate variable
E	E	intermedate variable
TN,N	n	real part of complex index of refraction
TK,K	k	index of extinction
TNP	n'	ratio of phase velocity of light in metal to that in vacuum
TKP	k'	alternate index of extinction
TNO	n_o	refractive index of transparent incident medium
SIGMA	σ	electrical conductivity
EPSILON	ε	dielectric constant
PD		penetration depth

3. Input Data for Program "AXCON"

The input data for the program AXCON are punched on cards as illustrated below

Card	Col. 1	Col. 11	Col. 21
1	Title and comments (up to 80 columns)		
2	n_o	λ_o (Ew.d field may be used)	
3	ϕ_1	Δ_1	ψ_1
4	ϕ_2	Δ_2	ψ_2
5	ϕ_3	Δ_3	ψ_3
		etc.	

The first card is a title card and is printed verbatim at the head of the output. The second card should contain the refractive index of the transparent incident medium between columns 1 and 10 and the wavelength of the light used between columns 11 and 20. The cards that follow contain Δ and ψ at verious angles of incidence ϕ. There is no limit to the number of data cards that may be used. The last card must be followed by a blank card.

The calculated penetration depth will have unit similar to that of the input vacuum wavelength. If the wavelength is given in cm, then the penetration depth will also be given in centimeters and the other dimensional constants will be in gaussian units.

The program, together with a sample of output, is reproduced on the following pages.

```
      PROGRAM AXCON (INPUT,OUTPUT)
C     THIS PROGRAM FINDS THE METAL OPTICAL CONSTANTS N AND KAPPA WHICH
C     APPEAR IN THE COMPLEX INDEX OF REFRACTION, THE (REAL) RATIO OF
C     PHASE VELOCITIES N PRIME, THE PARAMETER KAPPA PRIME, THE (REAL)
C     ELECTRICAL CONDUCTIVITY SIGMA, THE (REAL) DIELECTRIC CONSTANT
C     EPSILON, AND THE ABSORPTION COEFFICIENT ALPHA AT WAVELENGTH OF
C     5461 ANGSTROMS.
      DIMENSION TITLE (8)
      READ 5, TITLE
      PRINT 6, TITLE
    1 FORMAT (////1X,5HTNO =,F10.5,2X,7HWAVEL =,E10.3)
    2 FORMAT (//2X, 107H   PHID       PSID     DELD          N       N PRIME
     C      K        K PRIME     SIGMA        EPSILON       PEN. DEPTH)
    3 FORMAT (7F10.5, 2X, 3(E11.4, 2X))
    4 FORMAT (3F10.5)
    5 FORMAT (8A10)
    6 FORMAT (1H1,///8A10)
    9 FORMAT (F10.5,E10.1)
      READ 9, TNO,WAVEL
      PRINT 1, TNO, WAVEL
      PRINT 2
      C = 2.99776
      PI = 3.1415927
      OMEGA = 2.0*PI*C/WAVEL
  100 READ 4, PHID,DELD,PSID
      IF (PHID.EQ.0.0) GO TO 400
  110 DEL = DELD*0.01745329252
      PSI = PSID*0.01745329252
      PHI = PHID*0.01745329252
   21 SPH = SIN(PHI)
      SPHQ = SPH*SPH
      CPH = COS(PHI)
      TPH = SPH/CPH
      SD = SIN(DEL)
      CD = COS(DEL)
      STPS = SIN(2.0*PSI)
      CTPS = COS(2.0*PSI)
      D = +SPH*TPH*CTPS/(1.0 + CD*STPS)
      DSQ = D*D
      E = +SPH*TPH*SD*STPS/(1.0 + CD*STPS)
      ESQ = E*E
      F = DSQ - ESQ + SPH*SPH
      TNSQ = 0.5*(SQRT(F*F+4.0*DSQ*ESQ) + F)*TNO**2
      IF (TNSQ) 150, 152, 152
  150 TN = 0.0
```

```
      GO TO 154
  152 TN = SQRT(TNSQ)
  154 TKSQ = TNO*TNO/2.*(SQRT(F*F+4.0*DSQ*ESQ)-F)
      IF (TKSQ) 156, 158, 158
  156 TK = 0.0
      GO TO 160
  158 TK = SQRT(TKSQ)
  160 TNP = SPH*SQRT(1.0 + (TPH**2*CTPS**2)/((1.0 + STPS*CD)**2))*TNO
      TKP = (TNO*SPH*TPH*STPS*SD)/(1.0 + STPS*CD)
      SIGMA = TN*TK*OMEGA/(2.0*PI)
      EPSILON = TNSQ - TKSQ
      PD=C/(2.0*OMEGA*TKP)
      PRINT 3, PHID,PSID,DELD,TN,TNP,TK,TKP,SIGMA,EPSILON,PD
      GO TO 100
  400 CONTINUE
      END
```

PROGRAM AXCON -- SAMPLE OUTPUT (SILVER)

TNO = 1.00000 WAVEL = 5.461E-05

PHID	PSID	DELD	N	N PRIME	K	K PRIME	SIGMA	EPSILON	PEN. DEPTH
2.00000	44.99910	179.96520	.20703	.20994	4.00221	4.00236	4.5483E+04	-1.5975E+01	1.0858E-06
40.00000	44.63550	164.86780	.19999	.67244	4.00001	4.05120	4.3914E+04	-1.5960E+01	1.0727E-06
45.00000	44.53170	160.29340	.19997	.73402	3.99999	4.06186	4.3909E+04	-1.5960E+01	1.0699E-06
50.00000	44.41140	154.78380	.19999	.79083	3.99999	4.07251	4.3913E+04	-1.5960E+01	1.0671E-06
70.00000	43.77840	115.79420	.19999	.95965	3.99999	4.10864	4.3914E+04	-1.5960E+01	1.0577E-06
75.00000	43.65930	97.62860	.20000	.98530	3.99999	4.11470	4.3916E+04	-1.5960E+01	1.0561E-06
80.00000	43.71020	72.86210	.19999	1.00377	3.99998	4.11915	4.3913E+04	-1.5960E+01	1.0550E-06

C. FORTRAN IV Computer Program "MER"

This program computes the parameters ψ, Δ, δ_s, δ_p, R_s and R_p for metallic reflection from given values of n, k and ϕ.

1. Equations Used in the Program

$$A^2 = \frac{1}{2\,n_o^{\,2}}\left[\sqrt{(n^2 - k^2 - n_o^{\,2}\sin^2\phi)^2 + 4n^2k^2} + (n^2 - k^2 - n_o^{\,2}\sin^2\phi)\right] \tag{19}$$

$$B^2 = \frac{1}{2\,n_o^{\,2}}\left[\sqrt{(n^2 - k^2 - n_o^{\,2}\sin^2\phi)^2 + 4n^2k^2} - (n^2 - k^2 - n_o^{\,2}\sin^2\phi)\right] \tag{20}$$

(Positive square root gives A and B)

$$R_s = \sqrt{\frac{A^2 + B^2 - 2A\cos\phi + \cos^2\phi}{A^2 + B^2 + 2A\cos\phi + \cos^2\phi}} \tag{17}$$

$$R_p = R_s\sqrt{\frac{A^2 + B^2 - 2A\sin\phi\tan\phi + \sin^2\phi\tan^2\phi}{A^2 + B^2 + 2A\sin\phi\tan\phi + \sin^2\phi\tan^2\phi}} \tag{18}$$

$$\tan\delta_s = -\frac{2B\cos\phi}{A^2 + B^2 - \cos^2\phi} \tag{23}$$

$$\tan\delta_p = \frac{2B\cos\phi\,(A^2 + B^2 - \sin^2\phi)}{A^2 + B^2 - 1/n_o^{\,4}(n^2 + k^2)^2\cos^2\phi} \tag{24}$$

$$\tan\Delta = -\frac{2B\sin\phi\tan\phi}{A^2 + B^2 - \sin^2\phi\tan^2\phi} \tag{21}$$

$$\tan^2\psi = \frac{A^2 + B^2 - 2A\sin\phi\tan\phi + \sin^2\phi\tan^2\phi}{A^2 + B^2 + 2A\sin\phi\tan\phi + \sin^2\phi\tan^2\phi} = \frac{R_p^{\,2}}{R_s^{\,2}} \tag{22}$$

2. Variables Employed in the Program

Name	Symbol	Description
TNO	n_o	refractive index of transparent incident medium
TN	n	real part of the complex refractive index of metal
TK	k	index of extinction
A	A	intermediate variable
B	B	intermediate variable
RS	R_s	modulus of the complex Fresnel reflection coefficient for the s polarization
RP	R_p	modulus of the complex Fresnel reflection coefficient for the p polarization
PHID	ϕ (degrees)	angle of incidence
PHI	ϕ (radians)	angle of incidence
DELD	Δ (degrees)	relative phase change $\delta_p - \delta_s$
DEL	Δ (radians)	relative phase change
TAND	$\tan \Delta$	
DELP	δ_p (radians)	"absolute" phase change with respect to incident wave (p polarization)
DELPD	δ_p (degrees)	" "
DELS	δ_s (radians)	"absolute" phase change with respect to incident wave (s polarization)
DELSD	δ_s (degrees)	" "
TANDP	$\tan \delta_p$	
TANDS	$\tan \delta_s$	
PSID	ψ (degrees)	arctangent of relative amplitude attenuation
PSI	ψ (radians)	" "
TAPSI	$\tan \psi$	relative amplitude attenuation of p to s polarization

3. Input Data for Program "MER"

The input data for the program MER are punched on cards as illustrated below

Card	Col. 1	Col. 11	Col. 21	Col. 31	Col. 41	Col. 51	Col. 61
1	Title and comments (up to 80 columns may be used)						
2	n_o						
3	n	k					
4	ϕ_1	ϕ_2	ϕ_3	ϕ_4	ϕ_5	ϕ_6	ϕ_7

Card 1 is printed verbatim on the first page of the printout. Cards 2, 3 and 4 constitute a set of input data. Any number of sets may follow the first one. The last set of cards must be followed by a blank card.

The program together with a sample output is reproduced on the following pages.

```
      PROGRAM MER (INPUT,OUTPUT)
C MER METALLIC REFLECTION
      DIMENSION PHI(7),PHID(7),ASQ(7),A(7),BSQ(7),B(7),RPSQ(7),
     CRP(7),RSSQ(7),RS(7),TAND(7),DEL(7),DELD(7),TANDS(7),DELS(7),
     CDELSD(7),TANDP(7),DELP(7),DELPD(7),TAPSI(7),PSI(7),PSID(7)
      DIMENSION TITLE (8)
    1 FORMAT (8A10)
    2 FORMAT (2F10.0)
    3 FORMAT (///)
    4 FORMAT (7F10.0)
    5 FORMAT (/48X,4HTN =,F7.4,10X,4HTK =,F7.4)
    6 FORMAT (///5X,4HPHID,8X,1HA,9X,1HB,8X,2HRS,8X,2HRP,7X,5HTANDS,5X,
     X5HTANDP,5X,4HTAND,5X,5HTAPSI,5X,5HDELSD,5X,5HDELPD,5X,4HDELD, 7X,
     X4HPSID/(1H ,13F10.5))
    7 FORMAT (1H1)
    8 FORMAT (1H1, ////8A10)
   10 FORMAT (59X,5HTNO =,F7.4)
   11 FORMAT (F10.5)
    9 READ 1, TITLE
      PRINT 8, TITLE
      N = 0
   20 READ 11, TNO
      IF(TNO.EQ.0.0) GO TO 310
      READ 2, TN , TK
      N = N + 1
      IF (N.EQ.4) GO TO 40
      GO TO 50
   40 PRINT 7
      N = 1
   50 CONTINUE
      READ 4, (PHID(M),M=1,7)
      DO 100 M=1,7
      PHI(M)=PHID(M)*0.01745329252
  100 CONTINUE
      DO 200 M=1,7
      SX=SIN (PHI(M))
      CX=COS (PHI(M))
      TX=SX/CX
      TEMP1 = TN**2-TK**2-TNO**2*SX**2
      TEMP2=TEMP1**2+4.0*TN**2*TK**2
      ASQ(M) = (SQRT(TEMP2)+TEMP1)/(2.0*TNO**2)
      IF(ASQ(M))110,112,112
  110 A(M)=0
      GO TO 114
  112 A(M)=SQRT (ASQ(M))
  114 BSQ(M) = (SQRT(TEMP2)-TEMP1)/(2.0*TNO**2)
      IF(BSQ(M))116,118,118
  116 B(M)=0
      GO TO 120
  118 B(M)=SQRT (BSQ(M))
  120 RSSQ(M)=(ASQ(M)+BSQ(M)-2.0*A(M)*CX+CX*CX)/(ASQ(M)+BSQ(M)+2.0*A(M)
     C*CX+CX*CX)
      IF(RSSQ(M))122,124,124
  122 RS(M)=0
      GO TO 126
```

```
124 RS(M)= SQRT (RSSQ(M))
126 RPSQ(M)=RSSQ(M)*(ASQ(M)+BSQ(M)-2.0*A(M)*SX*TX+SX*SX*TX*TX)/(ASQ(M)
   C+BSQ(M)+2.0*A(M)*SX*TX+SX*SX*TX*TX)
    IF(RPSQ(M))128,130,130
128 RP(M)=0
    GO TO 132
130 RP(M)= SQRT (RPSQ(M))
132 TEMP1=2.0*B(M)*CX
    TEMP2=ASQ(M)+BSQ(M)-CX*CX
    TANDS(M)=-TEMP1/TEMP2
    DELS(M) = ATAN (-TEMP1/TEMP2)
    DELSD(M)=DELS(M)/0.01745329252
    IF(DELSD(M)) 133, 133, 134
133 DELSD(M) = DELSD(M) + 180.0
134 CONTINUE
    TEMP3=2.0*B(M)*CX*(ASQ(M)+BSQ(M)-SX*SX)
    TEMP4=(ASQ(M)+BSQ(M))-((1.0/TNO**4)*(TN**2+TK**2)**2*CX**2)
    TANDP(M)=+TEMP3/TEMP4
    TEMP5=2.0*B(M)*SX*TX
    TEMP6=ASQ(M)+BSQ(M)-SX*SX*TX*TX
    TAND(M)=-TEMP5/TEMP6
    DEL(M) = ATAN (-TEMP5/TEMP6)
    DELD(M)=DEL(M)/0.01745329252
    IF(DELD(M)) 136, 135, 135
136 DELD(M) = DELD(M) + 180.0
135 CONTINUE
    DELPD(M) = DELSD(M) + DELD(M)
    TAPSI(M)=RP(M)/RS(M)
    PSI(M)=ATAN (TAPSI(M))
    PSID(M)=PSI(M)/0.01745329252
200 CONTINUE
    PRINT 10, TNO
    PRINT 5, TN, TK
    PRINT 6,(PHID(M),A(M),B(M),RS(M),RP(M),TANDS(M),TANDP(M),TAND(M)
   X,TAPSI(M),DELSD(M),DELPD(M),DELD(M),PSID(M),M=1,7)
250 PRINT 3
300 GO TO 20
310 CONTINUE
    END
```

PROGRAM MER -- SAMPLE OUTPUT

TNO = 1.0000

TN = .1000 TK = .2000

PHID	A	B	RS	RP	TANDS	TANDP	TAND	TAPSI	DELSD	DELPD	DELD	PSID
2.00000	.09880	.20243	.82661	.82269	.42679	.41535	-.00972	.99527	23.11252	202.55536	179.44283	44.86404
40.00000	.03001	.66639	.95639	.91520	7.19770	.07321	-4.66590	.95693	82.09034	184.18702	102.09668	43.73924
45.00000	.02745	.72853	.96304	.92745	-32.70020	.06122	-32.70020	.96304	91.75161	183.50322	91.75161	43.92150
50.00000	.02545	.78579	.96876	.93823	-4.92914	.05123	6.66238	.96848	101.46824	182.93283	81.46459	44.08268
70.00000	.02093	.95575	.98621	.97225	-.82037	.02209	.85802	.98584	140.63545	181.26572	40.63027	44.59159
75.00000	.02038	.98154	.98982	.97946	-.56652	.01625	.58819	.98953	150.46769	180.93125	30.46356	44.69850
80.00000	.02000	1.00012	.99328	.98642	-.35790	.01069	.37031	.99309	160.30772	180.61258	20.30486	44.80123

TNO = 1.0000

TN = 1.0000 TK = .3000

PHID	A	B	RS	RP	TANDS	TANDP	TAND	TAPSI	DELSD	DELPD	DELD	PSID
2.00000	.99944	.30017	.14851	.14817	-6.65145	-6.68198	-.00067	.99777	98.54999	278.51150	179.96151	44.93591
40.00000	.79869	.37561	.23430	.07695	-2.99458	2.57391	-.83015	.32843	108.46603	248.76813	140.30210	18.18158
45.00000	.75389	.39794	.26461	.07002	-2.48237	.96176	-2.48237	.26461	111.94159	223.88318	111.94159	14.82126
50.00000	.70876	.42328	.30247	.08481	-2.02797	.27029	5.08612	.28039	116.24814	195.12490	78.87675	15.66320
70.00000	.56017	.53555	.55117	.36166	-.75748	-.22412	.45595	.65616	142.85686	167.36757	24.51071	33.27112
75.00000	.53732	.55833	.64164	.47865	-.54177	-.18454	.32477	.74598	151.55241	169.54445	17.99204	36.72232
80.00000	.52112	.57568	.74524	.61928	-.34903	-.12933	.21021	.83097	160.75946	172.63090	11.87144	39.72565

TNO = 1.0000

TN = .2000 TK = 4.0000

PHID	A	B	RS	RP	TANDS	TANDP	TAND	TAPSI	DELSD	DELPD	DELD	PSID
2.00000	.19999	4.00015	.97681	.97678	-.53153	-.53230	-.00061	.99997	152.00823	331.97341	179.96517	44.99913
40.00000	.19747	4.05119	.98240	.96998	-.39124	-.73995	-.27042	.98736	158.63253	323.50027	164.86776	44.63549
45.00000	.19695	4.06187	.98378	.96783	-.35818	-.82179	-.35818	.98378	160.29346	320.58691	160.29346	44.53164
50.00000	.19644	4.07252	.98529	.96525	-.32297	-.93627	-.47091	.97966	162.10136	316.88522	154.78386	44.41137
70.00000	.19471	4.10864	.99221	.95078	-.16727	-3.42013	-2.06913	.95824	170.50396	286.29823	115.79427	43.77837
75.00000	.19442	4.11471	.99411	.94864	-.12602	-128.40848	-7.46613	.95426	172.81749	270.44619	97.62870	43.65932
80.00000	.19421	4.11917	.99605	.95218	-.08427	2.48071	3.24296	.95596	175.18280	248.04513	72.86233	43.71013

TNO = 1.5000

TN = 1.5000 TK = .3000

PHID	A	B	RS	RP	TANDS	TANDP	TAND	TAPSI	DELSD	DELPD	DELD	PSID
2.00000	.99941	.20012	.09962	.09939	-9.97637	-10.02379	-.00047	.99766	95.72403	275.69713	179.97310	44.93283
40.00000	.79241	.25562	.16321	.04276	-4.31868	2.41879	-.71326	.26200	103.03721	247.53834	144.50113	14.68159
45.00000	.73130	.27349	.18752	.03516	-3.52923	.61616	-3.52923	.18752	105.81996	211.63991	105.81996	10.62050
50.00000	.67832	.29485	.21940	.05108	-2.83146	-.15054	1.87969	.23284	109.45196	171.43893	61.98696	13.10694
70.00000	.49210	.40642	.46693	.32059	-.95746	-.47093	.33533	.68658	136.24488	154.78285	18.53797	34.47286
75.00000	.46255	.43239	.56833	.44072	-.67028	-.36259	.24753	.77547	146.16682	160.06966	13.90284	37.79256
80.00000	.44174	.45275	.68871	.58837	-.42501	-.24376	.16423	.85430	156.97415	166.30082	9.32667	40.50731

TNO = 1.5000

TN = .3000 TK = 4.0000

PHID	A	B	RS	RP	TANDS	TANDP	TAND	TAPSI	DELSD	DELPD	DELD	PSID
2.00000	.19998	2.66689	.95211	.95204	-.86626	-.86785	-.00091	.99993	139.09904	319.04697	179.94793	44.99805
40.00000	.19446	2.74264	.96407	.93865	-.60260	-1.33770	-.40701	.97363	148.92689	306.78004	157.85316	44.23446
45.00000	.19335	2.75835	.96698	.93504	-.54589	-1.55526	-.54589	.96698	151.37012	302.74024	151.37012	44.03817
50.00000	.19226	2.77397	.97010	.93112	-.48727	-1.90190	-.73421	.95982	154.02162	297.73498	143.71336	43.82554
70.00000	.18868	2.82661	.98427	.92102	-.24449	6.75863	-10.73438	.93574	166.26126	261.58364	95.32238	43.09873
75.00000	.18810	2.83540	.98811	.92643	-.18328	2.25460	4.15474	.93758	169.61393	246.08088	76.46695	43.15485
80.00000	.18767	2.84186	.99203	.94046	-.12213	1.07293	1.37527	.94801	173.03691	227.01492	53.97801	43.47134

TNO = 1.5000

TN = 1.5000 TK = .4500

PHID	A	B	RS	RP	TANDS	TANDP	TAND	TAPSI	DELSD	DELPD	DELD	PSID
2.00000	.99944	.30017	.14851	.14817	-6.65145	-6.68198	-.00067	.99777	98.54999	278.51150	179.96151	44.93591
40.00000	.79869	.37561	.23430	.07695	-2.99458	2.57391	-.83015	.32843	108.46603	248.76813	140.30210	18.18158
45.00000	.75389	.39794	.26461	.07002	-2.48237	.96176	-2.48237	.26461	111.94159	223.88318	111.94159	14.82126
50.00000	.70876	.42328	.30247	.08481	-2.02797	.27029	5.08612	.28039	116.24814	195.12490	78.87675	15.66320
70.00000	.56017	.53555	.55117	.36166	-.75748	-.22412	.45595	.65616	142.85686	167.36757	24.51071	33.27112
75.00000	.53732	.55833	.64164	.47865	-.54177	-.18454	.32477	.74598	151.55241	169.54445	17.99204	36.72232
80.00000	.52112	.57568	.74524	.61928	-.34903	-.12933	.21021	.83097	160.75946	172.63090	11.87144	39.72565

D. FORTRAN IV Computer Program "LAYER"

The program "LAYER" finds the thickness and complex refractive index of a single, absorbing film on an absorbing substrate. It does so by systematically combining all prescribed values of film thickness L and refractive index $n_f - ik_f$ and calculating the Δ and ψ for each combination. Whenever a particular combination of L, n_f and k_f yields agreement with the experimentally determined quantities Δ and ψ within a specified error ε_Δ and ε_ψ, this combination appears in the output as a solution.

1. Equations Evaluated by the Program

$$\cos \phi'_m = \sqrt{1 - \frac{n_o^2 \sin^2 \phi}{n_{cm}^2}} \tag{38}$$

$$\cos \phi' = \sqrt{1 - \frac{n_o^2 \sin^2 \phi}{n_{cf}^2}} \tag{37}$$

$$r_{1s} = \frac{n_o \cos \phi - n_{cf} \cos \phi'}{n_o \cos \phi + n_{cf} \cos \phi'} \tag{33}$$

$$r_{1p} = \frac{n_{cf} \cos \phi - n_o \cos \phi'}{n_{cf} \cos \phi + n_o \cos \phi'} \tag{34}$$

$$r_{2s} = \frac{n_{cf} \cos \phi' - n_{cm} \cos \phi'_m}{n_{cf} \cos \phi' + n_{cm} \cos \phi'_m} \tag{35}$$

$$r_{2p} = \frac{n_{cm} \cos \phi' - n_{cf} \cos \phi'_m}{n_{cm} \cos \phi' + n_{cf} \cos \phi'_m} \tag{36}$$

$$d = \frac{4\pi L}{\lambda_o} n_{cf} \cos \phi' \qquad (31)$$

$$r_s = \frac{r_{1s} + r_{2s} e^{-id}}{1 + r_{1s} r_{2s} e^{-id}} \qquad (29)^*$$

$$r_p = \frac{r_{1p} + r_{2p} e^{-id}}{1 + r_{1p} r_{2p} e^{-id}} \qquad (30)^*$$

$$\rho = \frac{r_p}{r_s} \qquad (3)$$

$$\tan \Delta = \mathrm{Im}(\rho)/\mathrm{Re}(\rho) \qquad \text{from (6)}$$

$$\tan \psi = |\rho| \qquad \text{from (6)}$$

$$\Delta = \tan^{-1} (\tan \Delta)$$

$$\psi = \tan^{-1} (\tan \psi)$$

2. Variables Used in the Program

a. Real Quantities

Name	Symbol	Description
DELM	Δ (measured)	relative phase change (degrees)
DELC	Δ (calculated)	relative phase change (degrees)
DTN	δn_f	iteration increment of film refractive index n_f
DTNK	δk_f	iteration increment of index of extinction of film
DT	δL	iteration increment of film thickness L

*No error arises from dropping the common phase factor e^{id_o} appearing in Eqs. (29) and (30).

Name	Symbol	Description
EPSIM	ε_ψ	specified experimental error in ψ (degrees)
EDELM	ε_Δ	specified experimental error in Δ (degrees)
PHI1	ϕ (degrees)	angle of incidence
PHI	ϕ (radians)	angle of incidence
PSIM	ψ (measured)	arctangent of relative amplitude attenuation (degrees)
PSIC	ψ (calculated)	arctangent of relative amplitude attenuation (degrees)
TN1	n_o	refractive index of incident medium
TNS	n_m	refractive index of substrate
TNKS	k_m	index of extinction of substrate
TNI	n_{fi}	lower limit of iteration span of film index n_f
TN	n_f	refractive index of film
TNM	n_{fm}	upper limit of iteration span of film index n_f
TNKI	k_{fi}	lower limit of iteration span of k_f of film
TNK	k_f	index of extinction of film
TNKM	k_{fm}	upper limit of iteration span of k_f of film
TI	L_i	lower limit of iteration span for film thickness L
T	L	film thickness (units as for λ_o)
TM	L_m	upper limit of iteration span of film thickness
WL	λ_o	vacuum wavelength (units as for λ_o, preferably in angstroms)

b. Complex Quantities

Name	Symbol	Description
CPHI2	$\cos \phi'$	complex cosine of complex angle of refraction in film
CPHI3	$\cos \phi'_m$	complex cosine of complex angle of refraction in substrate
D	id	complex optical path length
R1S	r_{1s}	Fresnel reflection coefficient at film-air (or incident medium) interface. (For polarization normal to plane of incidence)
R1P	r_{1p}	Fresnel reflection coefficient at film-air (or incident medium) interface. (For polarization parallel to plane of incidence)
R2S	r_{2s}	Fresnel reflection coefficient at metal-film interface (normal polarization)
R2P	r_{2p}	Fresnel reflection coefficient at metal-film interface (parallel polarization)
RS	r_s	overall reflection coefficient for polarization normal to plane of incidence.
RP	r_p	overall reflection coefficient for polarization parallel to plane of incidence.
RHO	$\rho = r_p/r_s = \tan \psi \, e^{i\Delta}$	
TN3	$n_m - ik_m$	complex refractive index of substrate
TN2	$n_f - ik_f$	complex refractive index of film

3. Fortran Functions Used in the Program

Name	Evaluates	Converts
CSQRT (C)	$\sqrt{C}$	complex to complex
CEXP (C)	e^c	complex to complex
CABS (C)	$\lvert C \rvert$	complex to real
AIMAG (C)	finds the imaginary part of C	complex to real
REAL (C)	finds the real part of C	complex to real
COS (X)	cos X	real to real

Name	Evaluates	Converts
SIN (X)	sin X	real to real
ATAN (X)	$\tan^{-1}$ X	real to real
ATAN2 (X,Y)	$\tan^{-1}$ (x/y)	real to real
ABS (X)	|X|	real to real
CMPLX (A,B)	constructs A + iB from A,B	real to complex

Where C is complex, A, B, X, Y are real

4. Input Format for Program "LAYER"

Card	Col. 1	Col. 10	Col. 20	Col. 30	Col. 40	Col. 50
1 } 2 }	Title and comments (up to 80 columns each)					
3	n_o	λ_o	n_m	k_m		
4	n_{fi} (initial)	δn_f (increment)	n_{fm} (final)	k_{fi} (initial)	δk_f (increment)	k_{fm} (final)
5	L_i (initial)	δL (increment)	L_m (final)			
6	ϕ	ψ	Δ	ε_ψ	ε_Δ	

These six cards constitute a set. Any number of sets may follow. Three blank cards must follow the last set of data. Cards 1 and 2 of each set may contain any comments (or none at all) as desired. Their contents appear printed verbatim at the head of the output.

This program can be used to calculate theoretical values of Δ and ψ, with changes in film thickness or with different film constants, by punching numbers greater than (or equal to) 90 for ε_ψ and a number greater than (or equal to) 360 for ε_Δ. Entries for ψ and Δ can be blank or any values such as 0.0.

The program, together with a sample of output, is reproduced on the following pages.

```
      PROGRAM LAYER (INPUT,OUTPUT)
C     THIS PROGRAM CALCULATES THE THICKNESS AND COMPLEX REFRACTIVE
C     INDEX OF A SINGLE ABSORBING FILM ON AN ABSORBING SUBSTRATE
      COMPLEX TN2, TN3, CPHI2, CPHI3, R1S, R1P, R2S, R2P, D, RS, RP, RHO
      DIMENSION TITLE (8), RANGE (8)
    1 READ 2, TITLE,RANGE
    2 FORMAT (8A10/8A10)
    3 PRINT 4, TITLE,RANGE
    4 FORMAT (1H1, 8A10//8A10)
    5 READ 9, TN1,WL,TNS,TNKS
      IF (TN1) 3000, 3000, 6
    6 READ 10, TNI,DTN,TNM,TNKI,DTNK,TNKM
    7 READ 11, TI,DT,TM
    8 READ 12, PHI1,PSIM,DELM,EPSIM,EDELM
    9 FORMAT (F9.0, 3F10.0)
   10 FORMAT (F9.0, 5F10.0)
   11 FORMAT (F9.0, 2F10.0)
   12 FORMAT (F9.0, 4F10.0)
   13 FORMAT (1H0,/6HPHI = ,F5.2,10X,4HN = ,F7.4, 10X, 13HWAVELENGTH = ,
     C F5.0, 11H  ANGSTROMS//33H REFRACTIVE INDEX OF SUBSTRATE = , F7.4,
     C 2X, 4H-  I, F7.4)
   14 FORMAT (1H0, 27HREFRACTIVE INDEX OF FILM = , F7.4, 2X,
     C 4H-  I, F7.4//18H FILM THICKNESS = , F7.2, 10H ANGSTROMS,
     C //8H PSIC = , F10.5, 10X, 7HDELC = , F10.5,
     C //8H PSIM = , F10.5, 10X, 7HDELM = , F10.5)
   15 FORMAT (1H0, 7HPSIM = , F10.5,10X,  7HDELM = , F10.5//32H NO SOLUT
     CION WITHIN GIVEN LIMITS)
      M = 1
      PHI = 0.01745329252*PHI1
      CP = COS(PHI)
      SP = SIN(PHI)
      TN3 = CMPLX(TNS,-TNKS)
      CPHI3 = CSQRT(1.0 - TN1**2*SP**2/(TN3**2))
      TN = TNI
   20 TNK = TNKI
   30 T = TI
  100 TN2 = CMPLX(TN,-TNK)
      CPHI2 = CSQRT(1.0 - TN1**2*SP**2/(TN2**2))
      R1S = (TN1*CP - TN2*CPHI2)/(TN1*CP + TN2*CPHI2)
      R1P =-(TN1*CPHI2 - TN2*CP)/(TN1*CPHI2 + TN2*CP)
      R2S = (TN2*CPHI2 - TN3*CPHI3)/(TN2*CPHI2 + TN3*CPHI3)
      R2P =-(TN2*CPHI3 - TN3*CPHI2)/(TN2*CPHI3 + TN3*CPHI2)
      D = (0.0,1.0)*(4.0*3.1415927*T/WL)*TN2*CPHI2
      RS= (R1S + R2S*CEXP(-D))/(1.0 + R1S*R2S*CEXP(-D))
      RP = (R1P + R2P*CEXP(-D))/(1.0 + R1P*R2P*CEXP(-D))
      RHO = RP/RS
      PSIC = ATAN(CABS(RHO))/0.01745329252
      DELC = ATAN2(AIMAG(RHO), REAL(RHO))/0.01745329252
      IF (DELC) 140,140,150
  140 DELC = DELC + 360.00
  150 IF (EPSIM - ABS(PSIC - PSIM)) 400, 200, 200
  200 IF (EDELM - ABS(DELC - DELM)) 400, 300, 300
  300 PRINT 13, PHI1,TN1,WL,TNS,TNKS
      PRINT 14, TN,TNK,T,PSIC,DELC,PSIM,DELM
      M = 2
```

```
 400 IF(TM -T) 600,600,500
 500 T = T + DT
     GO TO 100
 600 IF(TNKM - TNK) 800,800,700
 700 TNK = TNK + DTNK
     GO TO 30
 800 IF(TNM - TN) 1000,1000,900
 900 TN = TN + DTN
     GO TO 20
1000 GO TO (2000, 1) M
2000 PRINT 13, PHI1,TN1,WL,TNS,TNKS
     PRINT 15, PSIM,DELM
     GO TO 1
3000 CONTINUE
     END
```

```
 SAMPLE OUTPUT  -- PROGRAM  LAYER
TRANSPARENT FILM ON ABSORBING SUBSTRATE   TANTALUM OXIDE ON TANTALUM

PHI = 75.00          N =  1.0000          WAVELENGTH =  5461  ANGSTROMS
 REFRACTIVE INDEX OF SUBSTRATE =  3.5000  -  I 2.4000
 REFRACTIVE INDEX OF FILM =  2.2600  -  I 0.
 FILM THICKNESS =    0.   ANGSTROMS
 PSIC =   18.38686          DELC =  104.82163
 PSIM =   18.38000          DELM =  104.82000

PHI = 75.00          N =  1.0000          WAVELENGTH =  5461  ANGSTROMS
 REFRACTIVE INDEX OF SUBSTRATE =  3.5000  -  I 2.4000
 REFRACTIVE INDEX OF FILM =  2.2600  -  I 0.
 FILM THICKNESS =  100.00 ANGSTROMS
 PSIC =   23.86772          DELC =   79.89817
 PSIM =   18.38000          DELM =  104.82000

PHI = 75.00          N =  1.0000          WAVELENGTH =  5461  ANGSTROMS
 REFRACTIVE INDEX OF SUBSTRATE =  3.5000  -  I 2.4000
 REFRACTIVE INDEX OF FILM =  2.2600  -  I 0.
 FILM THICKNESS =  200.00 ANGSTROMS
 PSIC =   28.77966          DELC =   62.11156
 PSIM =   18.38000          DELM =  104.82000

PHI = 75.00          N =  1.0000          WAVELENGTH =  5461  ANGSTROMS
 REFRACTIVE INDEX OF SUBSTRATE =  3.5000  -  I 2.4000
 REFRACTIVE INDEX OF FILM =  2.2600  -  I 0.
 FILM THICKNESS =  300.00 ANGSTROMS
 PSIC =   33.66301          DELC =   48.15683
 PSIM =   18.38000          DELM =  104.82000

PHI = 75.00          N =  1.0000          WAVELENGTH =  5461  ANGSTROMS
 REFRACTIVE INDEX OF SUBSTRATE =  3.5000  -  I 2.4000
 REFRACTIVE INDEX OF FILM =  2.2600  -  I 0.
```

```
 FILM THICKNESS =  400.00 ANGSTROMS
 PSIC =   40.23194          DELC =   34.38292
 PSIM =   18.38000          DELM =  104.82000

PHI = 75.00          N =  1.0000          WAVELENGTH =  5461  ANGSTROMS
 REFRACTIVE INDEX OF SUBSTRATE =  3.5000  -  I 2.4000
 REFRACTIVE INDEX OF FILM =  2.2600  -  I 0.
 FILM THICKNESS =  500.00 ANGSTROMS
 PSIC =   48.60562          DELC =    8.70889
 PSIM =   18.38000          DELM =  104.82000

PHI = 75.00          N =  1.0000          WAVELENGTH =  5461  ANGSTROMS
 REFRACTIVE INDEX OF SUBSTRATE =  3.5000  -  I 2.4000
 REFRACTIVE INDEX OF FILM =  2.2600  -  I 0.
 FILM THICKNESS =  600.00 ANGSTROMS
 PSIC =   45.54824          DELC =  330.96808
 PSIM =   18.38000          DELM =  104.82000

PHI = 75.00          N =  1.0000          WAVELENGTH =  5461  ANGSTROMS
 REFRACTIVE INDEX OF SUBSTRATE =  3.5000  -  I 2.4000
 REFRACTIVE INDEX OF FILM =  2.2600  -  I 0.
 FILM THICKNESS =  700.00 ANGSTROMS
 PSIC =   36.58898          DELC =  311.26812
 PSIM =   18.38000          DELM =  104.82000

PHI = 75.00          N =  1.0000          WAVELENGTH =  5461  ANGSTROMS
 REFRACTIVE INDEX OF SUBSTRATE =  3.5000  -  I 2.4000
 REFRACTIVE INDEX OF FILM =  2.2600  -  I 0.
 FILM THICKNESS =  800.00 ANGSTROMS
 PSIC =   30.26527          DELC =  297.05548
 PSIM =   18.38000          DELM =  104.82000

PHI = 75.00          N =  1.0000          WAVELENGTH =  5461  ANGSTROMS
```

```
REFRACTIVE INDEX OF SUBSTRATE =  3.5000  -  I 2.4000
REFRACTIVE INDEX OF FILM =  2.2600  -  I 0.
FILM THICKNESS =  900.00 ANGSTROMS
PSIC =   24.81020          DELC =  280.02744
PSIM =   18.38000          DELM =  104.82000

PHI = 75.00          N =  1.0000          WAVELENGTH =  5461  ANGSTROMS
REFRACTIVE INDEX OF SUBSTRATE =  3.5000  -  I 2.4000
REFRACTIVE INDEX OF FILM =  2.2600  -  I 0.
FILM THICKNESS = 1000.00 ANGSTROMS
PSIC =   19.10487          DELC =  256.27882
PSIM =   18.38000          DELM =  104.82000
```

E. FORTRAN IV Computer Program "SFILM"

The program "SFILM" employs a different iteration scheme from the program "LAYER" in that, rather than assuming a film thickness, this quantity is calculated from measured values of ψ and Δ with the assumed complex film index $n_f - ik_f$. Like the program "LAYER", "SFILM" finds the thickness and complex refractive index of a single, absorbing film on an absorbing substrate. It does so by making successive iterations of film index and calculating L, Δ, and ψ for each guess until agreement is reached with the experimentally determined quantities Δ and ψ (within specified error ε_Δ and ε_ψ).

1. Equations Evaluated by the Program

$$\cos \phi_m' = \sqrt{1 - \frac{n_o^2 \sin^2 \phi}{n_{cm}^2}} \tag{38}$$

$$\cos \phi_m' = \sqrt{1 - \frac{n_o^2 \sin^2 \phi}{n_{cf}^2}} \tag{37}$$

$$r_{1s} = \frac{n_o \cos \phi - n_{cf} \cos \phi'}{n_o \cos \phi + n_{cf} \cos \phi'} \tag{33}$$

$$r_{1p} = \frac{n_{cf} \cos \phi - n_o \cos \phi'}{n_{cf} \cos \phi + n_o \cos \phi'} \tag{34}$$

$$r_{2s} = \frac{n_{cf} \cos \phi' - n_{cm} \cos \phi_m'}{n_{cf} \cos \phi' + n_{cm} \cos \phi_m'} \tag{35}$$

$$r_{2p} = \frac{n_{cm} \cos \phi' - n_{cf} \cos \phi'_m}{n_{cm} \cos \phi' + n_{cf} \cos \phi'_m} \tag{36}$$

$$\rho_{meas} = \tan \psi_{meas} \, e^{i\Delta_{meas}} \tag{6}$$

$$A = (\rho r_{1p} - r_{1s}) \, r_{2s} \, r_{2p} \tag{50*}$$

$$B = \rho(r_{1p} \, r_{1s} \, r_{2p} + r_{2s}) - (r_{1s} \, r_{1p} \, r_{2s} + r_{2p}) \tag{51*}$$

$$C = \rho r_{1s} - r_{1p} \tag{52*}$$

$$X = [B^2 - 4 \, AC]^{1/2} \tag{53*}$$

$$E_{1,2} = (-B \pm X)/(2A) \tag{54*}$$

$$L_{1,2} = \frac{\lambda_o}{4\pi \, n_{cf} \cos \phi'} \left[-\tan^{-1}\left(\frac{\mathrm{Im}\, E_{1,2}}{\mathrm{Re}\, E_{1,2}} \right) + i \, \mathrm{Log} \, |E_{1,2}| \right] \tag{55*}$$

L = real part of L_1 or L_2, which ever has smaller imaginary part.

$$d = \frac{4\pi L}{\lambda_o} \, n_{cf} \cos \phi' \tag{31}$$

$$r_s = \frac{r_{1s} + r_{2s} \, e^{-id}}{1 + r_{1s} \, r_{2s} \, e^{-id}} \tag{29}$$

---

* These equations are obtained by applying complex algebra to Eq. (3) with the help of Eqs. (29), (30), and (31), (Ref. 11, 12, 2). A and B on this page are intermediate variables for the evaluation of the film thickness. They are not related to A and B of Eqs. (19) and (20).

$$r_p = \frac{r_{1p} + r_{2p}\, e^{-id}}{1 + r_{2p}\, r_{1p}\, e^{-id}} \qquad (30)^*$$

$$\rho = \frac{r_p}{r_s} \qquad (3)$$

$$\tan \Delta = \mathrm{Im}(\rho)/\mathrm{Re}(\rho) \qquad \text{from (6)}$$

$$\tan \psi = |\rho| \qquad \text{from (6)}$$

$$\Delta = \tan^{-1}(\tan \Delta)$$

$$\psi = \tan^{-1}(\tan \psi)$$

2. Variables Used in the Program

a. Real Quantities

Name	Symbol	Description
CDR	0.01745329252	conversion factor, degrees to radians
DELC	Δ (calculated)	relative phase change (degrees)
DELM	Δ (measured)	relative phase change (degrees)
DN	δn_f	iteration increment of film refractive index n_f
DNK	δk_f	interation increment of film index of extinction k_f
EDELM	ε_Δ	experimental error in Δ (degrees)
EPSIM	ε_ψ	experimental error in ψ (degrees)
ERROR		imaginary part of film thickness
P	$\lambda_o/4\pi$	

*Again, the common factor e^{id_o} in Eqs. (29) and (30) is dropped without introducing any error.

Name	Symbol	Description
PHI	ϕ	angle of incidence (degrees)
PSIC	ψ (calculated)	arctangent of relative amplitude attenuation (degrees)
PSIM	ψ (measured)	" "
N	n_f	real part of film complex refractive index
N1	n_o	refractive index of incident medium
NI	n_{fi}	lower limit of iteration span of n_f of film
NK	k_f	imaginary part of film complex refractive index
NKI	k_{fi}	lower limit of iteration span of k_f of film
NM	n_{fm}	upper limit of iteration span of n_f of film
NKM	k_{fm}	upper limit of iteration span of k_f of film
NS	n_m	real part of the complex refractive index of substrate
NKS	k_m	index of extinction of substrate
T	L	film thickness (same units as λ_o)
WL	λ_o	vacuum wavelength (same units as L, preferably in angstroms)

b. Complex Variables

Name	Symbol	Description
A	A	intermediate variable
B	B	intermediate variable
C	C	intermediate variable
CPHI2	$\cos \phi'$	cosine of complex angle of refraction in film
CPHI3	$\cos \phi'_m$	cosine of complex angle of refraction in substrate
D	-id-	complex optical path length

Name	Symbol	Description
E1,E2	e^{-id}	
I	$\sqrt{-1} = i$	imaginary unit
N2	$n_f - ik_f$	complex refractive index of film
N3	$n_m - ik_m$	complex refractive index of substrate
R1S	r_{1s}	Fresnel reflection coefficient at film-air (or incident medium) interface for polarization normal to plane of incidence
R1P	r_{1p}	Fresnel reflection coefficient at film-air (or incident medium) interface for polarization parallel to plane incidence
R2S	r_{2s}	Fresnel reflection coefficient at film-substrate interface for polarization normal to plane of incidence.
R2P	r_{2p}	Fresnel reflection coefficient at film-substrate interface for polarization parallel to plane of incidence.
RS	r_s	overall reflection coefficient for polarization normal to the plane of incidence
RP	r_p	overall reflection coefficient for polarization parallel to the plane of incidence
RHO	$\rho=r_p/r_s=\tan\psi\, e^{i\Delta}$ (caluclated)	complex relative amplitude attenuation
RHOM	$\rho=r_p/r_s=\tan\psi\, ^{i\Delta}$ (measured)	" "
T1,T2	L_1,L_2	calculated complex film thickness

3. Fortran Functions Used in the Program

See Appendix I-D Fortran Program "LAYER"

4. Input Format for the Program "SFILM"

Card	Col. 1	Col. 10	Col. 20	Col. 30	Col. 40	Col. 50
1, 2	Title and comments (up to 80 columns each)					
3.	n_o	λ_o	n_m	k_m		
4.	n_{fi} (initial)	δn_f (increment)	n_{fm} (final)	k_{fi} (initial)	δk_f (increment)	k_{fm} (final)
5.	ϕ	ψ	Δ	ε_ψ	ε_Δ	

These five cards constitute a set. Any number of sets may follow. Three blank cards must follow card 5 of the last set of data. All numbers punched on cards 3 through 5 should contain a decimal point and may be located anywhere in the field of column 1-9, 10-19, etc.

A reproduction of the program SFILM appears after the next page, followed by a sample output. The output also gives the calculated imaginary part of the film thickness. The set of output which gives the smallest imaginary part of the film thickness (ideally zero) is taken as the correct one.

5. A Note To Program "SFILM"

The program SFILM as it stands now is not very useful in calculating the film thickness from experimental values of ψ and Δ. A few modifications are needed:

1. The program should be prevented to calculate negative thicknesses. In evaluating the complex exponential e^{-id}, the program will calculate a small negative film thickness rather than a correct large positive film thickness value. A scheme should be added to the program to convert the calculated small negative film thickness to the correct large film thickness.

2. The way that the input data are used now, the choice of the result with the smallest imaginary film thickness may not be absolutely correct. The program will give a smallest imaginary film thickness when the calculated ψ and Δ are identical to the input (experimental) ψ and Δ. No consideration of experimental errors ε_ψ and ε_Δ enters the calculation except to control the output of results. It is believed that if the values in increments of Δ and ψ tried within the experimental errors $\pm\varepsilon_\psi$ and $\pm\varepsilon_\Delta$ are fed as input data, a correct film thickness may be obtained from the printed results where the imaginary film thickness is the smallest.

It should be noted that the film constants are very sensitive to changes in ψ and Δ. In using the program, approximate film constants should be known.

```
      PROGRAM SFILM (INPUT,OUTPUT)
      THIS PROGRAM CALCULATES THE THICKNESS AND COMPLEX REFRACTIVE
      INDEX OF A SINGLE ABSORBING FILM ON AN ABSORBING SUBSTRATE
      COMPLEX CPHI2, CPHI3, N2, N3, R1S, R1P, R2S, R2P, RS, RP, RHO
      COMPLEX A, B, C, D, E1, E2, I, RHOM, T1, T2, X
      REAL N1, NS, NKS, NI, NM, NKI, NKM, N, NK
      DIMENSION TITLE(8), RANGE(8)
      CDR = 0.01745329252
      I = CMPLX(0.0, 1.0)
    1 READ 2, TITLE,RANGE
    2 FORMAT (8A10/8A10)
    3 PRINT 4, TITLE, RANGE
    4 FORMAT (1H1, 8A10//8A10)
    5 READ 8, N1,WL,NS,NKS
      IF (N1) 1000, 1000, 6
    6 READ 9, NI,DN,NM,NKI,DNK,NKM
    7 READ 10, PHI,PSIM,DELM,EPSIM,EDELM
    8 FORMAT (F9.0, 3F10.0)
    9 FORMAT (F9.0, 5F10.0)
   10 FORMAT (F9.0, 4F10.0)
   11 FORMAT (1H0,/6HPHI = ,F5.2,10X,4HN = ,F7.4, 10X, 13HWAVELENGTH = ,
     C F5.0, 11H  ANGSTROMS//33H REFRACTIVE INDEX OF SUBSTRATE = , F7.4,
     C 2X, 4H-  I, F7.4)
   12 FORMAT (1H0, 27HREFRACTIVE INDEX OF FILM = , F7.4, 2X,
     C 4H-  I, F7.4//18H FILM THICKNESS = , F7.2, 10H ANGSTROMS//
     C 36H IMAGINARY PART OF FILM THICKNESS = , F10.5, 10H ANGSTROMS,
     C //8H PSIC = , F10.5, 10X, 7HDELC = , F10.5,
     C //8H PSIM = , F10.5, 10X, 7HDELM = , F10.5)
   13 FORMAT (1H0, 7HPSIM = , F10.5,10X,  7HDELM = , F10.5//32H NO SOLUT
     CION WITHIN GIVEN LIMITS)
      M = 1
      N3 = CMPLX(NS,-NKS)
      RHOM = TAN(PSIM*CDR)*CEXP(I*DELM*CDR)
      SP = SIN(PHI*CDR)
      CP = COS(PHI*CDR)
      CPHI3 = CSQRT(1.0 - N1**2*SP**2/(N3**2))
      P = WL/(4.0*3.1415927)
      N = NI
   20 NK = NKI
  100 N2 = CMPLX(N,-NK)
      CPHI2 = CSQRT(1.0 - N1**2*SP**2/(N2**2))
      R1S = (N1*CP - N2*CPHI2)/(N1*CP + N2*CPHI2)
      R1P =-(N1*CPHI2 - N2*CP)/(N1*CPHI2 + N2*CP)
      R2S = (N2*CPHI2 - N3*CPHI3)/(N2*CPHI2 + N3*CPHI3)
      R2P =-(N2*CPHI3 - N3*CPHI2)/(N2*CPHI3 + N3*CPHI2)
      A = (RHOM*R1P - R1S)*R2S*R2P
      B = RHOM*(R1P*R1S*R2P + R2S) - (R1S*R1P*R2S + R2P)
      C = RHOM*R1S - R1P
      X = CSQRT(B**2 - 4.0*A*C)
      E1 = (-B + X)/(2.0*A)
      E2 = (-B - X)/(2.0*A)
      T1 =P*(-ATAN2(AIMAG(E1), REAL(E1)) + I*ALOG(CABS(E1)))/(N2*CPHI2)
      T2 =P*(-ATAN2(AIMAG(E2), REAL(E2)) + I*ALOG(CABS(E2)))/(N2*CPHI2)
      IF (ABS(AIMAG(T1)) - ABS(AIMAG(T2))) 110, 110, 120
  110 T = REAL (T1)
```

```
      ERROR = AIMAG(T1)
      GO TO 130
  120 T = REAL(T2)
      ERROR = AIMAG(T2)
  130 D =-(4.0*3.1415927*T/WL)*I*N2*CPHI2
      RS = (R1S + R2S*CEXP(D))/(1.0 + R1S*R2S*CEXP(D))
      RP = (R1P + R2P*CEXP(D))/(1.0 + R1P*R2P*CEXP(D))
      RHO = RP/RS
      PSIC = ATAN(CABS(RHO))/CDR
      DELC = ATAN2(AIMAG(RHO), REAL(RHO))/CDR
      IF (DELC) 140,140,150
  140 DELC = DELC + 360.0
  150 IF (EPSIM - ABS(PSIC - PSIM))400, 200, 200
  200 IF (EDELM - ABS(DELC - DELM))400, 300, 300
  300 PRINT 11, PHI,N1,WL,NS,NKS
      PRINT 12, N,NK,T,ERROR,PSIC,DELC,PSIM,DELM
      M = 2
  400 IF (NKM - NK) 600,600,500
  500 NK = NK + DNK
      GO TO 100
  600 IF (NM - N) 800,800,700
  700 N = N + DN
      GO TO 20
  800 GO TO (900, 1) M
  900 PRINT 11,PHI,N1,WL,NS,NKS
      PRINT 13, PSIM,DELM
      GO TO 1
 1000 CONTINUE
      END
```

SAMPLE OUTPUT

CARBON MONOXIDE ADSORPTION ON PLATINUM CRYSTAL

```
PHI = 45.00          N = 1.0000          WAVELENGTH = 5461  ANGSTROMS
 REFRACTIVE INDEX OF SUBSTRATE = 2.8600  - I 4.4200
 REFRACTIVE INDEX OF FILM = 1.1000  - I 0.
 FILM THICKNESS =    8.84 ANGSTROMS
 IMAGINARY PART OF FILM THICKNESS =    -.06913 ANGSTROMS
 PSIC =   40.94841          DELC = 166.90696
 PSIM =   40.94786          DELM = 166.90693

PHI = 45.00          N = 1.0000          WAVELENGTH = 5461  ANGSTROMS
 REFRACTIVE INDEX OF SUBSTRATE = 2.8600  - I 4.4200
 REFRACTIVE INDEX OF FILM = 1.1100  - I 0.
 FILM THICKNESS =    8.14 ANGSTROMS
 IMAGINARY PART OF FILM THICKNESS =    -.05722 ANGSTROMS
 PSIC =   40.94835          DELC = 166.90696
 PSIM =   40.94786          DELM = 166.90693

PHI = 45.00          N = 1.0000          WAVELENGTH = 5461  ANGSTROMS
 REFRACTIVE INDEX OF SUBSTRATE = 2.8600  - I 4.4200
 REFRACTIVE INDEX OF FILM = 1.1200  - I 0.
 FILM THICKNESS =    7.56 ANGSTROMS
 IMAGINARY PART OF FILM THICKNESS =    -.04721 ANGSTROMS
 PSIC =   40.94830          DELC = 166.90695
 PSIM =   40.94786          DELM = 166.90693

PHI = 45.00          N = 1.0000          WAVELENGTH = 5461  ANGSTROMS
 REFRACTIVE INDEX OF SUBSTRATE = 2.8600  - I 4.4200
 REFRACTIVE INDEX OF FILM = 1.1300  - I 0.
 FILM THICKNESS =    7.07 ANGSTROMS
 IMAGINARY PART OF FILM THICKNESS =    -.03864 ANGSTROMS
 PSIC =   40.94824          DELC = 166.90695
 PSIM =   40.94786          DELM = 166.90693

PHI = 45.00          N = 1.0000          WAVELENGTH = 5461  ANGSTROMS
 REFRACTIVE INDEX OF SUBSTRATE = 2.8600  - I 4.4200
 REFRACTIVE INDEX OF FILM = 1.1400  - I 0.
 FILM THICKNESS =    6.64 ANGSTROMS
 IMAGINARY PART OF FILM THICKNESS =    -.03119 ANGSTROMS
 PSIC =   40.94819          DELC = 166.90695
 PSIM =   40.94786          DELM = 166.90693

PHI = 45.00          N = 1.0000          WAVELENGTH = 5461  ANGSTROMS
 REFRACTIVE INDEX OF SUBSTRATE = 2.8600  - I 4.4200
 REFRACTIVE INDEX OF FILM = 1.1500  - I 0.
 FILM THICKNESS =    6.28 ANGSTROMS
 IMAGINARY PART OF FILM THICKNESS =    -.02462 ANGSTROMS
 PSIC =   40.94813          DELC = 166.90694
 PSIM =   40.94786          DELM = 166.90693

PHI = 45.00          N = 1.0000          WAVELENGTH = 5461  ANGSTROMS
 REFRACTIVE INDEX OF SUBSTRATE = 2.8600  - I 4.4200
 REFRACTIVE INDEX OF FILM = 1.1600  - I 0.
 FILM THICKNESS =    5.96 ANGSTROMS
 IMAGINARY PART OF FILM THICKNESS =    -.01876 ANGSTROMS
 PSIC =   40.94808          DELC = 166.90694
 PSIM =   40.94786          DELM = 166.90693

PHI = 45.00          N = 1.0000          WAVELENGTH = 5461  ANGSTROMS
 REFRACTIVE INDEX OF SUBSTRATE = 2.8600  - I 4.4200
 REFRACTIVE INDEX OF FILM = 1.1700  - I 0.
 FILM THICKNESS =    5.68 ANGSTROMS
 IMAGINARY PART OF FILM THICKNESS =    -.01348 ANGSTROMS
 PSIC =   40.94803          DELC = 166.90694
 PSIM =   40.94786          DELM = 166.90693

PHI = 45.00          N = 1.0000          WAVELENGTH = 5461  ANGSTROMS
 REFRACTIVE INDEX OF SUBSTRATE = 2.8600  - I 4.4200
 REFRACTIVE INDEX OF FILM = 1.1800  - I 0.
 FILM THICKNESS =    5.43 ANGSTROMS
 IMAGINARY PART OF FILM THICKNESS =    -.00867 ANGSTROMS
 PSIC =   40.94797          DELC = 166.90693
 PSIM =   40.94786          DELM = 166.90693

PHI = 45.00          N = 1.0000          WAVELENGTH = 5461  ANGSTROMS
 REFRACTIVE INDEX OF SUBSTRATE = 2.8600  - I 4.4200
 REFRACTIVE INDEX OF FILM = 1.1900  - I 0.
 FILM THICKNESS =    5.20 ANGSTROMS
 IMAGINARY PART OF FILM THICKNESS =    -.00426 ANGSTROMS
 PSIC =   40.94792          DELC = 166.90693
 PSIM =   40.94786          DELM = 166.90693
```

```
PHI = 45.00          N = 1.0000          WAVELENGTH = 5461  ANGSTROMS
 REFRACTIVE INDEX OF SUBSTRATE = 2.8600  -  I 4.4200
 REFRACTIVE INDEX OF FILM = 1.2000  -  I 0.
 FILM THICKNESS =    5.00 ANGSTROMS
 IMAGINARY PART OF FILM THICKNESS =    -.00019 ANGSTROMS
 PSIC =   40.94786          DELC =  166.90693
 PSIM =   40.94786          DELM =  166.90693

PHI = 45.00          N = 1.0000          WAVELENGTH = 5461  ANGSTROMS
 REFRACTIVE INDEX OF SUBSTRATE = 2.8600  -  I 4.4200
 REFRACTIVE INDEX OF FILM = 1.2100  -  I 0.
 FILM THICKNESS =    4.82 ANGSTROMS
 IMAGINARY PART OF FILM THICKNESS =     .00360 ANGSTROMS
 PSIC =   40.94781          DELC =  166.90693
 PSIM =   40.94786          DELM =  166.90693

PHI = 45.00          N = 1.0000          WAVELENGTH = 5461  ANGSTROMS
 REFRACTIVE INDEX OF SUBSTRATE = 2.8600  -  I 4.4200
 REFRACTIVE INDEX OF FILM = 1.2200  -  I 0.
 FILM THICKNESS =    4.65 ANGSTROMS
 IMAGINARY PART OF FILM THICKNESS =     .00714 ANGSTROMS
 PSIC =   40.94775          DELC =  166.90693
 PSIM =   40.94786          DELM =  166.90693

PHI = 45.00          N = 1.0000          WAVELENGTH = 5461  ANGSTROMS
 REFRACTIVE INDEX OF SUBSTRATE = 2.8600  -  I 4.4200
 REFRACTIVE INDEX OF FILM = 1.2300  -  I 0.
 FILM THICKNESS =    4.50 ANGSTROMS
 IMAGINARY PART OF FILM THICKNESS =     .01047 ANGSTROMS
 PSIC =   40.94770          DELC =  166.90692
 PSIM =   40.94786          DELM =  166.90693

PHI = 45.00          N = 1.0000          WAVELENGTH = 5461  ANGSTROMS
 REFRACTIVE INDEX OF SUBSTRATE = 2.8600  -  I 4.4200
 REFRACTIVE INDEX OF FILM = 1.2400  -  I 0.
 FILM THICKNESS =    4.36 ANGSTROMS
 IMAGINARY PART OF FILM THICKNESS =     .01363 ANGSTROMS
 PSIC =   40.94764          DELC =  166.90692
 PSIM =   40.94786          DELM =  166.90693

PHI = 45.00          N = 1.0000          WAVELENGTH = 5461  ANGSTROMS
 REFRACTIVE INDEX OF SUBSTRATE = 2.8600  -  I 4.4200
 REFRACTIVE INDEX OF FILM = 1.2500  -  I 0.
 FILM THICKNESS =    4.23 ANGSTROMS
 IMAGINARY PART OF FILM THICKNESS =     .01662 ANGSTROMS
 PSIC =   40.94759          DELC =  166.90692
 PSIM =   40.94786          DELM =  166.90693

PHI = 45.00          N = 1.0000          WAVELENGTH = 5461  ANGSTROMS
 REFRACTIVE INDEX OF SUBSTRATE = 2.8600  -  I 4.4200
 REFRACTIVE INDEX OF FILM = 1.2600  -  I 0.
 FILM THICKNESS =    4.12 ANGSTROMS
 IMAGINARY PART OF FILM THICKNESS =     .01947 ANGSTROMS
 PSIC =   40.94753          DELC =  166.90692
 PSIM =   40.94786          DELM =  166.90693

PHI = 45.00          N = 1.0000          WAVELENGTH = 5461  ANGSTROMS
 REFRACTIVE INDEX OF SUBSTRATE = 2.8600  -  I 4.4200
 REFRACTIVE INDEX OF FILM = 1.2700  -  I 0.
 FILM THICKNESS =    4.01 ANGSTROMS
 IMAGINARY PART OF FILM THICKNESS =     .02220 ANGSTROMS
 PSIC =   40.94747          DELC =  166.90692
 PSIM =   40.94786          DELM =  166.90693

PHI = 45.00          N = 1.0000          WAVELENGTH = 5461  ANGSTROMS
 REFRACTIVE INDEX OF SUBSTRATE = 2.8600  -  I 4.4200
 REFRACTIVE INDEX OF FILM = 1.2800  -  I 0.
 FILM THICKNESS =    3.91 ANGSTROMS
 IMAGINARY PART OF FILM THICKNESS =     .02483 ANGSTROMS
 PSIC =   40.94742          DELC =  166.90692
 PSIM =   40.94786          DELM =  166.90693

PHI = 45.00          N = 1.0000          WAVELENGTH = 5461  ANGSTROMS
 REFRACTIVE INDEX OF SUBSTRATE = 2.8600  -  I 4.4200
 REFRACTIVE INDEX OF FILM = 1.2900  -  I 0.
 FILM THICKNESS =    3.81 ANGSTROMS
 IMAGINARY PART OF FILM THICKNESS =     .02735 ANGSTROMS
 PSIC =   40.94736          DELC =  166.90692
 PSIM =   40.94786          DELM =  166.90693
```

0 0 0 0 3 6 0 7 1 5 9

F. FORTRAN IV Computer Program "FPLOT"

The program "FPLOT" (Film Plot) calculates theoretical quantities of ψ and Δ with changes in film thickness. Depending on the code number M, results are tabulated (as program LAYER) or given as curves or both.

The equations and variables used in this program are similar to those used in program LAYER (see Appendix I-D).

Input data for program "FPLOT" are arranged on cards as illustrated below:

Card	Col. 1	Col. 10	Col. 20	Col. 30	Col. 40	Col. 50
1, 2	Title and comments (up to 80 columns)					
3	n_o	λ_o	n_m	k_m		
4	n_{fi} (initial)	δn_f (increment)	n_{fm} (final)	k_{fi} (initial)	δk_f (increment)	k_{fm} (final)
5	L_i	δL	L_m (limited to 200 points)			
6	ϕ	M				

These six cards constitute a set. Any number of sets may follow. In each set, the values of the optical constants of the film may be varied in increments if one desired. Three blank cards must follow the last set of cards.

M is the code number. The integer used for M determines how the results will be presented.

Format of Results

0 Results will be tabulated and given as three curves

a) ψ versus Δ curve with thickness as parameter

b) ψ versus film thickness

c) Δ versus film thickness

M	Format of Results
1	Results will be tabulated and only the ψ versus Δ curve is plotted.
2	Results will be tabulated and two curves will be plotted
	a) ψ versus film thickness
	b) Δ versus film thickness
3	Results will be given only as three curves
	a) ψ versus Δ
	b) ψ versus film thickness
	c) Δ versus film thickness
4	Output has only the ψ versus Δ curve
5	Two curves will be given
	a) ψ versus film thickness
	b) Δ versus film thickness

The maximum number of data points for L (thickness) is 200. If the ψ versus thickness and Δ versus thickness curves are to be plotted, the maximum number is reduced to 101. The program "LAYER" should be used instead, if only tabulated results are wanted.

This program "FPLOT" has to utilize the subroutines "PRNPLT" and "PLSCAL" written by M. S. Itzkowitz to do the plotting of the curves. These two subroutines are library subroutines and they are stored in the computer (control data 7600 system) at Lawrence Berkeley Laboratory.

A reproduction of the main program and the two subroutines is given on the following pages. A sample of the three output curves is also given.

```
      PROGRAM FPLOT (INPUT,OUTPUT)
C     THIS PROGRAM CALCULATES DELC AND PSIC FROM FILM THICKNESS
C     IT ALSO PLOTS PSIC VERSUS DELC CURVE WITH FILM THICKNESS AS PARAMETERS
C     AND PSIC VERSUS FILM THICKNESS, DELC VERSUS FILM THICKNESS.
      COMPLEX TN2, TN3, CPHI2, CPHI3, R1S, R1P, R2S, R2P, D, RS, RP, RHO
      DIMENSION TITLE (8), RANGE (8)
      DIMENSION XPLOT(200), YPLOT(200), ZPLOT(200)
    1 READ 2, TITLE,RANGE
    2 FORMAT (8A10/8A10)
    3 PRINT 4, TITLE,RANGE
    4 FORMAT (1H1, 8A10//8A10)
    5 READ 9, TN1,WL,TNS,TNKS
      IF (TN1) 3000, 3000, 6
    6 READ 10, TNI,DTN,TNM,TNKI,DTNK,TNKM
    7 READ 11, TI,DT,TM
      IF (TI.NE.0.0) TD=TM-TI
    8 READ 12, PHI1,M
    9 FORMAT (F9.0, 3F10.0)
   10 FORMAT (F9.0, 5F10.0)
   11 FORMAT (F9.0, 2F10.0)
   12 FORMAT (F9.0, I1 )
   13 FORMAT (1H0,/6HPHI = ,F5.2,10X,4HN = ,F7.4, 10X, 13HWAVELENGTH = ,
     C F5.0, 11H  ANGSTROMS//33H REFRACTIVE INDEX OF SUBSTRATE = , F7.4,
     C 2X, 4H-  I, F7.4)
   14 FORMAT (1H0, 27HREFRACTIVE INDEX OF FILM = , F7.4, 2X,
     C 4H-  I, F7.4//18H FILM THICKNESS = , F8.2, 10H ANGSTROMS,
     C //8H PSIC = , F10.5, 10X, 7HDELC = , F10.5)
   15 FORMAT (1H1)
   16 FORMAT (22HPSIC VERSUS DELC CURVE)
   17 FORMAT (6HPHI = ,F5.2,10X,4HN = ,F7.4,10X,13HWAVELENGTH = ,
     C F5.0,4H  A ,5X,13HNM  -  IKM = ,F7.4,2X,4H-  I,F7.4)
   18 FORMAT (13HNF  -  IKF = ,F7.4,2X,4H-  I,F7.4)
   19 FORMAT (26HDELC VERSUS FILM THICKNESS)
   21 FORMAT (26HPSIC VERSUS FILM THICKNESS)
      PHI = 0.01745329252*PHI1
      CP = COS(PHI)
      SP = SIN(PHI)
      TN3 = CMPLX(TNS,-TNKS)
      CPHI3 = CSQRT(1.0 - TN1**2*SP**2/(TN3**2))
      TN = TNI
   20 TNK = TNKI
   30 T = TI
      NPOINT = 1
  100 TN2 = CMPLX(TN,-TNK)
      CPHI2 = CSQRT(1.0 - TN1**2*SP**2/(TN2**2))
      R1S = (TN1*CP - TN2*CPHI2)/(TN1*CP + TN2*CPHI2)
      R1P =-(TN1*CPHI2 - TN2*CP)/(TN1*CPHI2 + TN2*CP)
      R2S = (TN2*CPHI2 - TN3*CPHI3)/(TN2*CPHI2 + TN3*CPHI3)
      R2P =-(TN2*CPHI3 - TN3*CPHI2)/(TN2*CPHI3 + TN3*CPHI2)
      D = (0.0,1.0)*(4.0*3.1415927*T/WL)*TN2*CPHI2
      RS= (R1S + R2S*CEXP(-D))/(1.0 + R1S*R2S*CEXP(-D))
      RP = (R1P + R2P*CEXP(-D))/(1.0 + R1P*R2P*CEXP(-D))
      RHO = RP/RS
      PSIC = ATAN(CABS(RHO))/0.01745329252
      DELC = ATAN2(AIMAG(RHO), REAL(RHO))/0.01745329252
```

```
      IF (DELC) 140,140,150
  140 DELC = DELC + 360.00
  150 IF(M.GT.2) GO TO 300
      PRINT 13, PHI1,TN1,WL,TNS,TNKS
      PRINT 14, TN,TNK,T,PSIC,DELC
  300 XPLOT(NPOINT) = DELC
      YPLOT(NPOINT) = PSIC
      IF(M.EQ.1.OR.M.EQ.4) GO TO 400
      IF(TI.EQ.0.0) GO TO 3500
      ZPLOT(NPOINT) = T - TD
      GO TO 400
 3500 ZPLOT(NPOINT) = T
  400 NPOINT = NPOINT + 1
      IF(TM -T) 600,600,500
  500 T = T + DT
      GO TO 100
  600 NPOINT = NPOINT - 1
      IF(M.EQ.2.OR.M.EQ.5) GO TO 1500
      PRINT 15
      PRINT 16
      PRINT 17, PHI1,TN1,WL,TNS,TNKS
      PRINT 18, TN,TNK
      CALL PRNPLT(XPLOT,YPLOT,360.,5.0,90.,2.0,0.,0.,NPOINT)
      IF(M.EQ.1.OR.M.EQ.4) GO TO 1100
 1500 PRINT 15
      PRINT 21
      PRINT 17, PHI1,TN1,WL,TNS,TNKS
      PRINT 18, TN,TNK
      IF(TI.EQ.0.0) GO TO 3100
      PRINT 3300, TD
 3300 FORMAT (5HADD  ,F8.2,17HTO SCALE READINGS)
      CALL PRNPLT(ZPLOT,YPLOT,TD,100.,90.,2.,0.,0.,NPOINT)
      GO TO 3400
 3100 CALL PRNPLT(ZPLOT,YPLOT,TM,100.,90.,2.,0.,0.,NPOINT)
 3400 PRINT 15
      PRINT 19
      PRINT 17, PHI1,TN1,WL,TNS,TNKS
      PRINT 18, TN,TNK
      IF(TI.EQ.0.0) GO TO 3200
      PRINT 3300, TD
      CALL PRNPLT(ZPLOT,XPLOT,TD,100.,360.,10.,0.,0.,NPOINT)
      GO TO 1100
 3200 CALL PRNPLT(ZPLOT,XPLOT,TM,100.,360.,10.,0.,0.,NPOINT)
 1100 IF(TNKM - TNK) 800,800,700
  700 TNK = TNK + DTNK
      GO TO 30
  800 IF(TNM - TN) 1000,1000,900
  900 TN = TN + DTN
      GO TO 20
 1000 GO TO 1
 3000 CONTINUE
      END
```

```
              SUBROUTINE PRNPLT(X,Y,XMAX,XINCR,YMAX,YINCR,ISX,ISY,NPTS)
        C  PRINTER PLOT ROUTINE        M.S.ITZKOWITZ     MAY,1967
        C
        C   PLOTS THE #NPTS# POINTS GIVEN BY #X(I),Y(I)# ON A 51 X 101 GRID
        C   USING A TOTAL OF 56 LINES ON THE PRINTER
        C     IF #ISX# OR #ISY# ARE NON-ZERO, THE CORRESPONDING MAXIMUM AND
        C      INCREMENTAL STEP SIZE ARE COMPUTED
        C     IF EITHER INCREMENTAL STEP SIZE IS ZERO, THE PROGRAM EXITS
        C     NEITHER OF THE INPUT ARRAYS ARE DESTROYED.  IF SCALING IS DONE
        C     THE CORRESPONDING NEW VALUES OF MAXIMUM AND STEP SIZE ARE RETURNED
        C
000013        DIMENSION X(NPTS),Y(NPTS),IGRID(105),XAXIS(11)
        C
000013        INTEGER BLANK,DOT,STAR,IGRID,PLUS
000013        DATA BLANK,DOT,STAR,PLUS / 1H ,1H.,1H*,1H+ /
        C
000013  901   FORMAT(14X,105A1)
000013  902   FORMAT(1XE10.3,2X,1H+,105A1,1H+)
000013  903   FORMAT(15X,103(1H.))
000013  904   FORMAT(7X,11(F10.0),2H (,I4,5H PTS)  )
000013  905   FORMAT(16X,11(1H+,9X))
000013  9800  FORMAT(46H1SCALING ERROR IN PRNPLT, EXECUTION TERMINATED )
        C
000013        IF(ISX.NE.0) CALL PLSCAL(X,XMAX,XINCR,NPTS,100)
000017        IF(ISY.NE.0) CALL PLSCAL(Y,YMAX,YINCR,NPTS,50)
000030        IF(XINCR.EQ.0..OR.YINCR.EQ.0.) GO TO 800
000042        YAXMIN=0.01*YINCR
000043        XAXMIN=0.01*XINCR
000043        IZERO=YMAX/YINCR+1.5
000046        JZERO=103.5-XMAX/XINCR
000050        IF(JZERO.GT.103.OR.JZERO.LT.4) JZERO=2
000062        PRINT 905
000066        PRINT 903
000075        DO 10 I=1,51
000102        IF ( I.NE.IZERO) GO TO 16
000104        DO 14 J=1,105
000111  14    IGRID(J)=PLUS
000112        GO TO 15
000116  16    DO 11 J=1,105
000124  11    IGRID(J)=BLANK
000131  15    IGRID(JZERO)=PLUS
000132        IGRID(104)=DOT
000135        IGRID(2)=DOT
000136        DO 12 K=1,NPTS
000140        ITEST =(YMAX-Y(K))/YINCR+1.5
000144        IF(ITEST .NE.I) GO TO 12
000146        J=103.5-(XMAX-X(K))/XINCR
000152        IF(J.GT.103)J=105
000156        IF(J.LT.3) J=1
000161        IGRID(J)=STAR
000163  12    CONTINUE
000167        IF(MOD(I,10).EQ.1) GO TO 13
000174        PRINT 901,IGRID
000201        GO TO 10
000205  13    YAXIS=YMAX-(I-1)*YINCR
000211        IF(ABS(YAXIS).LT.YAXMIN) YAXIS=0.
000216        PRINT 902,YAXIS,(IGRID(J),J=1,105)
000232  10    CONTINUE
```

```
000234        PRINT 903
000240        PRINT 905
000247        DO 20 M=1,11
000260        XAXIS(M)=XMAX-XINCR*(FLOAT(11-M))*10.0
000264        IF(ABS(XAXIS(M)).LT.XAXMIN)XAXIS(M)=0.
000267  20    CONTINUE
000270        PRINT 904,XAXIS,NPTS
000303        RETURN
000304  800   PRINT 9800
000310        CALL EXIT
000311        END
```

```
                SUBROUTINE PLSCAL(V,VMAX,VINCR,NPTS,NDIVIS)
          C
          C     SCALING PROGRAM FOR USE WITH PRNPLT    M.S.ITZKOWITZ  MAY,1967
          C  THIS VERSION ADJUSTS THE FULL SCALE TO 2.5,5.0, OR 10. TIMES 10**N
          C  AND ADJUSTS THE MAXIMUM POINT TO AN INTEGER MULTIPLE OF 5*VINCR
          C
000007          DIMENSION V(NPTS)
          C
000007          VMIN=V(1)
000010          VMAX=V(1)
000011          DO 10 I=1,NPTS
000016          IF(V(I).LT.VMIN) VMIN=V(I)
000021          IF(V(I).GT.VMAX) VMAX=V(I)
000024          ORANGE=VMAX-VMIN
000025    10    CONTINUE
000026          IF(ORANGE.EQ.0.) GO TO 8000
000032          ORANGE=0.4342944*ALOG(ORANGE)
000035          IF(ORANGE)20,20,30
000042    30    IRANGE=ORANGE
000044          GO TO 40
000045    20    IRANGE=-ORANGE
000046          IRANGE=-IRANGE-1
000051    40    ORANGE=ORANGE-FLOAT(IRANGE)
000053          RANGE=10.**ORANGE
          C
          C   RANGE IS BETWEEN 1.0 AND 10.0
          C
000056    43    IF(RANGE.GT.2.5) GO TO 41
000062          RANGE=2.5
000062          GO TO 50
000063    41    IF(RANGE.GT.5.0) GO TO 42
000067          RANGE=5.0
000067          GO TO 50
000070    42    RANGE=10.0
000072    50    TRANGE=RANGE*(10.**IRANGE)
          C
          C   TRANGE IS NOW 2.5,5.0, OR 10.0 TIMES A POWER OF TEN
          C
000076          VINCR=TRANGE/FLOAT(NDIVIS)
000100          IF(VMAX)51,51,52
000104    52    IMAX=VMAX/(5.0*VINCR)
000105          XMAX=5.0*VINCR*FLOAT(IMAX+1)
000110          GO TO 53
000113    51    IMAX=-VMAX/(5.0*VINCR)
000114          XMAX=5.0*VINCR*FLOAT(-IMAX+1)
000117    53    IF(VMIN.GT.XMAX-TRANGE) GO TO 100
000124          RANGE=RANGE*2.0
000125          IF(RANGE-10.) 43,43,54
000130    54    RANGE=RANGE/10.
000132          IRANGE=IRANGE+1
000133          GO TO 43
000134    100   VMAX=XMAX
000135          VMIN=XMAX-TRANGE
000137          RETURN
000140    8000  PRINT 9800
000144    9800  FORMAT(45H1PLSCAL CALLED TO SCALE ARRAY WITH ZERO RANGE)
000147          CALL EXIT
000150          END
```

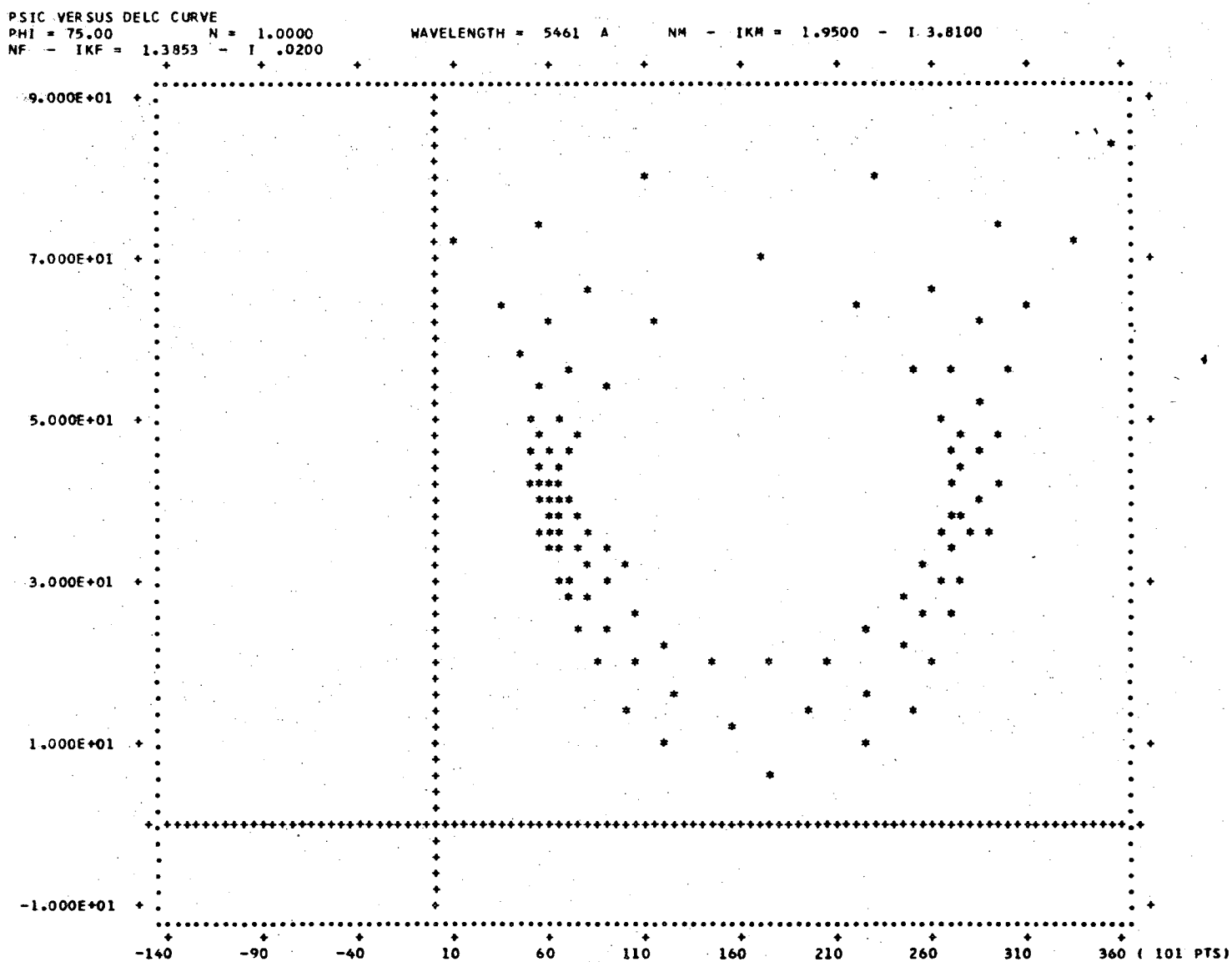
PSIC VERSUS DELC CURVE
PHI = 75.00 N = 1.0000 WAVELENGTH = 5461 A NM - IKM = 1.9500 - I 3.8100
NF - IKF = 1.3853 - I .0200
9.000E+01
7.000E+01
5.000E+01
3.000E+01
1.000E+01
-1.000E+01
-140
-90
-40
10
60
110
160
210
260
310
360 (101 PTS)

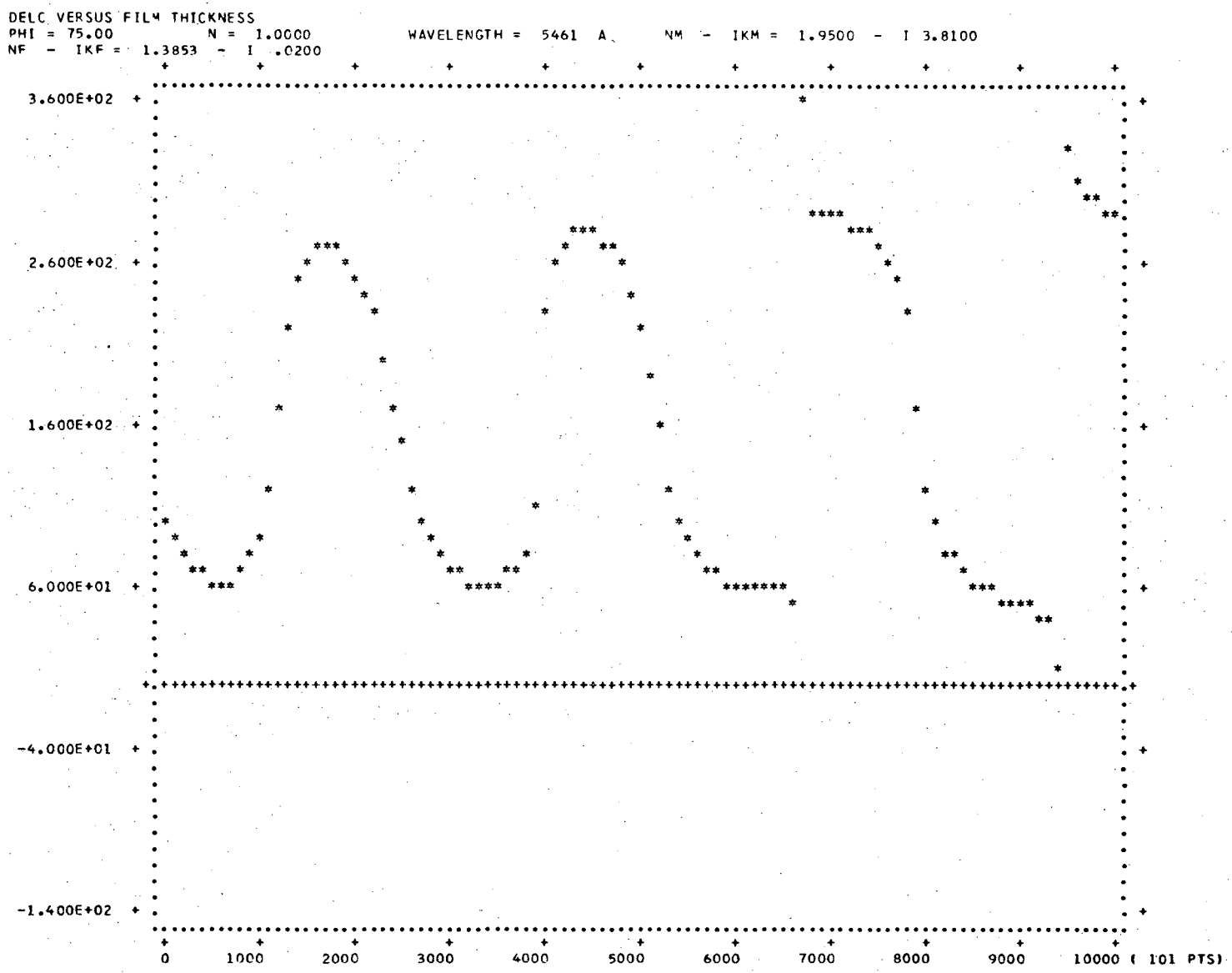
DELC VERSUS FILM THICKNESS
PHI = 75.00 N = 1.0000 WAVELENGTH = 5461 A NM - IKM = 1.9500 - I 3.8100
NF - IKF = 1.3853 - I .0200
3.600E+02
2.600E+02
1.600E+02
6.000E+01
-4.000E+01
-1.400E+02
0
1000
2000
3000
4000
5000
6000
7000
8000
9000
10000 (101 PTS)

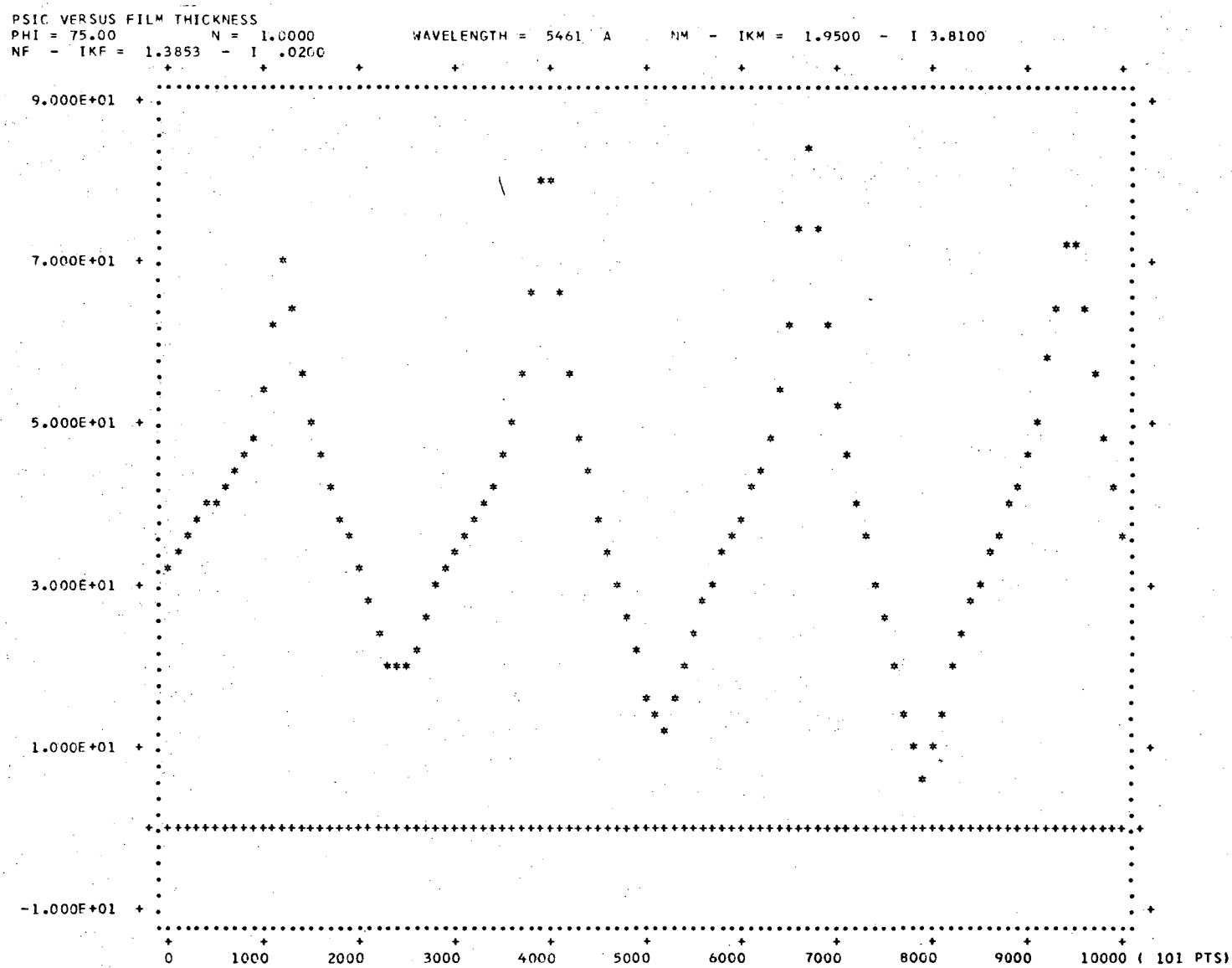
PSIC VERSUS FILM THICKNESS
PHI = 75.00 N = 1.0000 WAVELENGTH = 5461 A NM - IKM = 1.9500 - I 3.8100
NF - IKF = 1.3853 - I .0200
9.000E+01
7.000E+01
5.000E+01
3.000E+01
1.000E+01
-1.000E+01
0
1000
2000
3000
4000
5000
6000
7000
8000
9000
10000 (101 PTS)

G. FORTRAN IV Computer Program "DLVPS"

This program is used to plot the experimental ψ versus Δ curve so that it can be compared with the theoretical curve.

The subroutines "PRNPLT" and "PLSCAL" written by M. S. Itzkowitz are used to do the plottings.

1. Variables Used in the Program

Name	Symbol	Description
TN1	n_o	refractive index of incident medium
WL	λ_o	vacuum wavelength (Å)
TNS	n_m	real part of complex refractive index of substrate
TNKS	k_m	index of extinction of substrate
PHI	ϕ	angle of incidence (degree)
T		time (hr)
DELM	Δ (measured)	relative phase change (degree)
PSIM	ψ (measured)	arctangent of relative amplitude attenuation (degree)
P		position (cm)

2. Input Format for Program "DLVPS"

Card	Col. 1	Col. 10	Col. 20	Col. 30	Col. 40
1 2	Title and comments (up to 80 columns)				
3	n_o	λ_o	n_m	k_m	ϕ
4	$time_1$	$position_1$	Δ_1	ψ_1	
5	$time_2$	$position_2$	Δ_2	ψ_2	
etc ⋮ N					
N+1	0.0				

These cards constitute a set. Cards 1 to 3 are used for identification and will be printed out in the output. Data are entered in cards 4 through N. The N+1 card is used to signal the end of one set of data. Any number of sets may follow. Three blank cards must follow the last set of data.

A reproduction of the main program DLVPS appears on the next page. The subroutines employed can be found in Appendix I-F.

```
      PROGRAM DLVPS (INPUT,OUTPUT)
C     THIS PROGRAM PLOTS THE MEASURED VALUES OF PSI VERSUS DEL
      DIMENSION TITLE(8), RANGE (8), DELM (50), PSIM (50), T (50),P(50)
    1 READ 2, TITLE,RANGE
    2 FORMAT (8A10/8A10)
      PRINT 4, TITLE, RANGE
    4 FORMAT (1H1,8A10//8A10///)
      READ 9, TN1, WL, TNS, TNKS, PHI
      IF (TN1) 11,11,6
    9 FORMAT (F9.0, 4F10.0)
    6 PRINT 12, PHI, TN1, WL, TNS, TNKS
   12 FORMAT (1H0,/6HPHI = ,F5.2,10X,4HN = ,F7.4, 10X, 13HWAVELENGTH = ,
     C F5.0, 11H  ANGSTROMS//33H REFRACTIVE INDEX OF SUBSTRATE = , F7.4,
     C 2X, 4H-  I, F7.4/)
      PRINT 13
   13 FORMAT(1H0,8HTIME(HR),5X,12HPOSITION(CM),10X,4HPSIM,10X,4HDELM//)
      NPOINT = 1
    3 READ 5, T(NPOINT),P(NPOINT),DELM(NPOINT),PSIM(NPOINT)
    5 FORMAT (F9.0,3F10.0)
      IF(DELM(NPOINT).EQ.0) GO TO 10
      PRINT 8, T(NPOINT),P(NPOINT),PSIM(NPOINT),DELM(NPOINT)
    8 FORMAT (2X,F5.2,10X,F5.2,11X,F10.3,4X,F10.3)
      NPOINT = NPOINT + 1
      GO TO 3
   10 NPOINT = NPOINT - 1
      PRINT 7
    7 FORMAT (1H1, 22HPSIM VERSUS DELM CURVE)
      CALL PRNPLT(DELM,PSIM,360.,5.,90.,2.,0.,0.,NPOINT)
      GO TO 1
   11 CONTINUE
      END
```

APPENDIX II

ALIGNMENT AND CALIBRATION OF THE ELLIPSOMETER ON LEED SETUP

A. Alignment of the Ellipsometer

Due to the constraint imposed by the LEED Chamber, the angle of incidence used is fixed at 45°. This means that the optical axes of the polarizer telescope and the analyzer telescope should be perpendicular to each other. A prism with two reflecting faces at 90° (plus 40 sec) to each other (Fig. A1) was used to align the optical axes. The following procedure was followed:

1. With the Quarter wave plate removed, the alignment prism resting on a precision tripoid is positioned between the telescopes so that the perpendicular surfaces of the prism are facing the telescopes.
2. Using an Abbe Lamont Autocollimating eyepiece, one face of the prism is brought to be perpendicular to the optical axis of one telescope by adjusting the tripoid legs to bring the crosshairs of the eyepiece and their reflected image into coincidence (Fig. A2a).
3. The same autocollimation procedure is then carried out with the second telescope. However, the crosshairs and their images are brought into coincidence by adjusting the position screws on the telescope (Fig. A2a).
4. Looking through a pinhole eyepiece placed on the collimator and closing down the iris diaphragm on the polarizer, the target on one face of the prism is centered in the view of the collimator. The centering is done by shifting the prism and varying the height of the tripoid table.
5. With the pinhole eyepiece on the analyzer telescope, the target on the prism is viewed by the analyzer telescope. The target is centered in the horizontal sense by sliding the prism. If at this

point the target is not centered vertically (Fig. A2b) in the view of the analyzer telescope, the level of the analyzer telescope is adjusted (adjustment of the dovetail mount carrier) so that the target is centered vertically.

The two optical axes of the telescopes are now lying in one plane and the angle between them is at 90° (Fig. A2c).

To check the alignment, the pinhole is placed in the polarizer and the eyepiece in the analyzer. A mercury light is used to illuminate the pinhole. By rotating the prism table approximately 45°, one face of the prism is used as the reflecting surface. The image of the pinhole is observed through the eyepiece. Without adjusting the legs of the tripoid, one should be able to place the image of the pinhole at the center of the crosshairs. If not, the alignment procedure should be repeated.

B. Calibration of the Polarizer and the Analyzer Circles

The Calibration of the polarizer and the analyzer circles on the LEED set up presents some difficulties. The main one is that the two telescopes can not be arranged in the straight through position. Therefore, the way to determine the correction factors for the circle readings will depend on finding the minimum intensity at extinction settings of the polarizer and the analyzer. The extinction setting of the analyzer will depend on the setting of the polarizer. However, extinction intensity would be at a minimum when the transmission axis of the polarizer is either parallel to the plane of incidence (p-position) or perpendicular to the plane of incidence (s-position).

A stainless steel alignment mirror was used as the reflecting surface and the procedure below was followed.

1. Turn the polarizer to s-position (0° on circle reading).*
2. Turn the analyzer to p-position (90° on circle reading).*
3. Adjust polarizer and analyzer for minimum photomultiplier current. Note dial recorder reading.
4. Return polarizer to 0° circle reading and analyzer to 90° circle reading.
5. Loosen collar screws of both the polarizer and the analyzer carrier and rotate them until the minimum reading obtained in step (3) is reached. Tighten the screws.

To determine correction factors for the polarizer circle readings.

6. Set polarizer at 0° and find the extinction setting of the analyzer by the method of taking two equal intensity readings around null.
7. Repeat step (6) at 0.1° (or 0.05°) steps from 0° until a noticeable increase in photomultiplier current at extinction setting of the analyzer is obtained.
8. Do the same at minus 0.1° (or -0.05°) steps from 0°.
9. Using a chart recorder instead of the dial,** reset all the extinction settings of the polarizer and analyzer and display the photomultiplier current on the chart recorder.
10. Analyze the chart recorder display of the photomultiplier current. The polarizer and analyzer settings (0° + dP and 90° + dA) that give the minimum photomultiplier current are the settings when the polarizer transmission axis is at s-position and that of the analyzer

---

* With the arrangement of optical components that we used (light source, polarizer, compensator, sample, analyzer and detector), the circle reading of this particular ellipsometer is based on an angle measured counterclockwise from the plane perpendicular to the plane of incidence when looking into the beam.

** Because the noise level of the photomultiplier is high at low intensity of light, it is difficult to read a dial recorder.

at p-position. The values -dP and -dA are chosen as correction factors.

C. Calibration of the Compensator Circle Setting

1. Insert quarter-wave plate and rotate compensator circle to s-position (circle reading 0°).
2. With the polarizer and the analyzer set at s- and p-position respectively, rotate the quarter-wave plate in its holder until a minimum photomultiplier current is reached.
3. Determine the circle reading of the compensator at minimum intensity.
4. If the circle reading is 0° + dQ, then the corrected compensator setting would be Q + dQ (for example, 45° +dQ or 135° +dQ) during measurement.

0 0 0 0 3 6 0 7 1 6 6

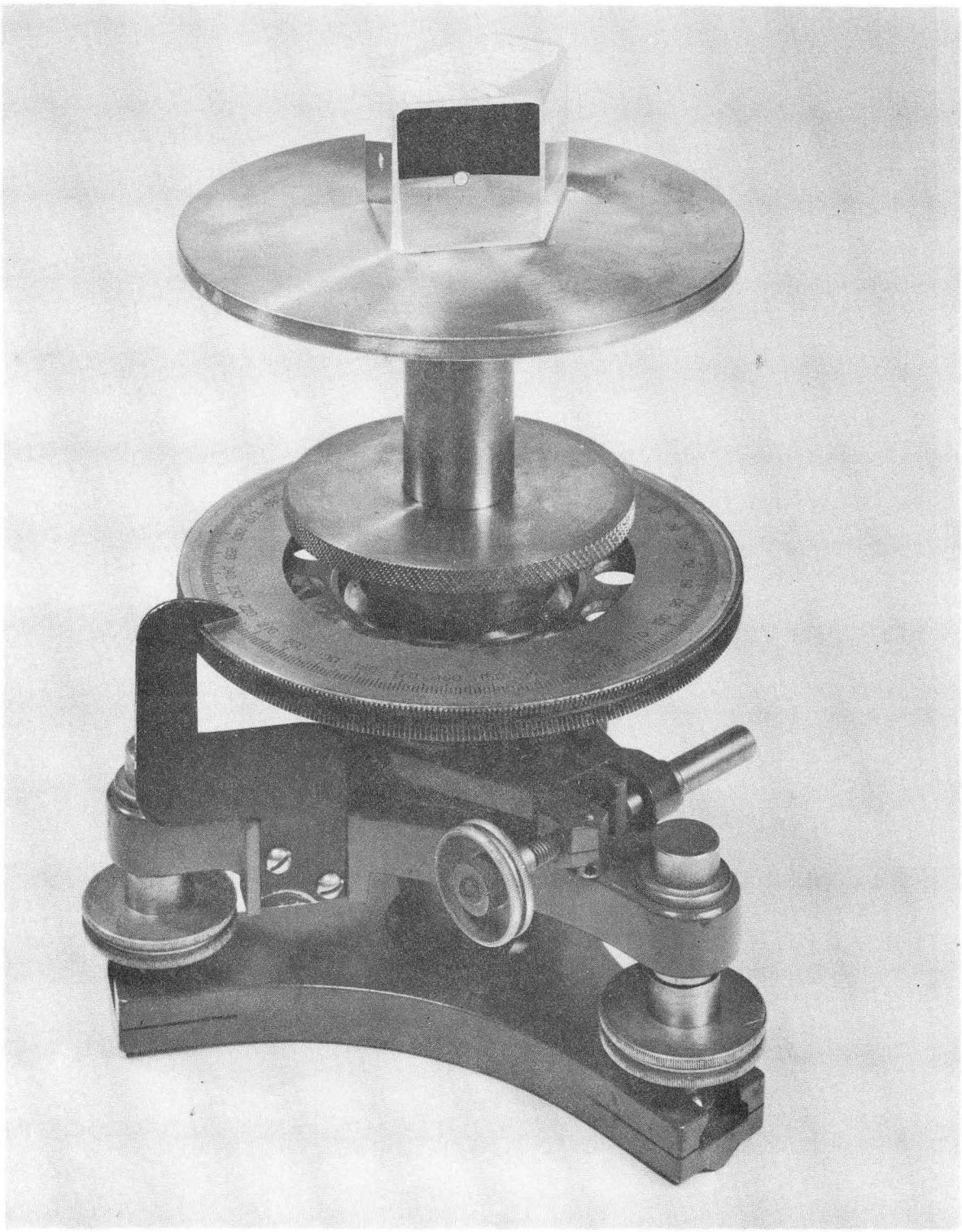

XBB 7110-4914

Fig. A1 Alignment prism (reflecting faces at 90°) and tripoid for use with LEED setup.

Fig. A2

Schematic of alignment procedures on LEED setup.

Λ - Plane of table

χ - Plane of tripoid table before adjustment

μ - Plane of tripoid table after adjustment.

ξ,β - Reflecting faces of prism

I,II - Planes containing the telescope axes

AB,CB' - Telescope axes

ef,gh - Normals of prism reflecting faces

<u>Refer to Appendix I-A</u>

a. Step 2 brought ef to align with AB by tilting the tripoid table an angle α. Step 3 brought CB' to align with gh.

b. AB, CB' both perpendicular to the faces of the prism β and ξ respectively but AB, CB' do not intercept.

c. AB, CB' intercept each other and are normal to each other.

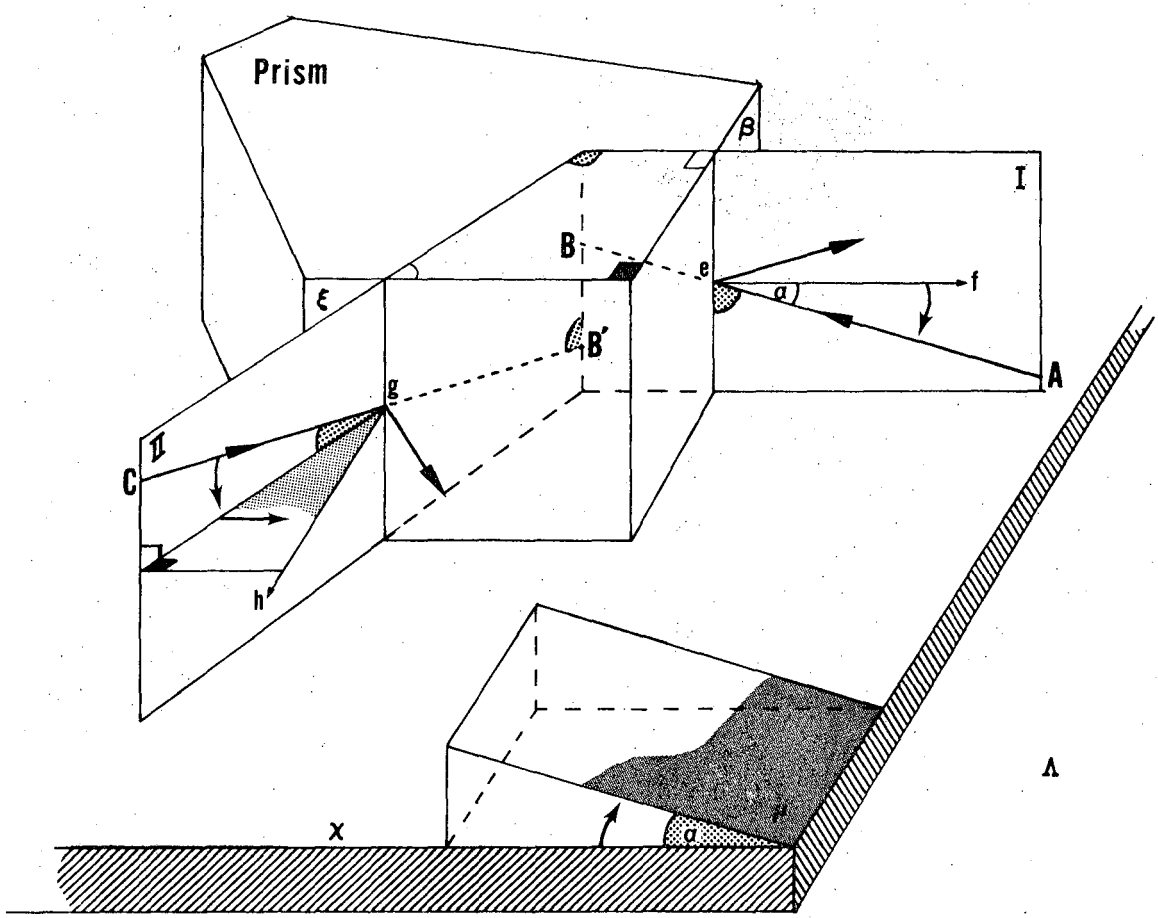

XBL 7110-7459

Fig. A2a

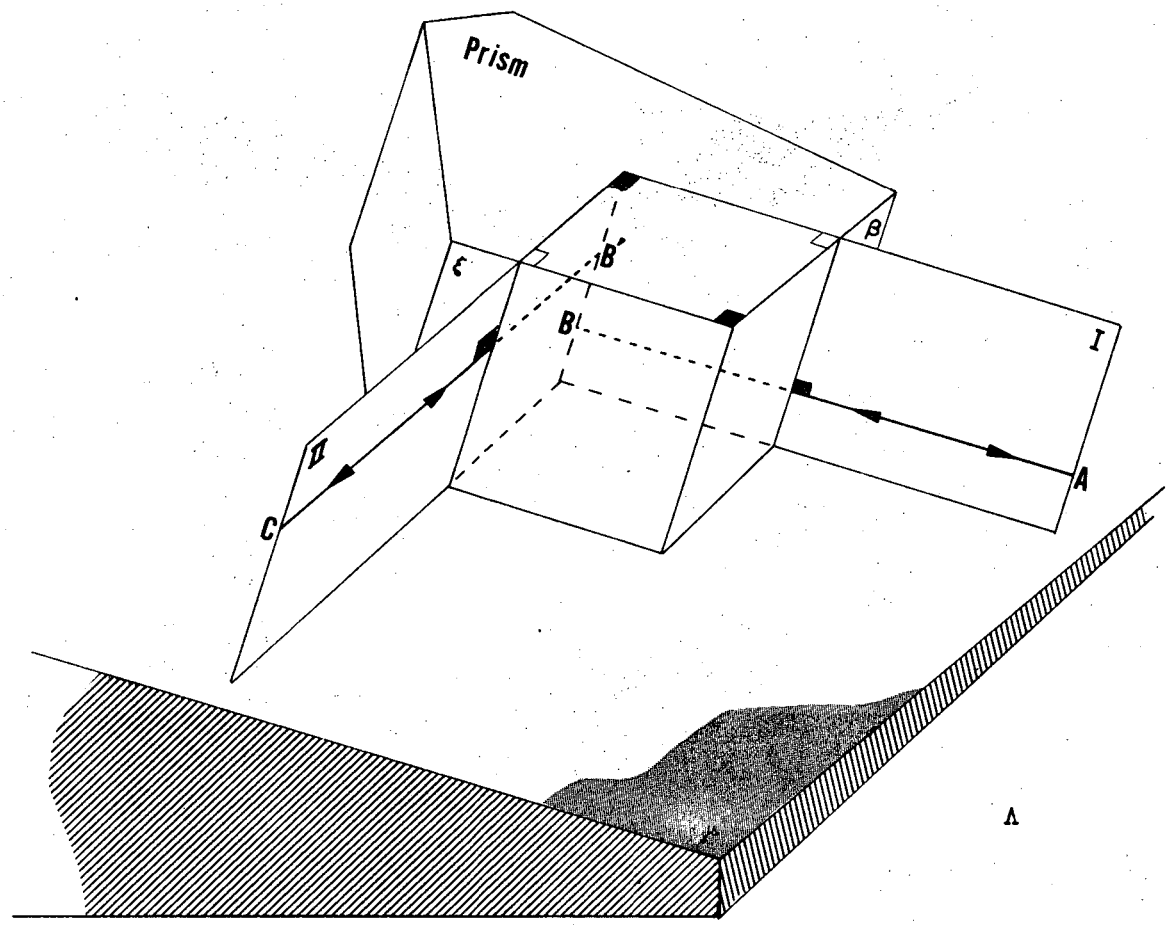

XBL 7110-7460

Fig. A2b

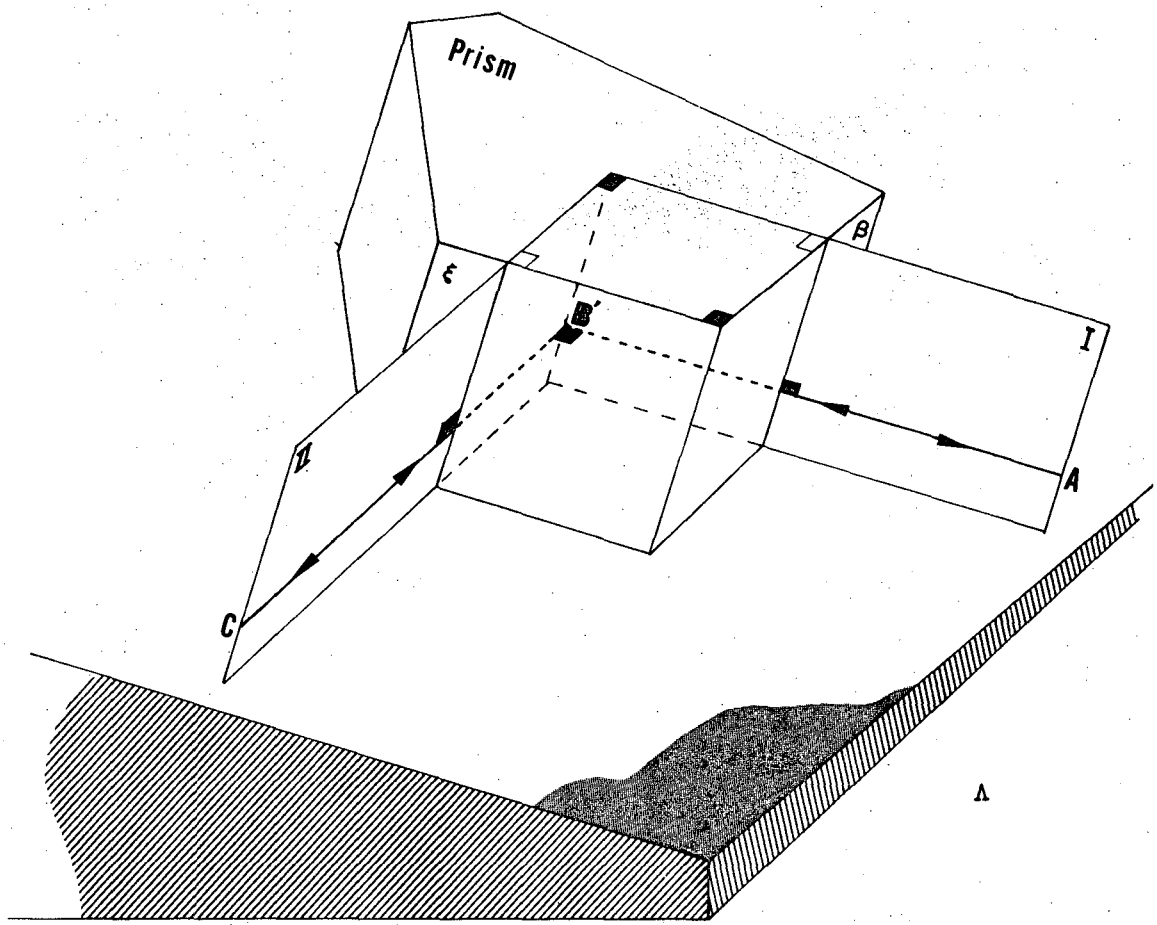

XBL 7110-7461

Fig. A2c

APPENDIX III

ALIGNMENT AND CALIBRATION OF THE ELLIPSOMETER (VARIABLE ANGLE OF INCIDENCE SETUP)

A. Adjustment of the Collimator and Telescope Axes to be Coplanar and to Intersect the Rotational Axis of the Sample Table at Right Angles

1. Remove quarter wave plate. Place pinhole in fixed telescope (collimator with polarizer) and illuminate it with the lamp.
2. Swing the moveable telescope (with analyzer) to in line position with the fixed telescope. (The pinhole image is centered on the vertical cross-hair of the analyzer eyepiece. The horizontal scale reading, or angle of incidence reading should be approximately 180°.)
3. Center the pinhole image on the eyepiece cross-hairs by adjusting the vertical screw of the moveable telescope (see Fig. A3a).
4. Place the alignment mirror* on the sample table and autocollimate the analyzer with the mirror (to get the mirror normal to the optical axis of the telescope). The cross-hairs and their reflections are brought to coincidence by adjusting the table (Fig. A3b).
5. Rotate the table with mirror 180° and autocollimate with the fixed telescope (collimator with polarizer). Correct half of the error by adjusting the table and half by adjusting the vertical screw of the collimator (Fig. A3c).
6. Remove mirror and repeat steps 1 and 3, and then 4 and 5 until no further adjustments are necessary (Fig. A3d).

Steps 1 to 6 have set the optical axes of the telescopes parallel to each other and perpendicular to the axis of rotation of the table.**

---

*A vertical mirror with target in the middle and mounted on an aluminum block.

**The optical axes of the telescopes are both parallel to a plane which is normal to the rotational axis of the sample table.

Steps 7 through 10 will set the table surface perpendicular to its rotational axis.

7. Keep moveable telescope in 180° position.
8. Place mirror on table in same position as before, then rotate mirror on fixed table by 90°.
9. Return mirror by rotating the table to autocollimate with moveable telescope. Errors are corrected by adjusting the table (Fig. A3e).
10. Repeat step 9 with mirror at different positions on the table. Final error due to deviation of right angle mirror mount should stay the same during a full rotation of the mirror with respect to the table.

The following steps will bring the two optical axes of the telescopes to lie in the same plane normal to the rotational axis of the sample table and to intercect the rotational axis at a common point (Fig. A3f).

11. Place alignment mirror on table and observe target on mirror through fixed telescope with pinhole. Move target on table until target shows no lateral motion upon rotation of the table (target in table axis).
12. Closing down the iris diaphragm, center the target in the view of the telescope in vertical direction by raising or lowering the table.
13. Use lateral adjustment on fixed telescope (screws at dovetail) to center target in the horizontal direction.
14. Rotate table with mirror 180° and observe target through moveable telescope with pinhole.
15. Closing down the iris diaphragm, center target in the view of the

telescope in the vertical direction by placing shims under moveable telescope at dovetail connection.

16. Use lateral adjustment screws on moveable telescope to center target in horizontal direction.

17. Remove mirror. Place pinhole in fixed telescope and illuminate it. Center pinhole image in analyzer eyepiece by adjusting the vertical screw of the moveable telescope (this is necessary only when the shimming of step 15 is necessary).

B. Adjustment of the Horizontal Circle Readings (Angle of Incidence Readings)

1. Put pinhole in fixed telescope and illuminate it.
2. Put eyepiece with cross-hairs in moveable telescope.
3. Move telescope such that the image of the pinhole is centered on the cross-hairs.
4. Set horizontal circle to read 180° by adjusting the screw at the base of the fixed telescope and compensator mount.

The above procedures of setting the angle of incidence circle readings is based on the assumption that the rotational axis of the sample table is in line with the rotational axis of the moveable telescope. Section C outlines a prodecure to check the alignment of the rotational axes of table and telescope and a way to correct the error when necessary.

C. Alignment of Rotational Axes of Table and Telescope

1. Misalignment Check

a. Translatory Movement

(1) Place alignment mirror on center of table as described in A-11.

(2) Rotate table and moveable telescope, target should stay centered laterally.

b. Tilting Movement

(1) Check autocollimation with moveable telescope in 180° position.

(2) Check autocollimation for different positions of moveable telescope by rotating the table with mirror unchanged. Variations in autocollimation are due to angle between axes of rotation.

This alignment check was not necessary before the modification of the original ellipsometer when the table was mounted on the same axis as the telescope. After the modification, the table was mounted on a dovetail carrier and the rotational axis of the table was made to coincide with that of the telescope at the time of assembly.

2. Alignment of Rotational Axes

Alignment of the rotational axes of the telescope and the table, involves adjusting the dovetail carrier on which the sample table is situated. A polygonal mirror* (or the 90° prism as mentioned in Appendix II) can be used to assist in the alignment.

a. Place the polygonal mirror* on the table and check autocollimation with the moveable telescope in 180° position. Any error is corrected by adjusting the table. Make sure that the table surface is perpendicular to the rotational axis. (Section A, steps 7-10)

b. With the table unchanged, rotate the polygonal mirror to any angle (such as 90° or 120°).

*A polygonal mirror is a device with a vertical mirror which can be rotated with respect to the base. The angle of rotation is indicated by the scale on the side to a precision of 1 degree. (accuracy 0.25")

c. Rotate the moveable telescope to the same angle as the mirror.

d. Autocollimate the telescope with the mirror. Any error is corrected by adjusting the rotational axis of the table.

e. Check the alignment with the mirror rotated to different angles.

D. Calibration of Polarizer and Analyzer Circles

1. Insert pinhole in fixed telescope and illuminate it.
2. Remove quarter-wave plate and with the moveable telescope in 180° position, check the centering of the pinhole image and then insert photomultiplier.
3. Turn the polarizer to s-position (circle reading at 0°).
4. Extinguish with analyzer. The analyzer circle reading should be approximately 90°. If the reading is very different from 90°, note photomultiplier current.
5. Loosen collar screw of analyzer carrier and rotate to minimum intensity reading as noted in step 4 with circle set at 90°.
6. Determine again the extinguishing reading of the analyzer circle which is probably $90° + \Delta A$.
7. Place test mirror* on sample table and reflect light off test mirror near principal angle of incidence (75°). The telescope should be in 150° position on horizontal circle (angle of incidence circle) reading. Center pinhole image on cross-hairs of eyepiece and then insert photomultiplier.
8. Set analyzer circle reading at 90° (p-position) and adjust polarizer to obtain minimum photomultiplier current. The polarizer circle reading should be $0° + dP$. Note photomultiplier current.

---

*The test mirror is a stainless mirror which has approximately a principal angle of incidence of 75°.

9. Set analyzer at +0.05 (or smaller) steps from 90° and adjust polarizer for minimum photomultiplier current until a noted increase in photomultiplier current is observed. This will give sets of polarizer and analyzer circle readings--0° + dP and 90° + dA.
10. Repeat step 9 in -0.05 (or smaller) steps from 90°.
11. The set of readings that gives dA - dP = ΔA is chosen as the correct set. The correction factors that apply to measurements will be -dP and -dA.

E. Calibration of the Quarter-Wave Plate

1. With the telescope in 180° position (straight through position), insert quarter-wave plate.
2. Set the polarizer circle at 0° + dP and the analyzer circle at 90° + dA.
3. With the compensator circle set at 0°, rotate the quarter-wave plate in its holder until a minimum photomultiplier current is obtained.
4. Determine the compensator circle reading at minimum photomultipler current. The reading will probably be 0° + dQ. The setting of the compensator circle reading during measurement will therefore be Q + dQ (such as 45° + dQ or 135° + dQ).

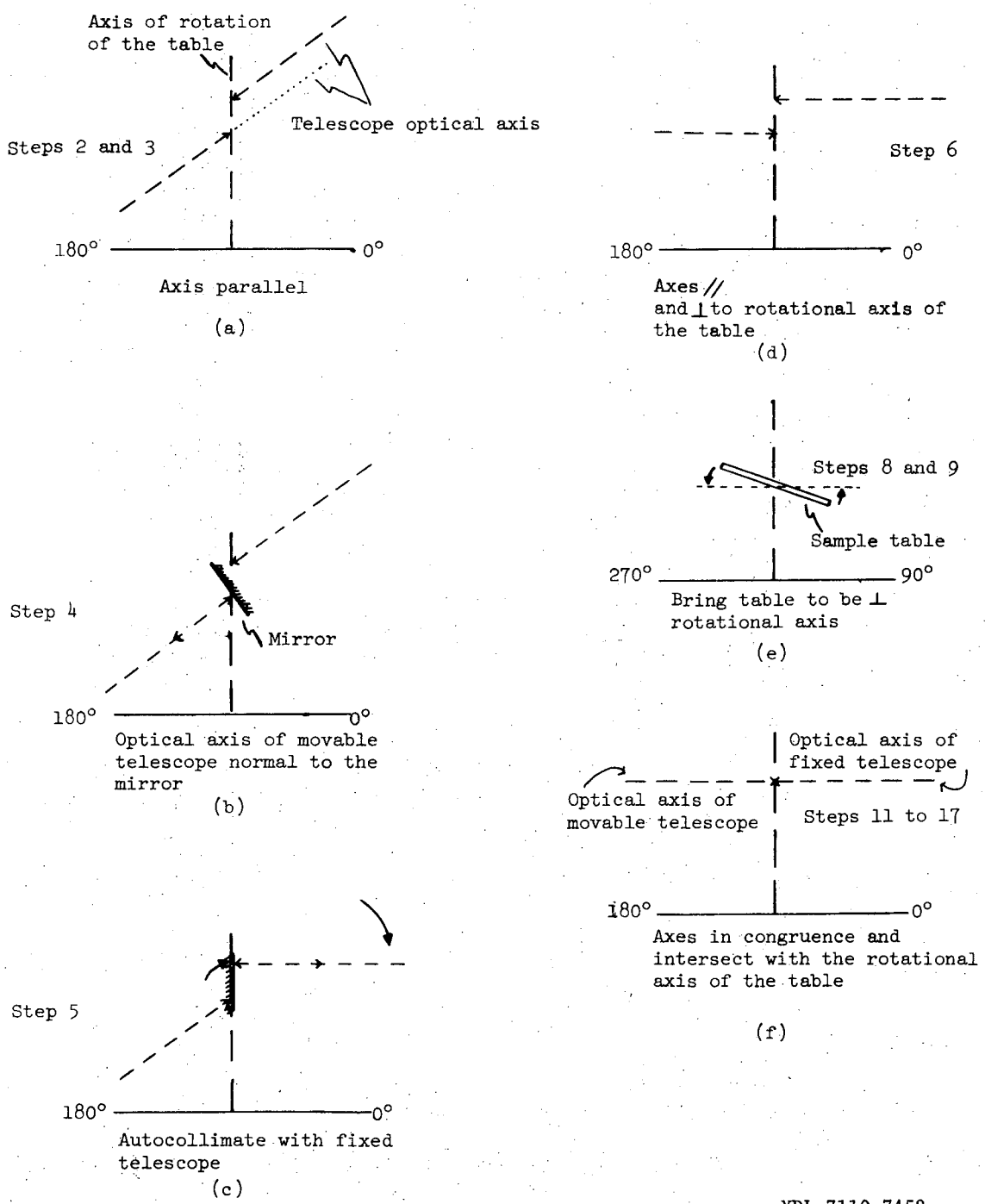

XBL 7110-7458

Fig. A3 Schematic of alignment procedures of ellipsometer with variable angle of incidence. (See Appendix III-A)

APPENDIX IV

POINCARÉ SPHERE

The use of a sphere for the representation of the state of polarization of light was introduced by the French scholar H. Poincaré in the 18th century. In ellipsometry, the Poincaré sphere[11,79-83] can be used to follow step by step the change of polarization caused by each optical component of the ellipsometer. The inter-relationship between parameters and the relative intensity change of the light can also be readily determined by the use of Poincaré sphere.

The representation of ellipsometric parameters on a Poincaré sphere is shown in Fig. A4. Point H, which lies on the equator, represents any arbitrary reference plane and is chosen here as the plane of incidence. Points on the equator will be states of linear polarization. The points L and R represent circular polarized light. Any point between the north pole L, and the equator designates elliptically polarized light with counterclockwise rotation (left-hand or positive polarization) when looking toward the light source. Points between the south pole R, and the equator designate elliptically polarized light with a clockwise rotation (right-hand or negative polarization). The angle θ is the azimuth angle of the polarized light (see Fig. A5). For a plane polarized light, θ is the angle between the plane of incidence and the electric vector whereas for an elliptically polarized light, it is chosen as the angle between the plane of incidence and the major axis of the ellipse. θ is measured counterclockwise from H when looking down from the pole L. The angle γ is a measurement of the ellipticity of the polarized light (see Fig. A5) and is defined as positive on the northern hemisphere (left-hand polarization) and negative on the southern hemisphere (right-hand polarization).

The relative phase change Δ, is measured counterclockwise when looking from the reference point H. The arctangent of the relative amplitude attenuation ψ, is measured from the opposite end of the sphere's diameter (V) that passes through H (measured from the plane normal to the reference plane). The retardation of the compensator δ_Q is measured counterclockwise when looking from the point F. Point F represents the fast axis azimuth angle of the compensator. The orientation of the transmission axis of the polarizer, analyzer, and the fast axis of the compensator* are represented in the same way as θ on the Poincare sphere.

With a system such as the one shown in Fig. 2, the representation of the change of state of polarization on a Poincaré sphere is illustrated in Fig. A6. When the ellipsometeric system is at null, the polarizer is set at an azimuth angle of p from the plane of incidence. The light, after passing through the polarizer (linearly polarized) is represented by point P on the equator with an angle of 2p from H. The quarter-wave plate, with its fast axis (F) at azimuth 45° (90° on the sphere), will cause a phase shift (δ_Q) of 90° and brings the state of polarization to E. Since E is located on the lower hemisphere, the light is right-hand elliptically polarized. The effect of the reflection is represented on the Poincaré sphere as two parts--phase change and amplitude change. The phase change Δ restores the elliptically polarized light to linearly polarized light and brings it back to the point F on the equator. The amplitude change will cause an azimuth angle change and brings the polarization state to A'. With the analyzer transmission axis A, set at 90° (180° from A' on the Poincaré sphere) to the light

*All azimuth angles are measured counterclockwise from the plane of incidence when looking into the light source (or looking against the polarizational vector).

vector, the light is extinguished. With reference to Fig. A6, we note that

$$\Delta = \widehat{EF} = \widehat{PF} \quad \text{(from spherical trigonometry, Law of sines)}$$

or

$$\Delta = \widehat{HF} - \widehat{HP} = 90^\circ - 2p \tag{A1}$$

and also,

$$\widehat{VA'} = \widehat{AH}$$

$$2\psi = 360 - 2a$$

$$\psi = 180 - a \tag{A2}$$

The Eqs. (A1) and (A2) derived above can be used to obtain Δ and ψ from polarizer and analyzer circle readings for this special zone. Relations between Δ,ψ and p, a for other zones can be derived on the Poincaré sphere following the same treatment as mentioned.* If the stereographic projection of the Poincaré sphere is used (right-hand columns of Fig. A4), quantitative treatment on the Poincaré sphere can be applied with the help of Wulff's net.[37]

---

*See Appendix V for the conversion of p and a to Δ and ψ respectively for different zones.

POINCARÉ SPHERE

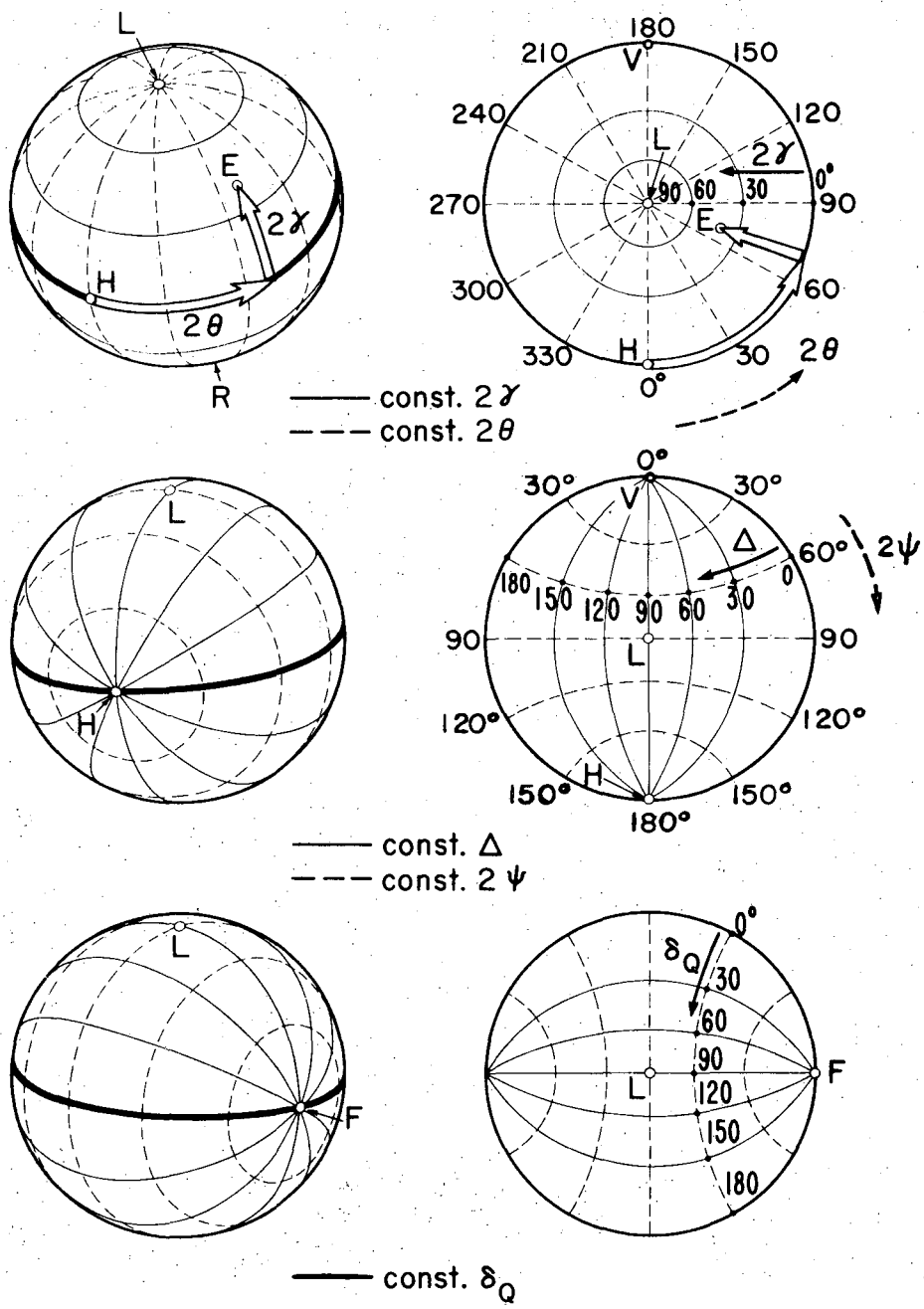

Fig. A4 XBL685-2759-A

Representation of ellipsometric parameters on Poincaré Sphere (left) and its stereographic projection (right) seen from the north pole L (left-hand circular polarization). H denotes the reference plane. Top: grid for geometric parameters θ and γ, center: grid for physical parameters ψ and Δ, bottom: grid for retardation δ_Q of a compensator with fast axis F.[85]

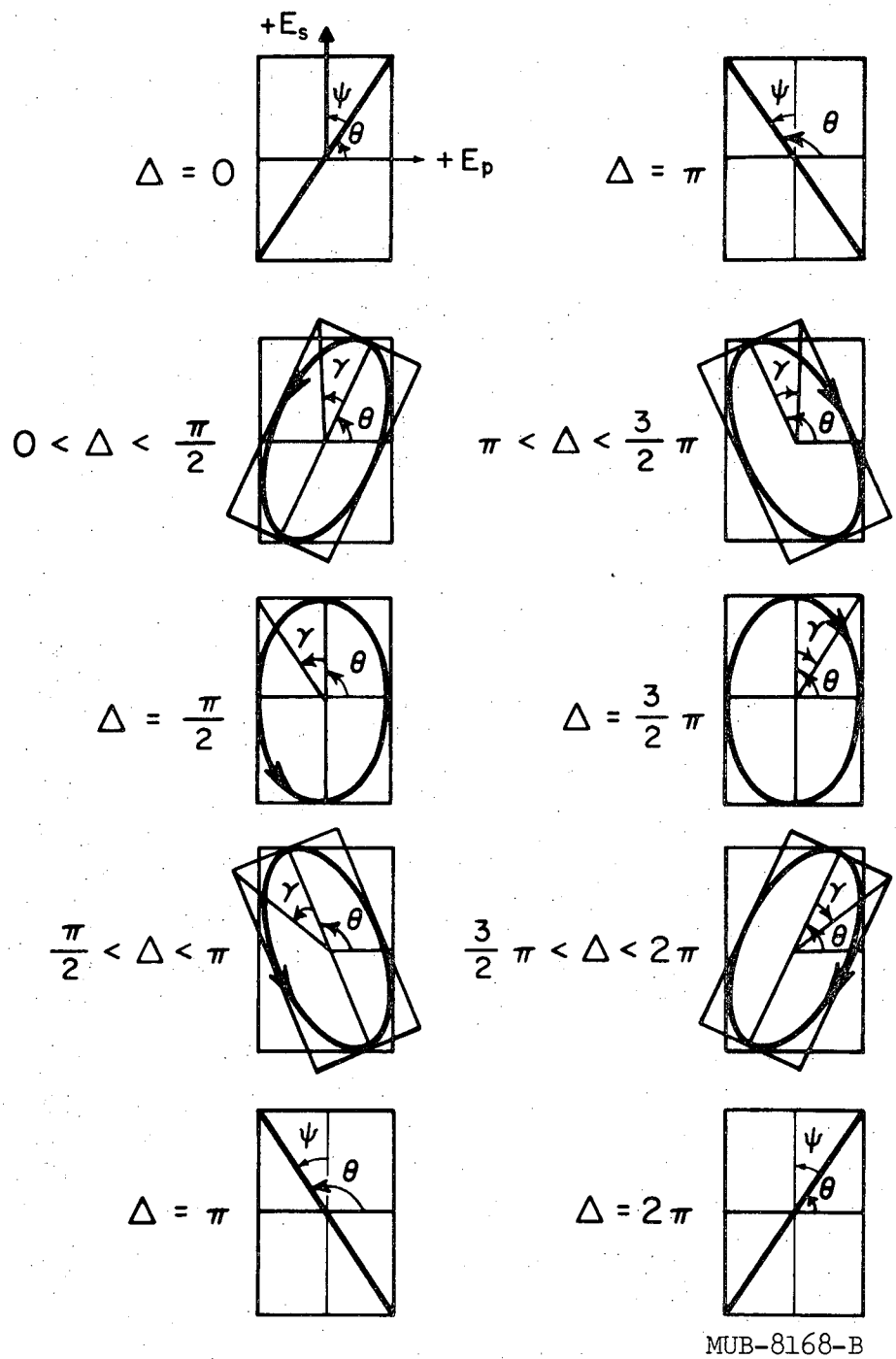

Fig. A5 Dependence of elliptical polarization on relative plane change Δ. γ is the ellipticity, θ, the azimuth angle of polarization and ψ, the arctangent of relative amplitude attenuation.[85]

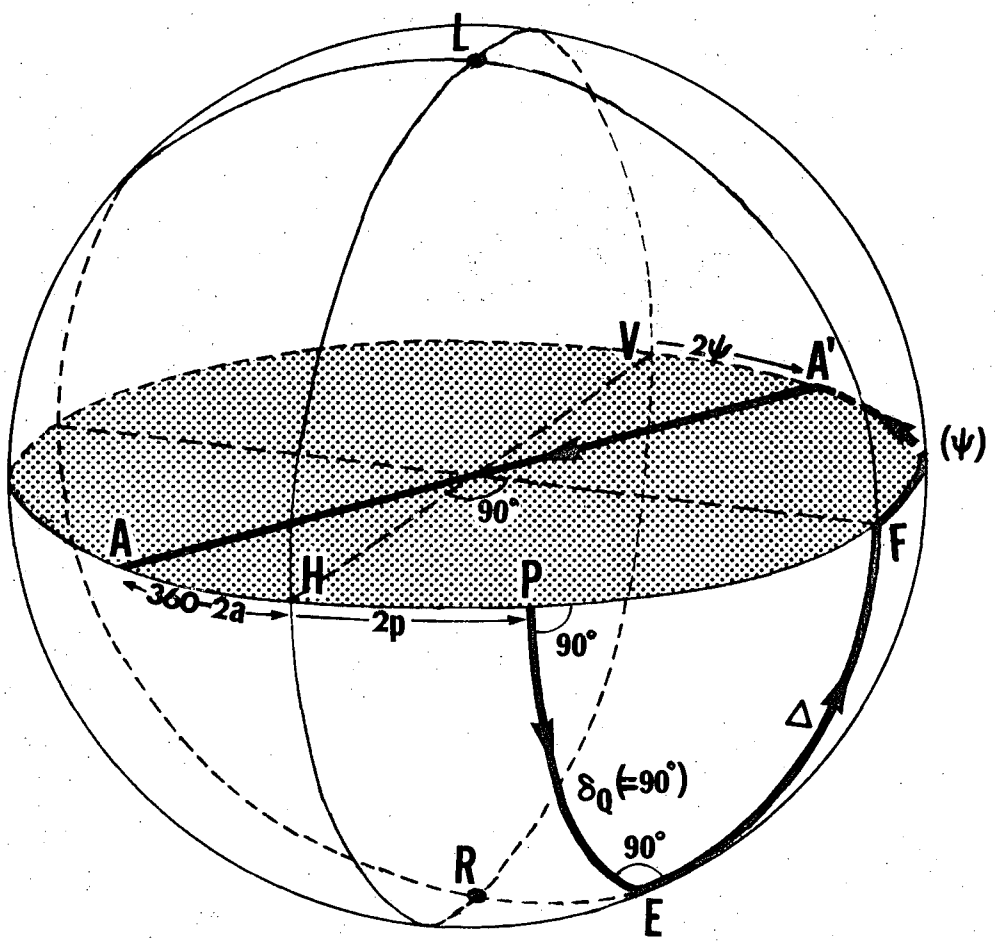

XBL 7110-7421

Fig. A6 Poincaré Sphere representation of the changes in the state of polarization through the components of an ellipsometer arrangement in Fig. 2.

$\widehat{HP} = 2p$ $\widehat{VA'} = 2\psi$ $\widehat{PE} = \delta_Q$ $\widehat{EF} = \Delta$

and $\widehat{HFVA} = 2a$

APPENDIX V

Ellipsometric parameters Δ and ψ from polarizer and analyzer circle readings in different zones.

Zone	Polarizer Circle Reading (P)	Azimuth of Transmission Axis (p)	Compensator Circle Reading (Q)	Azimuth of Quarter wave Plate Fast Axis (q)	Analyzer Circle Reading (A)	Azimuth of Transmission Axis (a)	Relative Phase Change (Δ)	Arctangent of Relative Amplitude Attenuation (ψ)
	A (Δ from 0° to 90°)							
A1	90-135	0-45	135	45	0-90	90-180	90 - 2p 270 - 2P	180 - a 90 - A
A2	135-180	45-90	45	135	0-90	90-180	2p - 90 2P - 270	180 - a 90 - A
A3	0-45	90-135	135	45	90-180	0-90	270 - 2p 90 - 2P	a A - 90
A4	45-90	135-180	45	135	90-180	0-90	2p - 270 2P - 90	a A - 90
	B (Δ from 90° to 180°)							
B1	90-135	0-45	45	135	90-180	0-90	90 + 2p 2P - 90	a A - 90
B2	135-180	45-90	135	45	90-180	0-90	270 - 2p 450 - 2P	a A - 90
B3	0-45	90-135	45	135	0-90	90-180	2p - 90 2P + 90	180 - a 90 - A
B4	45-90	135-180	135	45	0-90	90-180	450 - 2p 270 - 2P	180 - a 90 - A
	C (Δ from 180° to 270°)							
C1	90-135	0-45	135	45	90-180	0-90	270 - 2p 450 - 2P	a A - 90
C2	135-180	45-90	45	135	90-180	0-90	2p + 90 2P - 90	a A - 90
C3	0-45	90-135	135	45	0-90	90-180	450 - 2p 270 - 2P	180 - a 90 - A
C4	45-90	135-180	45	135	0-90	90-180	2p - 90 2P + 90	180 - a 90 - A
	D (Δ from 270° to 360°)							
D1	90-135	0-45	45	135	0-90	90-180	2p + 270 2P + 90	180 - a 90 - A
D2	135-180	45-90	135	45	0-90	90-180	450 - 2p 630 - 2P	180 - a 90 - A
D3	0-45	90-135	45	135	90-180	0-90	2p + 90 2P + 270	a A - 90
D4	45-90	135-180	135	45	90-180	0-90	630 - 2p 450 - 2P	a A - 90

REFERENCES

1. R. H. Muller, Surface Science 16, 14 (1969).

2. J. R. Mowat and R. H. Muller, Reflection of Polarized Light From Absorbing Media, University of California, Lawrence Berkeley Laboratory, UCRL 11813, (1966).

3. C. E. Leberknight and B. Lustman, J. Opt. Soc. Am., 29, 59 (1939).

4. T. C. Fry, J. Opt. Soc. Am. 16, 1 (1928).

5. A. B. Winterbottom, Det Kongelige Norske Videnskabers Selskabs Skrifter, (1955).

6. J. M. Stone, Radiation and Optics, (McGraw-Hill Co., New York, 1963) Ch. 15, 16.

7 J. R. Mowat and R. H. Muller, Reflection of Polarized Light From Film-Covered Surfaces, University of California, Lawrence Berkeley Laboratory, UCRL 17128, (1967).

8. L. Tronstad, Trans. Faraday Soc. 31, 1151 (1935).

9. A. Rothen, Rev. Sci. Instr. 16, 26 (1945).

10. J. O'M. Bockris, A. K. N. Reddy and B. Rao, J. Electrochem. Soc. 113, 1133 (1966).

11. F. L. McCrackin, E. Passaglia, R. R. Stromberg and H. L. Steinberg, J. Research Nat'l. Bur. Standards 67A, 363 (1963).

12. F. L. McCrackin and J. P. Colson, U. S. Dept. of Commerce, NBS Tech. Note 242.

13. H. E. Bennett, D. K. Burge, R. L. Peck, and J. M. Bennett, J. Opt. Soc. Am. 59, 675 (1969).

14. F. L. McCracken and J. P. Colson, U. S. Dept. of Commerce, NBS Micellaneous Pub., 256 (1964).

15. C. S. Stracken, Proc. Cambridge Phil. Soc. 29, 116 (1953).

16. D. V. Sivukhis, Soviet Physics JETP 3, 269 (1956).

17. C. A. Fenstermaker and F. L. McCrackin, Surface Science 16, 85 (1969).

18. D. W. Berreman, J. Opt. Soc. Am. 60, 499 (1970).

19. R. H. Muller, Rev. Sci. Instr. 39, 1593 (1968).

20. R. H. Muller, R. F. Steiger, G. A. Somorjai, and J. M. Morabito, Surface Science 16, 234 (1969).

21. A. J. Melmed, H. P. Layer, and J. Kruger, Surface Science 9, 476 (1968).

22. J. J. Vrakking and F. Meyer, Applied Phys. Letters 18, 226 (1971).

23. E. U. Condon and H. Odishaw, Handbook of Physics, (McGraw-Hill Book Co., 1958).

24. R. J. Archer and G. W. Gobeli, J. Phys. Chem. Solids 26, 343 (1965).

25. R. J. Archer, J. Electrochem. Soc. 104, 619 (1957).

26. R. J. Archer, Manual of Ellipsometry, (Gaertner Scientific Corp., Chicago, 1968).

27. J. H. Turney, M. S. Thesis, Department of Chemical Engineering, University of California, Berkeley, Aug. 1971. (LBL 171).

28. S. S. So, W. H. Knausenberger and K. Vedam, J. Opt. Soc. Am. 61, 124 (1971).

29. R. H. Muller, J. Electrochem. Soc. 113, 943 (1966).

30. R. B. Bird, W. E. Stewart, and E. N. Lightfoot, Transport Phenomena, (J. Wiley and Sons, Inc., 1960).

31. International Critical Table.

32. L. J. Aplet and J. W. Carson, Appl. Optics 3, 544 (1964).

33. C. C. Robinson, Applied Optics 3, 1163 (1964).

34. B. Pogany, Ann. Phys. 49, 531 (1916).

35. P. Drude, The Theory of Optics, (Dover Publ., New York, N. Y., 1959), p. 366.

36. Y. C. Chiu and M. A. Genshaw, J. Phys. Chem. 73, 3571 (1969).

37. F. E. Wright, J. Opt. Soc. Am. 20, 529 (1930).

38. R. W. Ditchburn, Light, (Interscience Publ., 1964) Vol. II, p. 590.

39. W. Koenig, in Handbuch der Physik, Vol. XX, H. Geiger and K. Scheel, eds., Springer, Berlin, (1928).

40. R. J. King and M. J. Downs, Surface Sci. 16, 288 (1969).

41. A. C. Hall, Surface Science 16, 1 (1969).

42. L. E. Smith and R. R. Stromberg, J. Opt. Soc. Am. 56, 1539 (1966).

43. T. Smith, J. Opt. Soc. Am. 57, 1207 (1967).

44. R. J. Archer, Phys. Rev. 110, 354 (1958).

45. H. Yokota, H. Sakata, M. Nishibori and K. Kinosita, Surface Science 16, 265 (1969).

46. M. A. Barrett and A. B. Winterbottom, in First International Congress on Metallic Corrosion, (Butterworths, London, 1962) p. 657.

47. P. C. S. Hayfield, in First International Congress on Metallic Corrosion, (Butterworths, London, 1962) p. 653.

48. R. C. Menard, J. Opt. Soc. Am. 52, 427 (1962).

49. B. H. Clausen and M. Flower, J. Electrochem. Soc. 110, 983 (1963).

50. R. J. Archer, J. Opt. Soc. Am. 52, 970 (1962).

51. W. C. Malm, A. J. D. Liu and H. H. Soonpaa, Surface Science 16, 365 (1969).

52. J. L. Ord, Surface Science 16, 155 (1969).

53. H. Takasaki, Appl. Optics 5, 759 (1966).

54. A. B. Winterbotton, U. S. Dept. of Commerce, NBS Miscellaneous Publ., 256 (1964) p. 97.

55. H. P. Layer, Surface Science 16, 177 (1969).

56. C. W. Tucker, Surface Science 2, 516 (1964).

57. A. E. Morgan and G. A. Somorjai, J. Chem. Phys. 51, 3309 (1969).

58. J. J. Carroll and A. J. Melmed, Surface Science 16, 251 (1969).

59. L. S. Bartell and D. Churchill, J. Phys. Chem. 65, 2242 (1961).

60. B. J. Bornong, Surface Science 16, 321 (1969).

61. R. R. Stromberg, E. Passoglia, and D. J. Tutas, U. S. Dept. of Commerce, NBS Mics. Publ., 256 (1964) p. 281.

62. F. Meyer and G. A. Bootsma, Surface Science 16, 221 (1969).

63. R. S. Sirohi and M. A. Genshaw, J. Electrochem. Soc. 116, 910(1969).

64. R. M. Goldstein and R. J. Lederich, Thin Solid Films 5, R11 (1970).

65. A. K. N. Reddy, M. A. V. Devanathan, and J. O'M Bockris, J. Electroanal. Chem. 6, 61 (1963).

66. A. Rothen and M. Hanson, Rev. Sci. Instr. 20, 66 (1949).

67. F. G. Will, J. Electrochem. Soc. 110, 145 (1963).

68. F. G. Will, J. Electrochem. Soc. 110, 152 (1963).

69. D. N. Bennion and C. W. Tobias, J. Electrochem. Soc. 113, 589 (1966).

70. D. N. Bennion and C. W. Tobias, J. Electrochem. Soc. 113, 593 (1966).

71. H. J. R. Maget and R. Roethlein, J. Electrochem. Soc. 112, 1034 (1965).

72. H. C. Weber, H. P. Meissner, and D. A. Sama, J.Electrochem. Soc. 109, 884 (1962).

73. E. Justi and A. Winsel, Kalte Verbrennung, (Franz Steiner Verlag, Weisbaden, 1962), Ch. 3.

74. E. A. Grens, R. M. Turner, and T. Katan, Adv. Energy Conversion 4, 109 (1964).

75. J. A. Rockett and R. Brown, J. Electrochem. Soc. 113, 207 (1966).

76. T. Katan, S. Szpak, and E. A. Grens, J. Electrochem. Soc. 112, 1166 (1965).

77. R. Kh. Burshtein, M. R. Turasevich, S. F. Chernyshyov and V. V. Karasu, Soviet Electrochemistry, 3, 803 (1967).

78. R. P. Iczkowski, J. Electrochem. Soc., 111, 1078 (1964).

79. H. G. Jerrard, J. Opt. Soc. Am., 44, 634 (1954).

80. G. N. Ramachandran and S. Ramaseshan, in Encyclopedia of Physics, Vol. XXV/1, S. Fluegge, ed., Springer-Verlag, (1961), p. 1.

81. L. Tronstad, Det. Kgl. Norske Videnskabers Selskabs Skrifter (1931) nr. 1, F. Bruns, Trondheim, (1931).

82. M. Born and E. Wolf, Principles of Optics, (1970), 4th ed., Ch. I, p. 30.

83. J. M. Stone, Radiation and Optics, (McGraw-Hill Co., New York, 1963) Ch. 13.

84. R. H. Muller and R. F. Steiger, Inogranic Materials Research Division, Annual Report 1967, Lawrence Berkeley Laboratory, University of California, Berkeley, UCRL 18043, p. 48

85. R. H. Muller, in Advances in Electrochemistry and Electrochemical Engineering, Vol. 9, Interscience, to be published.

LEGAL NOTICE

This report was prepared as an account of work sponsored by the United States Government. Neither the United States nor the United States Atomic Energy Commission, nor any of their employees, nor any of their contractors, subcontractors, or their employees, makes any warranty, express or implied, or assumes any legal liability or responsibility for the accuracy, completeness or usefulness of any information, apparatus, product or process disclosed, or represents that its use would not infringe privately owned rights.

TECHNICAL INFORMATION DIVISION
LAWRENCE BERKELEY LABORATORY
UNIVERSITY OF CALIFORNIA
BERKELEY, CALIFORNIA 94720